UNIVERSIDADE FEDERAL DE SANTA CATARINA
CENTRO TECNOLÓGICO
PROGRAMA DE PÓS-GRADUAÇÃO EM ENGENHARIA QUÍMICA

JEOVANDRO MARIA BELTRAME

MODIFICATION OF POLYESTERS AND NANOMATERIAL PRODUCTION FOR BIOMEDICAL APPLICATIONS

FLORIANÓPOLIS
2022

Jeovandro Maria Beltrame

MODIFICATION OF POLYESTERS AND NANOMATERIALS PRODUCTION FOR BIOMEDICAL APPLICATIONS

Dissertação/Tese submetida ao Programa de Pós-Graduação em Engenharia Química da Universidade Federal de Santa Catarina para a obtenção do título de Doutor em Engenharia Química.
Orientador: Prof. Dr. Pedro Henrique Hermes de Araújo
Coorientadora: Profª. Drª. Claudia Sayer e Drª. Camila Guindani.

Florianópolis
2022

Ficha de identificação da obra elaborada pelo autor, através do Programa de Geração Automática da Biblioteca Universitária da UFSC

Beltrame, Jeovandro Maria
Modification of polyesters and nanomaterials production for biomedical applications / Jeovandro Maria Beltrame; orientador, Pedro Henrique Hermes de Araujo; coorientadora, Claudia Sayer; coorientadora, Camila Guindani. 2022.

131 p.

Tese (Doutorado) - Universidade Federal de Santa Catarina, Centro Tecnológico, Programa de Pós-Graduação em Engenharia Química, Florianópolis, 2022.

Inclui referências.

1. Engenharia Química. 2. N-acetilcisteína. 3. Cisteína. 4. Electrospining. 5. Electrospining. I. Hermes de Araujo, Pedro Henrique. II. Sayer, Claudia. III. Guindani, Camila. IV. Universidade Federal de Santa Catarina. Programa de Pós-Graduação em Engenharia Química. V. Título.

Jeovandro Maria Beltrame

MODIFICATION OF POLYESTERS AND NANOMATERIALS PRODUCTION FOR BIOMEDICAL APPLICATIONS

O presente trabalho em nível de doutorado foi avaliado e aprovado por banca examinadora composta pelos seguintes membros:

_____
Prof.(a), Dr.(a) Ana Paula Serafini Immich Boemo
Universidade Federal de Santa Catarina (UFSC)

_____
Prof., Dr. Alexandre Parize
Universidade Federal de Santa Catarina (UFSC)

_____
Prof., Dr. Alexandre D'Agostini Zottis
Instituto Federal de Santa Catarina (IFSC)

_____
Prof., Dr. Marco Augusto Stimamiglio
Fundação Oswaldo Cruz (Fiocruz-Curitiba/PR)

Certificamos que esta é a **versão original e final** do trabalho de conclusão que foi julgado adequado para obtenção do título de doutor em Engenharia Química.

_____
Profª. Drª. Débora de Oliveira
Coordenação do Programa de Pós-Graduação

Documento assinado digitalmente
Debora de Oliveira
Data: 20/10/2022 14:21:24-0300
CPF: ***.453.929-**
Verifique as assinaturas em https://v.ufsc.br
ICP-Edu

_____
Prof. Dr. Pedro Henrique Hermes de Araújo
Orientador

Documento assinado digitalmente
Pedro Henrique Hermes de Araujo
Data: 20/10/2022 13:57:46-0300
CPF: ***.308.657-**
Verifique as assinaturas em https://v.ufsc.br
ICP-Edu

Florianópolis, 2022.

Este trabalho é dedicado aos meus amigos e amigas,
namorada, irmãos e aos meus queridos pais.

AGRADECIMENTOS

Primeiramente a Deus, pela saúde, pela força e persistência.

A minha família, meus pais João e Lourdes, e aos meus irmãos Matheus e Jaqueline por proporcionaram esta oportunidade desde sempre, por se fazerem presentes mesmo com toda distância. Estando sempre comigo, incentivando, apoiando e, principalmente, por todo amor incondicional.

Ao meu avô Santo Maria em memória, pelo incondicional apoio.

A cunhada Juciane Araldi e sobrinhos José e Cristian por serem meus grandes amigos, sempre me incentivando com palavras de apoio e conforto e por inúmeros momentos de descontração.

A minha companheira Bárbara Rampa Dias, pelo incondicional companheirismo e compreensão. Por todo auxílio e atenção nas dificuldades e por me incentivar para poder tornar este trabalho possível. E a sua família pelo incondicional apoio.

Aos meus orientadores, professor Dr. Pedro Henrique Hermes de Araújo, professora doutora Claudia Sayer, pela oportunidade, pela confiança e liberdade em poder estar estudando a produção deste estudo contribuindo para com o meu crescimento pessoal e profissional.

A coorientadora e amiga Camila Guindani, pela oportunidade e confiança em aceitar o convite em poder estar trabalhando a aplicabilidade deste material desenvolvido contribuindo para com o meu crescimento pessoal e profissional.

Aos membros da banca examinadora, Ana Paula Serafini Immich Boemo, Alexandre Parize, Alexandre D'Agostini Zottis e Marco Augusto Stimamiglio por aceitarem o convite e contribuírem para a melhoria desse trabalho.

As professoras Dra. Rozângela C. Pedroza, Dra. Karina Bettega Felipe pelos diálogos esclarecedores que me auxiliaram na constituição da proposta de trabalho, com discussões acerca de potenciais de aplicação. E por todo auxílio na execução dos experimentos biológicos.

À Universidade Federal de Santa Catarina, especialmente ao programa de Pós-Graduação de Engenharia Química.

Ao secretário e a secretária da Pós-Graduação, Edevilson Silva e Lizi, pela disposição em sempre ajudar.

À CNPq pelo apoio financeiro.

A Central de Análise do Departamento de Engenharia Química e ao Técnico Leandro.

Ao Laboratório Central de Microscopia Eletrônica (LCME). Aos técnicos Deise e Américo pelo treinamento e análise de Microscopia Eletrônica de Varredura.

Ao Laboratório Multiusuários de Estudos em Biologia (LAMEB) pelo uso da microscopia óptica, para visualizar a formação das fibras poliméricas.

Ao Laboratório de Controle de Processos (LCP), pela utilização de equipamentos para a síntese do polímero e utilização do FT-IR para análise de bioatividade.

Ao Laboratório de Sistemas Porosos (LASIPO), ao Laboratório Interdisciplinar (Linden).

Agradecer ao grupo de pesquisa Nanotec do Instituto Federal de Santa Catarina pela cooperação de anos. Em especial o coordenador Alexandre D'Agostini Zottis pela amizade e pela confiança aos longos destes anos de aprendizado.

Aos amigos e amigas Brena Beatriz, Clara Calado, Sabryna Giordani e Costa, Valdelúcia Grinevicius, Marcel Martins Guimarães, Rodrigo Lucas, Graziani Fornari. Aos meus amigos do laboratório Heloisa Madalosso, Tamara Angner, Felipe Lima, José Francisco, Ricardo Cunha, João Santin, Thiago Ouriques por dividirem seus conhecimentos e possibilidades de novos engajamentos, pela compreensão e disponibilidade para auxílios com ensaios e discussões, além da amizade e convivência no dia a dia.

Aos amigos presentes ou distantes em todos os instantes Alexandre Erzen, Diego Coelho, Gabriele Ottero, Eduardo, Aline Suave, Maycon Bastos, Rosemeri Lopes, Renan Jesus que sempre de alguma forma colaboraram com discussões de vida ou de trabalho.

A todos, o meu muito obrigada.

“Nunca deixe que lhe digam que não vale a pena acreditar no sonho que se tem ou que os seus planos nunca vão dar certo ou que você nunca vai ser alguém” .... (Renato Russo, 1987)

RESUMO EXPANDIDO

Introdução

A necessidade de novos dispositivos inteligentes projetados para mimetizar propriedades e comportamentos biológicos vem despertando interesse constante no desenvolvimento de dispositivos voltados para aplicações biomédicas. A utilização de polímeros com características biocompatíveis e bioabsorvíveis é de particular interesse para aplicações biomédicas. Os poliésteres surgem como uma das classes de polímeros mais estudadas e promissoras para essas aplicações, devido à sua capacidade de serem biorreabsorvidos e/ou biodegradados, além de serem biocompatíveis. A polimerização de poliésteres por abertura de anel pode ser realizada por enzimas, consideradas catalisadores "verdes", pois seu uso não gera resíduos tóxicos e a reação pode ser conduzida de forma eficiente em condições brandas. Além disso, quando os poliésteres apresentam insaturações, eles podem ser modificados com N-acetilcisteína (NAC) e cisteína (Cys) por meio de reações tiol-eno, permitindo a incorporação dessas moléculas por ligação covalente com o viés de proporcionar uma redução na hidrofobicidade e cristalinidade dos polímeros. Este trabalho relata a síntese de poli(globalida-co-ε-caprolactona) por polimerização enzimática por abertura de anel (e-ROP) e sua posterior modificação com NAC e Cys. O PGlCL foi sintetizado com uma razão de comonômero Gl/CL de 50/50, usando tolueno como solvente. A modificação foi realizada utilizando uma fotorreação tiol-eno entre a insaturação presente no monômero Gl e o grupo tiol (S-H) das moléculas NAC e Cys.

Objetivo

O objetivo deste trabalho foi a síntese enzimática de poli(globalida-co-ε-caprolactona) (PGlCL) seguida de modificação via reação de tiol-eno utilizando o aminoácido Cisteína (Cys) e o derivado aminoácido N-acetilcisteína e (NAC) para obtenção de scaffolds baseados em PGlCLNAC para aplicações na regeneração tecidual e estabilização de nanopartículas magnéticas de óxido de ferro (SPION) com PGlCLCys conjugado a biomoléculas na superfície de SPION e liberação enzimática em ambiente controlado.

Metodologia

A síntese do copolímero foi realizada pelo método de polimerização enzimática por abertura de anel (e-ROP) de globalida (Gl) e ε-caprolactona (CL). Modificação de poli(globalida-co-ε-caprolactona) com N-acetilcisteína (NAC) e cisteína (Cys) empregando um método de reação tiol-eno um tipo de reação química de clique. O polímero modificado foi caracterizado em termos de propriedades físicoquímicas usando técnicas convencionais de espectrometria, calorimetria e espectroscopia para avaliar o grau de funcionalização. Posteriormente, o polímero modificado de PGlCLNAC foi utilizado para a produção do scaffold utilizando a técnica de eletrofiação de Electrospinning. A caracterização do Scaffold usando métodos físico-químicos para avaliar a cristalinidade e hidrofilicidade dos Scaffolds. Ensaios convencionais de citotoxicidade biológica para avaliar membranas de curto prazo e ensaio clonogênico de longo prazo. Seguido do ensaio de fluorescência para avaliar a estrutura nuclear da célula em contato com a membrana. Avaliar o potencial uso dessas membranas para regeneração de tecidos. O polímero foi modificado com PGlCLCys. Também foi caracterizado por métodos físicoquímicos e na sequência pelo método de coprecipitação foi utilizado para a estabilização de nanopartículas magnéticas de óxido de ferro (SPIONs). A caracterização físico-química das SPIONs foi realizada para determinar a morfologia, diâmetro, potencial de superfície, diâmetro hidrodinâmico, magnetismo, etc. modificação da superfície das SPIONs utilizando a reação química da carbodiimida para incorporação de biomoléculas. Ensaios de citotoxicidade de SPIONs e a liberação da biomolécula conjugada à superfície de SPIONs foram utilizados para validar a aplicação dessas nanopartículas na área biomédica.

Resultados e discussão

A modificação realizada tanto com NAC (PGlCLNAC) quanto com Cys (PGlCLCys) permitiu a obtenção de um copolímero com cristalinidade reduzida, evidenciado pela característica amorfo determinada com as análises térmicas e pela maior hidrofilicidade medida na interação com a água em testes de superfície. Essas características aumentam a degradabilidade e o potencial de aplicação desses copolímeros no desenvolvimento de dispositivos para

aplicações biomédicas. Visando potenciais aplicações na área da nanomedicina, primeiramente, o copoliéster modificado com NAC, PGlCLNAC, foi utilizado para a obtenção de fibras eletrofiadas pela técnica de eletrofiação em blenda com poli(ε-caprolactona) (PCL). Essas fibras apresentaram baixa hidrofobicidade e baixa cristalinidade, permitindo uma proliferação celular mais intensa do que as fibras PCL, possibilitando um uso futuro para aplicação na área de regeneração tecidual. O copoliéster modificado com Cys (PGlCLCys), em um segundo momento, foi utilizado para o revestimento de nanopartículas superparamagnéticas de óxido de ferro (SPION) tendo em vista sua hidrofilicidade e melhor cristalinidade, o que possibilita a obtenção de nanopartículas dispersas em meio aquoso. A incorporação de cisteína possibilita a conjugação de biomoléculas na superfície, o que permite seu uso no desenvolvimento de dispositivos inteligentes voltados para modificações de superfície, com a inserção de moléculas alvo que proporcionam mimetismo em locais específicos do ambiente celular específico.

Conclusão

Portanto, o uso do copolímero PGlCLCys se deve a uma estratégia de modificação de superfície via reação carbodiimida entre aminas e ácidos carboxílicos para formação de amidas, o que permite o desenvolvimento de biomateriais inteligentes possibilitando liberação enzimática desencadeada em pH controlado.

Palavras-chave: poli(globalida-co-ε-caprolactona). N-acetilcisteína. cisteína. Eletrofiação. Nanopartículas Superparamagnéticas de Óxido de Ferro.

RESUMO

A necessidade de novos dispositivos inteligentes e projetados para mimetizar propriedades e comportamentos biológicos vem despertando constante interesse para o desenvolvimento de dispositivos que visam as aplicações biomédicas. O uso de polímero com características biocompatível e biorreabsorvível possui um interesse particular para aplicações biomédicas. Poliésteres emergem como uma das classes de polímeros mais estudadas e promissoras para estas aplicações, devido a sua capacidade de serem biorreabsorvidos e/ou biodegradados, além de serem biocompatíveis. A polimerização de poliésteres por abertura de anel pode ser realizada por enzimas, consideradas catalisadores "verdes", visto que o seu uso não gera resíduos tóxicos e a reação pode ser conduzida em condições brandas de forma eficiente. Adicionalmente, quando os poliésteres possuem insaturações estas podem ser modificadas com N-acetilcisteína (NAC) e cisteína (Cys) via reações tiol-eno possibilitam a incorporação destas moléculas por ligação covalente com o viés de proporcionar uma redução na hidrofobicidade e cristalinidade dos polímeros. Este trabalho relata a síntese de poli(globalide-co-ε-caprolactona) (PGlCL) por polimerização por abertura de anel via enzimática (e-ROP) e sua posterior modificação com NAC e Cys. O PGlCL foi sintetizado com uma razão de comonômeros Gl/CL de 50/50, utilizando tolueno como solvente. A modificação foi realizada empregando uma fotoreação tiol-eno entre a insaturação presente no monômero de Gl e o grupo tiol (S-H) das moléculas de NAC e Cys. A modificação realizada tanto com NAC (PGlCLNAC), como com Cys (PGlCLCys) permitiu a obtenção de um copolímero com cristalinidade reduzida, evidenciada pela característica amorfa determinada com as análises térmicas e pela maior hidrofilicidade medida na interação com água em ensaio de superfície. Essas características aumentam a degradabilidade e potencial de aplicação desses copolímeros no desenvolvimento de dispositivos para aplicações biomédicas. Visando potenciais aplicações na área nanomedicina, primeiramente, o copoliéster modificado com NAC, o PGlCLNAC, foi utilizado para a obtenção de fibras eletrofiadas pela técnica *electrospinning* em uma blenda com poli(ε-caprolactona) (PCL). Estas fibras apresentaram baixa hidrofobicidade e baixa cristalinidade, permitindo uma proliferação celular mais intensa do que fibras de PCL, viabilizando uma futura utilização para a aplicação na área de regeneração tecidual. O copoliéster modificado com Cys (PGlCLCys), num segundo momento, foi utilizado para o recobrimento de nanopartículas superparamagnéticas de óxido de

ferro (SPION) tendo em vista a sua hidrofilicidade e cristalinidade melhorada, o que possibilita a obtenção de nanopartículas dispersas em meio aquoso. A incorporação cisteína viabiliza a conjugação de biomoléculas na superfície, o que possibilita o seu uso no desenvolvimento de dispositivos inteligentes com foco em modificações na superfície, com a inserção de moléculas alvos e que propiciam a mimetização em sítios específicos no ambiente celular especifico. Portanto, a utilização do copolímero PGlCLCys se deve a uma estratégia de modificação da superfície via reação carbodiimida entre aminas e ácidos carboxílicos para formação de amida, o que permite o desenvolvimento de biomateriais inteligentes viabilizando a liberação enzimática acionada em pH controlado.

Palavras-chave: poli(globalide-co-ε-caprolactona). N-acetilcisteína. Cisteína. Electrospining. Nanopartículas Superparamagnétcias de Óxido de Ferro.

ABSTRACT

The need for new intelligent devices designed to mimic biological properties and behaviors has been arousing constant interest in the development of devices aimed at biomedical applications. The use of polymers with biocompatible and bioresorbable characteristics is of particular interest for biomedical applications. Polyesters emerge as one of the most studied and promising polymer classes for these applications, due to their ability to be bioreabsorbed and/or biodegraded, in addition to being biocompatible. Polymerization of polyesters by ring-opening can be carried out by enzymes, which are considered green catalysts since their use does not generate toxic residues and the reaction can be efficiently carried out under mild conditions. Additionally, the modification of unsaturations in polyesters chains using N-acetylcysteine (NAC) and cysteine (Cys) via thiol-ene reactions allows the incorporation of these molecules by a covalent bond with the bias of providing a reduction in the hydrophilicity and crystallinity of the supports. This work reports the synthesis of poly(globalide-co-ε-caprolactone) (PGlCL) by enzymatic ring-opening polymerization (e-ROP) followed by its modification with NAC and Cys. PGlCL was synthesized by e-ROP using toluene as solvents, with a Gl/CL comonomer ratio of 50/50. The modification was performed using a photopolymerization reaction carried out in the unsaturation, present in the Gl monomer, with the (S-H) sulfur of the NAC and Cys molecules through thiol-ene reactions. The modification carried out in the PGlCLNAC and PGlCLCys copolymers in both cases allowed obtaining a copolymer with reduced crystallinity, evidenced by the amorphous characteristic obtained with the thermal analyzes and by the greater hydrophilicity measured by contact angle assays. These characteristics allow an improvement in terms of degradability and application potential of these copolymers in the development of devices for biomedical applications. Aiming at potential applications in the field of nanomedicine, first, the copolyester modified with NAC, PGlCLNAC, was used to obtain electrospun fibers using the Electrospinning technique in a blend with polycaprolactone (PCL). These fibers showed a reduction in the hydrophobicity and crystallinity of the blend, enabling the use of these fibers to obtain non-toxic membranes and with potential application in the area of tissue regeneration. The modified copolyester with Cys (PGlCLCys), in a second moment, was used for the coating of superparamagnetic iron oxide nanoparticles (SPION) because

of its hydrophilicity and improved crystallinity, which makes it possible to obtain nanoparticles dispersed in an aqueous medium. The incorporation of cysteine enables the conjugation of biomolecules on the surface, which allows its use in the development of smart devices with a focus on surface modifications, with the insertion of target molecules that provide mimicry at specific sites in the specific cellular environment. Therefore, the use of PGlCLCys copolymer is due to a surface modification strategy via carbodiimide reaction between amines and carboxylic acids for amide formation, which allows the development of intelligent biomaterials enabling the triggered enzymatic release at controlled pH.

Keywords: poly(globalide-co-ε-caprolactone). N-acetylcysteine. Cysteine. Electrospinning. SPIONS.

LIST OF FIGURES

LIST OF TABLES

LIST OF ABREVIATIONS AND SYMBOLS

AIBN – Azobisisobutyronitrile
Asp – Aspartate
BAET - 2-(Boc-amino)ethanethiol
BSA – Bovine Serum Albumin
CALB – Candida Antartica Lipase B
$CDCl_3$ – Deuterated chloroform
CL – ε-Caprolactone
CO_2 – Carbon dioxide
Cys – Cysteine
DAPI - 4′,6-Diamidino-2-phenylindole dihydrochloride
DCC - N,N-Dicyclohexylcarbodiimide
DCM – Dichloromethane
DFT - Density Functional Theory
DMF - Dimethylformamide
DMPA – 2,2-dimethoxy-2-phenylacetophenone
DMSO - Dimethyl sulfoxide
DLS – Dynamic Light Scattering
DSC – Differential Scanning Calorimetry
ECM - Extracellular Matrix
EDC - N-(3-dimethylaminopropyl)-N'-ethylcarbodiimide
EGMP – Ethylene glycol bis(3-mercapto propionate).
EtOH - Ethanol
e-ROP – Enzymatic Ring-opening Polymerization
FA – Folic Acid
FTIR-ATR – Fourier Transform Infrared Spectroscopy – Attenuated Total reflectance
G – Gibbs free energy
Gl – Globalide
GPC – Gel Permeation Chromatography
His – Histidine
HPLC - High-performance Liquid Chromatography
Log P - Logarithm of Partition Coefficient
$Log^{p0/w}$ – Logarithm of Partition Coefficients for n-octanol/water mixtures
Mn – Number average molecular weight
MTT – 3-(4,5-Dimethylthiazol-2-yl)-2,5-diphenyltetrazolium bromide

Mw – Weight average molecular weight
NAC – N-acetylcysteine
N-ACA – Nacetylcysteamine
NHS – N-hydroxysuccinimide
NMA – Nuclear Morphometric Analysis
NRU – Neutral Red Uptake
NZ435 – Novozym 435
P - Partition coefficient
PBS - Phosphate-buffered solution
PCL – Poly(ε-caprolactone)
PEG - Poly(ethylene glycol)
PGL – Polyglobalide
PGlCL – Poly(globalide-co-ε-caprolactone)
PGlCLCys - Poly(globalide-co-ε-caprolactone) covalently bonded with cysteine
PGlCL-NAC - Poly(globalide-co-ε-caprolactone) covalently bonded with N-acetylcysteine
PVP – Poly(vinylpyrrolidone)
PVA - Poly(vinyl alcohol)
^{1}H NMR - Proton Nuclear Magnetic Resonance
SAED - Selected area electron diffraction
$scCO_2$ – Supercritical Carbon dioxide
SEM – Scanning Electron Microscopy
Ser – Serine
SMD - Solvation Model Based on Electronic Density
SPION – Superparamagnetic Iron Oxide Nanoparticles
SPION@PGlCLCys – SPION coated with PGlCLCys
SPION@PGlCLCys_FA - SPION@PGlCLCys bioconjugated with folic acid
TEM – Transmission Electron Microscopy
THF – Tetrahydrofuran
UV – Ultraviolet
UV-Vis - Ultraviolet–visible
VSM - Vibrating Sample Magnetometer
XRPD – X-ray Powder Diffraction
TGA - Thermogravimetric analysis
T_m – Melting temperature
TMS – Tetramethylsilane
X_c – Degree of crystallinity
XRD - X-ray Diffraction
Đ – Dispersity

ΔG_{solv} – Gibbs free energy of solvation
ΔH_m – Fusion Heat

SUMARY

CONCEPTUAL DIAGRAM

"MODIFICATION OF POLYESTERS AND PRODUCTION NANOMATERIALS FOR BIOMEDICAL APPLICATIONS"

What?

Enzymatic synthesis of poly(globalide-co-ε-caprolactone) (PGlCL) followed by modification via thiol-ene reaction using the amino acid Cysteine (Cys) and the amino acid derivative N-acetylcysteine (NAC) for the obtaining scaffolds based on PGlCLNAC for applications in tissue regeneration and stabilization of magnetic iron oxide nanoparticles (SPION) with PGlCLCys conjugated with biomolecules on the surface of SPION and enzyme-triggered release in a controlled environment.

Why?

- The growing demand for the use of biocompatible and bioresorbable polymers in biomedical devices, aims to improve the efficiency of medical diagnoses and treatments, providing greater comfort and practicality to patients' lives.
- Globalide (Gl) and ε-caprolactone (CL) polyesters can be used to produce copolymers with interesting properties for biomedical applications;
- The presence of unsaturations in the copolymer allows modification reactions so that it is possible to produce a customized biomaterial for different purposes;
- The use of enzymes and the use of click chemistry reactions are ideal approaches for biomedical and pharmaceutical applications, setting a green perspective and dispensing the use of multi-step reactions for the bioconjugation of molecules leaving no toxic residues in the final product.

State of the art

- Enzymatic ring-opening polymerization (e-ROP) has been used with different monomers including Globalide (Gl) and ε-caprolactone (CL) for the synthesis of copolyesters providing good results.
- In the literature, there are few reports on the polymerization and modification of Globalide, but none using N-acetylcysteine (NAC) and its use in obtaining scaffolds in a blend with PCL;

- In the literature, there are few reports on the polymerization and modification of the Globalide, but none using such modified polymers in the stabilization of SPIONs;
- This is the first study to propose a PGlCLCys biomaterials platform with a triggered system for the enzymatic release of biomolecules in controlled environments.

Hypotheses

- Synthesis of PGlCL via enzymatic ring-opening polymerization (e-ROP) makes it possible to obtain a copolymer with strategic unsaturations;
- The use of amino acids (Cysteine – Cys) and derivatives (N-acetylcysteine – NAC) for the modification of PGlCL makes it possible to obtain copolymers with modified thermal properties;
- The thiol-ene modification of PGlCL with NAC reduces the crystallinity and hydrophobicity of the PGlCLNAC scaffold, and provides surface-cell interactions in the biological medium;
- The thiol-ene modification of PGlCL with Cys reduces hydrophobicity, which enables the use of the PGlCLCys copolymer for stabilization of SPIONs. This modification also provides amine site for covalent conjugation of molecules on the surface of the SPIONs;
- It is possible to produce covalent conjugates with folic acid molecules (SPION@PGlCLCys_FA), whose release can be triggered in a controlled environment.

Which steps?

- Enzymatic ring-opening copolymerization (e-ROP) of Gl and CL;
- Modification of PGlCL with NAC by thiol-ene reaction;
- Characterization of the modified copolymer PGlCLNAC;
- Obtaining the scaffold using the Electrospinning technique;
- Physicochemical characterization;
- Conducting biological assays;
- Modification of PGlCL with Cys by thiol-ene reaction;
- Characterization of the modified copolymer PGlCLCys;
- Stabilization of iron oxide magnetic nanoparticles (SPIONs);
- Physicochemical characterization of SPIONs;
- Conducting biological assays.

Expected results
•Understand how the modification of PGlCL with the amino acid (Cysteine-Cys) and with the amino acid derivative (N-acetylcysteine-NAC) influences the physicochemical properties of the copolymers; •To produce scaffold from electrospinning technique with PGlCLNAC with improved biocompatibility; •To produce SPIONs stabilized with PGlCLCys and with covalently conjugated biomolecules on the surface; •To perform enzyme-triggered release assays of surface conjugated biomolecules in controlled environments; •To produce a PGlCL nanoplatform with tunable properties for diverse biomedical applications.

THESIS METHODOLOGICAL SEQUENCE FLOWCHART

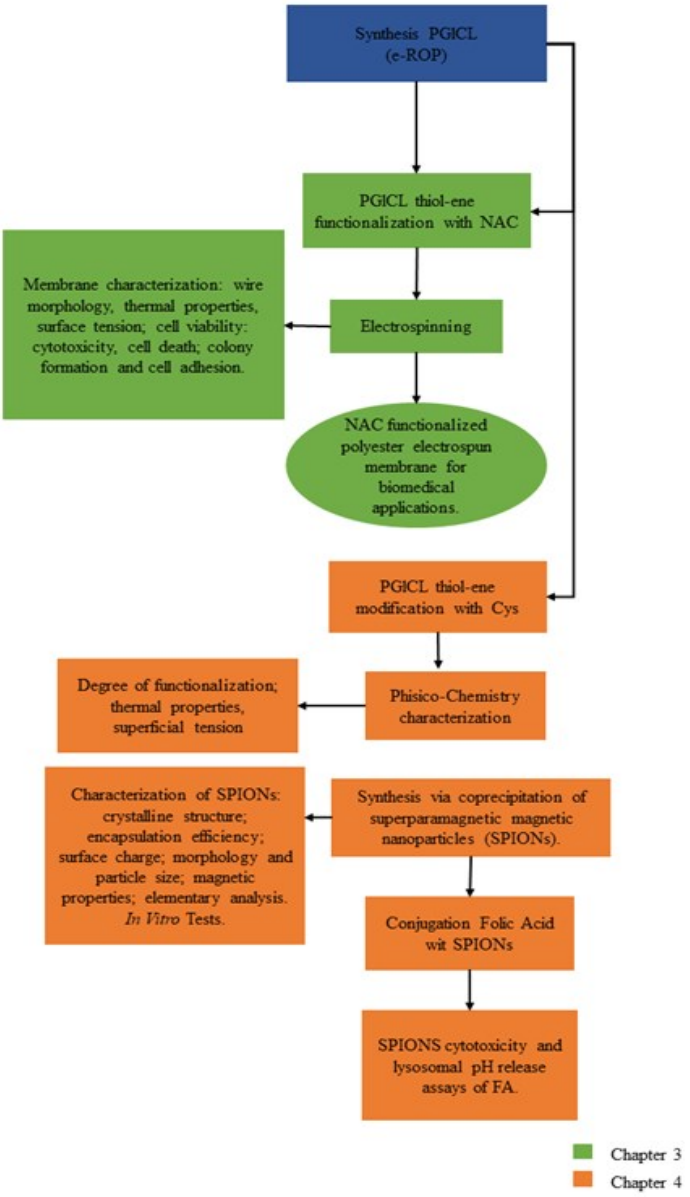

CHAPTER 1

1 INTRODUCTION

In the last two decades, significant advances have been made in the field of biodegradable polymers. Their application in the manufacture of biomaterials for medical applications has been receiving attention given their acceptance by the biological environment, internalization and elimination as progressively smaller polymer chains. The main degradation mechanism is the enzymatic hydrolysis of the ester bonds. Therefore, this class of polymers configures an attractive option of low production cost and reduction in the generation of plastic waste. Biodegradable polyesters, as for instance the copolymer poly(globalide-co-ε-caprolactone) derived from lactone (ε-caprolactone) and macrolactone (globalide), have been gaining notoriety due to the possibility of adjusting the rates of (co)monomers enabling the modulation of mechanical properties (cristalization and hidrophobicity), biocompatibility, and biodegradability. This class of polymers stands out due to its biocompatibility and biodegradability characteristics and has been gaining visibility due to the manipulation of the properties, mainly hydrophilicity and crystallinity, which can be adjusted according to the area of application: medicine, regeneration, of tissues, and organs; in the food industry, such as biodegradable packaging; and in the pharmaceutical industry as carriers for drug delivery (ATES ; HEISE, 2014; CLAUDINO et al., 2012; GUINDANI et al., 2020a; VAN DER MEULEN et al., 2008).

Synthesis processes of polyesters via the traditional route require some care regarding the purity of the monomer and the use of an inert atmosphere (KOBAYASHI; MAKINO, 2009). The ring-opening polymerization method using biological catalysts (enzymes) (e-ROP) can be performed under mild temperature conditions and reduces the generation of toxic waste, moreover, when immobilized enzymes are used as catalysts, they can be reused. Using unsaturated macrolactones, as for instance globalide, as monomers, the product of this polymerization is a linear-chain unsaturated polyester, which can undergo post-polymerization modifications (GUINDANI et al., 2019b), which allow the application of these polymers in different devices in the biomedical area (MARQUES et al., 2002; VERT, et al., 1992). Thiol-ene reactions are a useful technique for the modification of unsaturated polyesters,

since they promote high reaction rates and high yields, besides being insensitive to oxygen. In addition, a wide variety of thiol groups can be used, with emphasis on amino acids and their derivatives (BELTRAME et al., 2021; GUINDANI et al., 2020a; GUINDANI et al., 2020b; HOYLE et al., 2004).

The production of biodegradable scaffolds has recently aroused great interest in the medical field and a wide variety of polymers have been used to manufacture these structures. Poly(ε-caprolactone) (ε-PCL) polyesters have received increasing attention due to their biocompatibility, biodegradability, and mechanical properties suitable for making a structure that resembles the structure of the extracellular matrix. However, these polyesters are highly crystalline and hydrophobic, which reduces both: their degradation rate and their interaction with the biological environment. Thus, in view of the need to develop alternatives that minimize these effects, the covalent modification of PGlCL with N-acetylcysteine (PGlCL-NAC) aims to promote the formation of a copolymer with improved biocompatibility properties, while increasing the presence of interaction sites with the biological environment (GUINDANI, 2019b). In this way, PGlCL-NAC electrospinning in a blend with PCL enables the production of scaffolds with modified physical and chemical properties, emerging as alternative for the production of scaffolds for the regeneration of a wide variety of structural tissues (for example, bones, cartilage, skin and muscle tissues) (ATES; HEISE, 2014).

The versatility of polyesters allows their use in stabilizing superparamagnetic iron oxide nanoparticles (SPIONs) which are an important ally for the diagnosis/treatment of malignant tumors, configuring an important ally and having their use approved as these can be metabolized by the organism (PALANISAMY; WANG, 2019). To avoid embolism caused by these nanoparticles, they need to be coated with biocompatible and non-cytotoxic materials (SHEN et al., 2013). Synthetic polymers such as non-biodegradable poly(methyl methacrylate) have been used for this purpose. However, unsaturated polyesters obtained from lactones have several advantages over these polymers, as in addition to being biocompatible, they are biodegradable and may contain unsaturations in their main polymer chain. These unsaturations can be reacted with different molecules (ATES;HEISE, 2014), such as amino acids, and their derivatives useful as tools in breast cancer targeting both in diagnosis (DADFAR et al., 2019) and treatment (QU et al., 2018; YAO et al., 2019). Recent advances in polymerization and modification methods involving unsaturated polyesters have aroused

constant interest, as this procedure allows obtaining polymers with amphipathic characteristics (GUINDANI et al., 2019b). The modification of double bonds in the polymer backbone using the thiol-ene "click reaction" is a versatile and low-cost strategy that does not require the use of multiple synthesis steps. This strategy makes it possible to obtain a polymer with modified characteristics and properties, such as lower crystallinity and greater hydrophilicity, in addition to the absence of cytotoxicity. (GUINDANI et al., 2020b).

The present work aims to investigate the production of polyester nanoplatforms by green chemistry methods followed by modification with amino and their derivatives via thiol-ene reaction to obtain electrospun fibers and magnetic nanoparticles coating for applications such as biomedical devices, contributing to the development of modern health treatment techniques.

1.1 OBJECTIVES

1.1.1 General objetive

To investigate the synthesis of biocompatible polyesters and their post-polymerization modification with amino acids and derivatives for the production of scaffolds and stabilization of superparamagnetic iron oxide nanoparticles for biomedical applications.

1.1.2 Specific objetives

- To produce poly(globalide-co-ε-caprolactone) (PGlCL) by e-ROP and to carry out its modification by thiol-ene reactions with N-acetylcysteine (PGlCL-NAC).
- To produce electrospun scaffolds using poly(ε-caprolactone) (PCL) and PGlCL-NAC blends, and evaluate their *in vitro* biocompatibility with fibroblast cells (McCoy);
- To synthesize and characterize of Superparamagnetic Iron Oxide Nanoparticles (SPIONS) stabilized with PGlCLCys (SPION@PGlCLCys), followed by conjugation with folic acid (SPION@PGlCLCys_FA) via carbodiimide chemistry reaction;

- To evaluate the biocompatibility of SPIONS@PGlCLCys and SPION@PGlCLCys_FA, exposed to normal L929 fibroblast cells and MDA MB 231 human breast cancer cells.
- To evaluate the enzyme-triggered release of the folic acid conjugated to SPION@PGlCLCys_FA under lysosomal conditions.

CHAPTER 2

2 LITERATURE REVIEW

This chapter presents a brief review of the available literature on the issues relevant to this work. First, the classification of polyesters is presented, followed by the polyester synthesis method by ring-opening polymerization reactions catalyzed by enzymes (e-ROP). Subsequently, methods of modifying polyesters with amino acids and derivatives are shown. Finally, the application of modified polymers in different polymeric devices are introduced, with an especial focus on the biomedical application area: 1) electrospun fibers for tissue regeneration and 2) coating of magnetic nanoparticles for possible applications in the early detection of tumor cells are presented here.

2.1 POLYMERS: BIOCOMPATIBILITY, BIODEGRADABILITY, AND BIORESORPTION

Biocompatibility is related to the property of the biomaterial of being compatible with living tissue, promoting growth and differentiation between normal cells, maintaining orientation in space throughout the biomaterial. The elaborated biomaterial must exercise its function as a support for cell growth to avoid undesirable tissue damage while minimizing disturbances in the physiological regeneration process (WILLIAMS, 2008).

The classification of polymers presented *by the American Standards for Testing and Materials* (ASTM) establishes that biodegradable polymers are those in which degradation is performed by microorganisms, predominantly in a natural ecosystem (ASTM D-883, 2011). In addition, degradation is conditioned to the intrinsic characteristics of the polymeric species used for the construction of the biomaterial. However, the choice of biodegradable polymers is conditioned on the biocompatibility characteristics aiming at the applicability of the desired biomaterial. Biocompatibility and biofunctionality are considered as the main criteria for the evaluation of a biodegradable system (VERT et al., 1992).

Another important characteristic concerns polymers with bioabsorbable and bioreabsorbable properties, which can differ one from the other based on how degradation occurs (BARBANTI et al., 2005). *In*

vivo degradation of biodegradable polymers occurs through the clivage of macromolecular chains into smaller chains, without affecting the integrity of the material and without eliminating by-products in the body. On the other hand, other polymeric supports may suffer the action of extracellular enzymes and form degradation by-products that will be removed from the site of action (VERT et al., 1992).

Bioabsorbable polymers can integrate into body fluids without a division of the macromolecular chain or a decrease in molar mass. On the other hand, bioreabsorbable polymers when reabsorbed in vivo generate *metabolites* that can be eliminated from the body through metabolic pathways (VERT et al., 1992).

Additionally, the structural aspects of the materials should be considered, conditions of the microenvironment, such as the pH, in which it will be employed, and the surface area/volume ratio of the polymeric support, which influence the degradation process and which are determining factors for the construction and application of a biomaterial (LENZ, 1993).

2.1.1 Polyesters

The need for the development of nanomaterials from synthetic polymers that degrade in biological systems after performing a certain function has aroused interest in obtaining polyester polymers. These polymers have ester groups within the repeating units along the main chain which provides degradation by hydrolysis. Its applicability in biodevices is conditional on the fact that at least one subset of the polyester family is environmentally degradable (MILETIĆ et al., 2010).

Another relevant feature of polyesters is the versatility that polymers have associated with good mechanical properties and biocompatibility. These properties make them good candidates to be used in the biomedical and pharmaceutical industry as a reabsorbable implant material or as a carrier for the controlled release of drugs (ALBERTSSON; VARMA, 2003).

In addition to the biodegradation and bioresorption characteristics of polyesters as a due to of weight loss occurs from the fragmentation of polymer chains through the hydrolysis of the main chain ester bonds, so that the rate and extent of degradation are dependent on the hydrophilic and crystalline character of the polymer which influence the access of water in the polymer chain (GUINDANI et al., 2020b). So, hydrolysis occurs until the material reaches molecular mass around 4.000 Da. Degradation products with molecular mass less than 4.000 Da then

undergo a process of cell degradation (URBANEK et al., 2020). The final degradation and resorption of the material occur through the cells of the organism, such as macrophages, lymphocytes, and neutrophils (PACHENCE et al., 2007). This stage of degradation is characterized by the reduction of molecular mass, structural alteration, and mechanical properties such as loss of tensile strength, compressive strength, and hardness (ATHANASIOU et al., 1998; BARBANTI et al., 2005).

Some factors are crucial and have a marked influence on the degradation of polyesters, for example, kinetic factors; chemical composition and configurational structure; molecular weights (Mn and Mw); dispersion (Đ); environmental conditions; mechanical stress; crystallinity; chain orientation; distribution of chemically reactive compounds within the matrix; additives; general hydrophilicity and morphology (e.g.: porosity); and size of the polymeric device (GUINDANI, 2018).

Thus, the modulation of the physical and biodegradable properties of the aliphatic polyesters can be obtained from the adjustment in the structure and composition of the main polymer chains. To make the polymer chains more flexible, polar groups can be used, which plays an important role in the orientation and crystalline packaging, depending on the application that surrounds this polymer (ALBERTSSON e VARMA, 2003; COULEMBIER et al., 2006).

2.1.1.1 Poly(ε-caprolacactone)

Polycaprolactone (PCL) (Figure 1) is a polymer constantly used in the construction of materials both in the medical and biological fields. The biodegradation and bioresorption of polyesters such as PCL occur from the hydrolysis of ester bonds, which results in the reduction of molar mass without the loss of mass. Resorption continues through cells of the body, such as macrophages (PACHENCE et al., 2007). PCL can be biodegraded by the hydrolytic pathway without enzymatic degradation in the tissue, which makes the bioresorption/absorption process slower. (VERT, 2009).

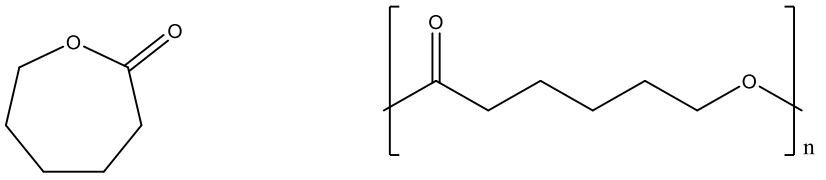

(a) (b)

Figure 1. The chemical structure of ε-caprolactone is represented in its cyclic form (a) and repetitive monomeric unit of poly (ε-caprolactone) (b).

2.1.1.2 Polyglobalide

Polyglobalide (PGl) (Figure 2) aliphatic polyester macrolactone and studies have reported its application in the development of devices with a focus on biomedical applications (ATES; HEISE, 2014; CLAUDINO et al., 2012; GUINDANI et al., 2019b; VAN DER MEULEN et al., 2008). The monomer, globalide (Gl), also known as 15-pentadecenolide-oxacyclohexadecen-2-one (IUPAC name), is applied more by the fragrance industry, due to the organoleptic properties of its musky odor and the slow loss of aroma . Thus, few studies on the synthesis of polyglobalides are found in the literature.

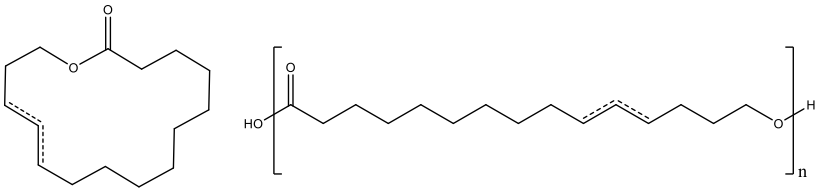

(a) (b)

Figure 2. The chemical structure of the globalide is represented in its cyclic form (a) and repetitive monomeric unit of the poly(globalide) (b).

2.2 ENZYMATIC SYNTHESIS OF POLYESTERS

2.2.1 Lipases

In nature, enzymes are divided into six distinct classes, such as oxide-reductases, transferases, hydrolases, lyases, isomerases, and ligases. Lipase stands out here, which is used for hydrolysis of fatty esters in nature, being particularly interesting for polymer synthesis. Lipases catalyze reactions in organic media, given their activity at the water-fat

interface in cells. They also do not require the use of a cocatalyst, thus demonstrating that it is the most efficient enzyme for polyester synthesis (GEUS, 2007). Lipases can be used for polycondensation and polyesterification reactions, as well as ring-opening polymerizations and polymer modification reactions (GUINDANI et al., 2017; HABEYCH et al., 2011; MILETIĆ et al., 2010).

Novozym® 435 is a commercially available immobilized lipase manufactured by Novozymes (Bagsvaerd, Denmark). Novozym® 435 is composed of the enzyme Candida Antarctica lipase B (CALB), which is immobilized (physically adsorbed) within the macroporous resin Lewatit VP OC 1600 is a macroporous adsorber in form of spherical beads. The copolymer poly[(methyl-co-butyl methacryhomee methacrylate]) copolymer matrix facilites its use for the imobilization of enzymes (especially lipases) (HABEYCH et al., 2011; ZHANG et al., 2014). Novozym® 435 is a catalyst that has wide versatility, thanks to its highly resistant support, which ensures that the enzyme maintains its activity on a variety of substrates in various organic solvents (GEUS, 2007).

Enzymatic ring-opening polymerizations (e-ROP) are a promising approach, especially due to the increasing progress of studies that report the efficiency of lipase-catalyzed reactions in different solvents and studies related to the reuse of the immobilized catalyst, which implies in the reduction of process costs (FUKUDA et al., 2001). Enzymatic catalysis can be seen as a highly promising and extremely necessary technique in expanding the development of environmentally friendly processes for polyester synthesis (GUINDANI et al., 2017).

2.2.2 Enzymatic ring-opening polymerization mechanism (e-ROP)

In contrast to condensation polymerizations, e-ROP polymerization has the convenience of not generating output groups during the reaction. This allows to obtain polyesters with a high degree of control about molecular mass and dispersion, under relatively moderate reaction conditions. Non-enzymatic ring opening polymerization using metal catalysts based on tin, zinc, and aluminum is commonly applied for the production of polycaprolactone (PCL) and polyglobalide (PGl), among other polyesters derived from cyclic esters (CLAUDINO et al., 2012; Li, et al., 2011). However, these catalysts can generate residues that may hamper the application of the obtained polymer in the biomedical

field. Thus, the use of biological catalysts can be an alternative due to lower toxicity and no waste generation (KOBAYASHI, 2009).

Lipases play a crucial role as biocatalysts within e-ROP, being responsible for the hydrolytic catalysis of the ester bond. This reaction occurs at the active site of the enzyme, where the catalytic triad is located: a nucleophilic serine residue activated by a hydrogen bond, stabilized by hydrogen bridge with a histidine (His), aspartate (Asp), or serine (Ser) (ALBERTSSON; SRIVASTAVA, 2008).

In the enzymatic transesterification mechanism presented in Figure 3, the catalytic triad present in lipase is electronically stabilized. Ester (e.g., present in the ε-caprolactone chain) functions as a substrate molecule and suffers a nucleophilic attack of the primary serine alcohol at the active enzyme site (I), which leads to the formation of an intermediate species (II). In transesterification, the alkoxy group (R_2-OH) is then released (III), forming a species of monomer activated by the enzyme (III). However, in the case of an e-ROP, the alcoxi group will not be released, considering that the lactones are cyclic. Thus, the nucleophile represented by the primary alcohol (R_3-OH) performs the attack on the species formed by the monomer activated by the enzyme (III). Thus, the formation of a new intermediate species is obtained in the (IV) stage. With this, there is the formation of the final product which is a short-chain polymer, and the regeneration of the active site of the enzyme (GEUS, 2007; MILETIĆ et al., 2010).

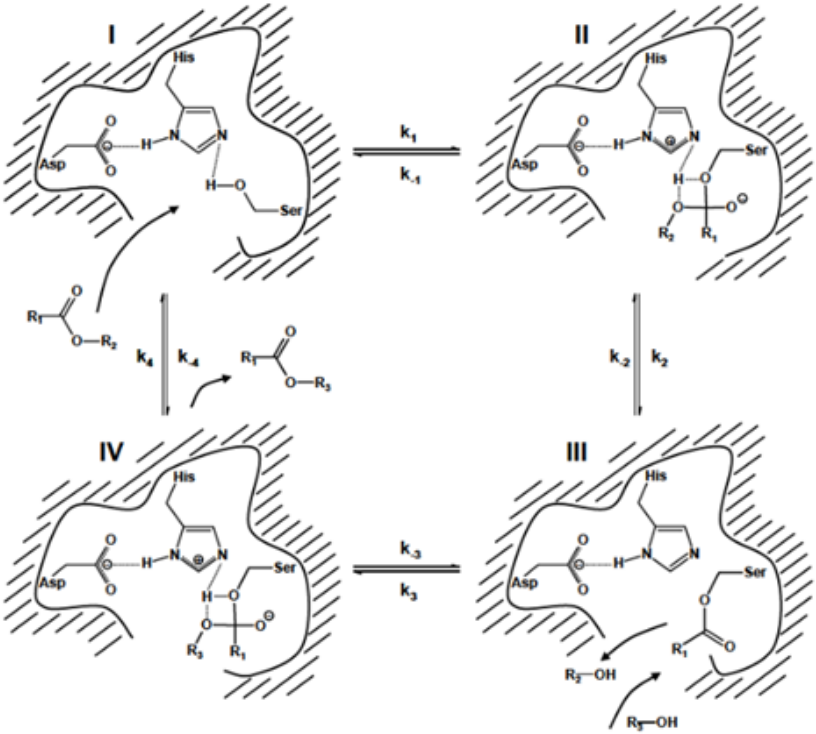

Figure 3. Mechanism for enzymatic transesterification proposed by Geus (2007). Source: (GEUS, 2007).

Figure 4 presents the e-ROP mechanism of caprolactone proposed by Johson et al. (2011).

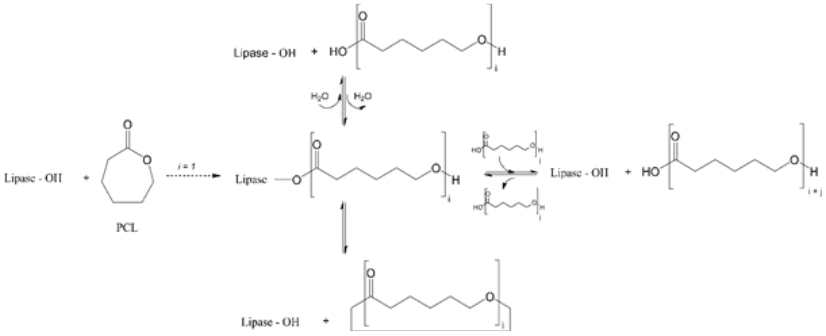

Figure 4. Enzymatic ring-opening polymerization mechanism. Adapted from (JOHNSON et al., 2011).

2.2.3 The main parameter affecting e-ROP

The need for the enzyme to use a small amount of water to activate its active site makes this characteristic the main parameter that affects the e-ROP reaction. The amount of water is related to the maintenance of the active three-dimensional conformation, its integrity, the polarity of the active site, flexibility, and stability of the protein regardless of whether it is in free form or covalently attached to a support. Thus, the presence of water functions as a nucleophile, when in the presence of other nucleophiles, it will result in the formation of chains with different terminal groups (HENDERSON et al., 1996). With this, some of the characteristics of the polymer, for example, molecular mass and terminal functionalization, can be obtained by adding different nucleophiles during polymerization (GUINDANI et al., 2019b).

The polymerization reaction itself occurs from the nucleophilic attack of the hydroxyl present in the oligomer chain, formed in stage III (Figure 3) (ALBERTSSON; SRIVASTAVA, 2008). From there, there is the formation of new complexes, formed by activation by the enzyme. These are generated as a result of the addition of more than one monomeric unit in the polymer chain, forming the final product. This process is cyclical and occurs successively along with polymerization and can be observed in Figure 4

During the propagation reaction, it is desirable to obtain linear chains as a final product, but the formation of cyclic chains or hydrolysis of the oligomeric/polymer chains may also occur. Figure 4 displays e-

ROP polymerization route of cyclic esters, performed with the use of the commercial biocatalyst Novozym 435 to obtain a linear polymer. The model presented can be applied to different species of lactones, macrolactons, lactams, and cyclic carbonates. (MEI et al., 2002).

2.3 POST-POLYMERIZATION MODIFICATION AND CONJUGATION USING PGlCL AND PGlCLCys

The post-polymerization reaction involving pre-synthesized linear chain polymer consists of modifying the polymer or copolymer chain to obtain a new material with altered physical and chemical properties to expand the possibilities of the application of the material. Among the properties that can be altered are viscosity, solubility, adhesion, crystallinity, and hydrophilicity. Furthermore, through this strategy it is possible to conjugate polymers/copolymers with more complex structures, such as proteins and antibodies, for example, aiming at materials that have specific interactions with cells (TREUEL et al., 2014; TUNCA, 2014).

2.3.1 Thiol-ene modification

The copolymer polyglobalide-co-ε-caprolactone may be modified via a thiol-ene *click-chemistry* reactions between the unsaturation present in the repetitive unit of globalide and a thiol group containing molecule as shown in Figure 5 (GUINDANI et al., 2019b). These reactions can be performed directly using either a thermal or a photoinitiator. However, the use of thermal initiators leads to polymers with lower molecular weights and low mechanical integrity. The use of the photoluminescent route (Figure 6) allows the production of polymers and crosslinker polymer with modified thermal properties (ATES et al., 2011; ATES e HEISE, 2014; LOWE, 2010).

Thiol-ene reaction is often regarded as a *click-chemistry* reaction, i.e., high-yield reactions with harmless by-products generation. The *click-chemistry* concept arises from the need to obtain a new method for conducting organic reactions that generate substances from the union of small units with heteroatom bonds (KOLB et al., 2001). The advantages of thiol-ene reaction is regioselective and does not require the use of mild conditions. In addition, these reactions are insensitive to the presence of oxygen and humidity (HOYLE; BOWMAN, 2010).

The main obstacle to the modification of the pre-synthesized copolymer is related to the chemical modification of the linear structure to obtain an amphiphilic copolymer. The most common is the use of successive synthetic procedures, which is a task considered difficult and ingenious, due to the linearity of polyesters. An alternative is the modification of the pre-synthesized polymer followed by modification procedures via direct synthesis methods, *click chemistry* reactions, which allows the addition of different molecules to the linear polymer structure (ATES et al., 2011).

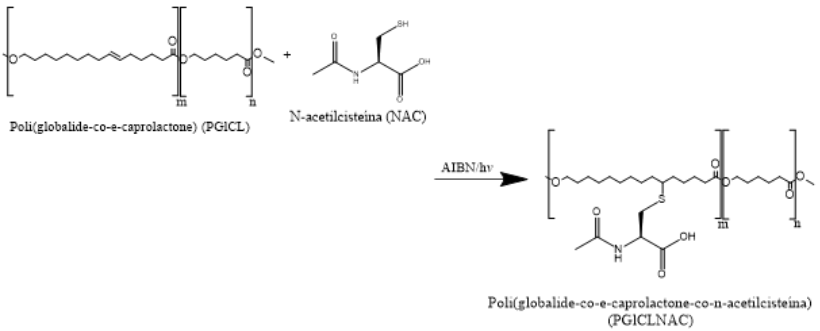

Figure 5. Mechanism of modification of the polymer PGlCL by thiol-ene reaction with N-acetylcysteine. Adapted from (GUINDANI et al., 2019b).

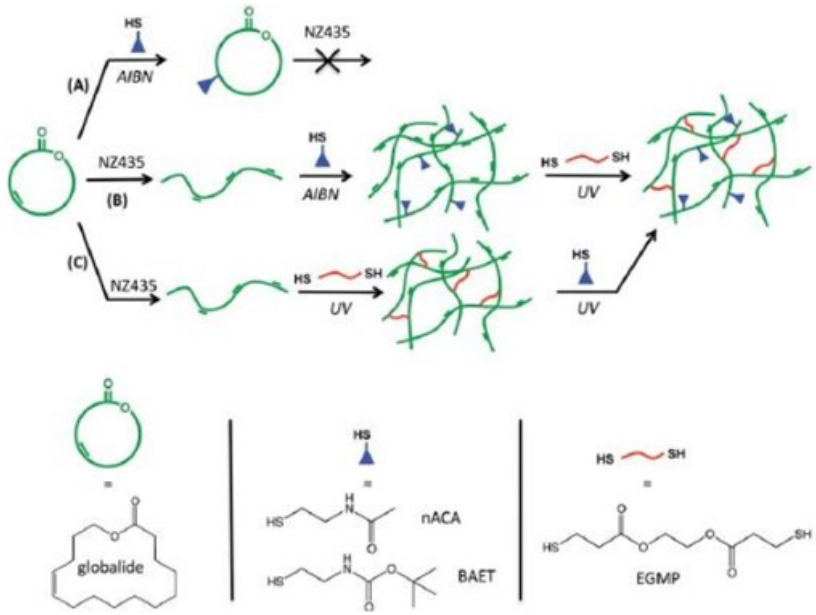

Figure 6. NZ435: Novozym 435; AIBN: azobisisobutyronitrile; N-ACA: Nacetylcysteamine; BAET: 2-(Boc-amino) ethanethiol; EGMP: ethylene glycol bis(3-mercapto propionate). (ATES; HEISE, 2014).

2.3.2 Carbodiimide conjugate macromolecules

The covalent chemical conjugation of macromolecules has attracted the scientific interest once it enables improving the properties of nanomaterials for biomedical applications. For instance, the conjugation of molecules on the surface of nanomaterials aims to modulate this surface, providing receptor-ligand interactions (LEIRO et al., 2018).

Covalent chemical conjugation involves the reaction between functional groups present in the device and biomolecules that have specific characteristics. A highlighted molecule is folic acid, commonly used for the functionalization of devices that target tumor cells. Many functional groups are described in the literature, with emphasis on the mechanisms that involve amine and carboxylic acid groups. Thus, based on the characteristic of the functional group and its reactivity, it is possible to predict and design which reactions they may undergo,

allowing the establishment of synthetic routes to prepare the conjugate of interest (LEIRO et al., 2018; MONTALBETTI; FALQUE, 2005).

Amine groups are good nucleophiles, thus, the use of molecules with this functional group is attractive for the modification of polyesters. The formation of an amide bond is the product of chemical conjugation, which consists of an equilibrium condensation reaction between a carboxylic acid and an amine. However, direct condensation is possible at temperatures of 200°C. This temperature is incompatible with the aimed application and may compromise the functionality of biomolecules/biopolymers. Thus, the use of strategies with milder temperatures allows the primary activation of the carboxylic acid with the use of a leaving group ends up being necessary before the attack of the amine group. In this way, the development of methods and strategies for the covalent coupling of molecules have been developed (LEIRO et al., 2018).

Carbodiimide chemistry was one of the first coupling routes reagents to be synthesized for covalently linking an amine group ($-NH_2$) to a carboxylic acid (-COOH) forming an amide bond ($-COONH_2$). Organic coupling agents (N,N-Dicyclohexylcarbodiimide - DCC) (Figure 7 A) or aqueous coupling agents (N-(3-dimethylaminopropyl)-N'-ethylcarbodiimide - EDC)) (Figure 7 B), are commonly used to promote carboxylic acid activation, being used together with the reagent N-hydroxysuccinimide (NHS), forming the O-acylisourea intermediate. This O-acylisourea can then react directly with the amine to produce the desired amide and generate an urea by-product. Also, part of the O-acylisourea may follow an undesired path to give an unreactive N-acyl urea by-product. Initially, DCC was the most commonly used carbodiimide. However, its use favors the formation of poorly soluble ureas in multiple purification steps. Thus, methods employing water-soluble carbodiimides (EDC) are more favorable due to the formation of

water-soluble ureas, facilitating purification processes (LEIRO et al., 2018; MONTALBETTI; FALQUE, 2005).

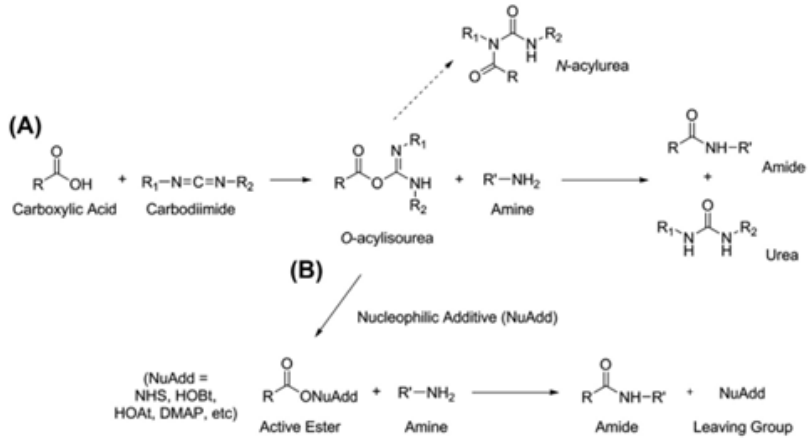

Figure 7: (A) Activation of carboxylic acid through carbodiimide coupling reagent and consecutive coupling to an amine using DCC and (B) use of nucleophilic additives to generate the activated ester and subsequent reaction with an amine using NHS (LEIRO et al., 2018; MONTALBETTI; FALQUE, 2005).

2.4 BIOMEDICAL APPLICATIONS

Some of the desirable properties in a biomaterial are biodegradability, biocompatibility, absence of toxicity, in addition, the generation of biocompatible non-toxic degradation products which makes modified polyesters potential polymers for the elaboration of biomaterials with appropriate characteristics.

2.4.1 Polymeric porous supports (scaffolds) and their applications

For the application of a biomaterial, it is necessary to develop a structure that provides characteristics and stimuli for the cell, which are identical to the natural environment, so that properties as porosity and structure are the main characteristics for the elaboration and preparation of the biomaterial. Thus, it is necessary to develop support that constitutes a temporary three-dimensional matrix with a specific structure and that

provides the development of a tissue (ATES; HEISE, 2014; HOKUGO et al., 2006; MAIA et al., 2013).

The supports can be used both for cell growth and as a mechanical support platform, which helps in the formation of the structure of the newly grown tissue (BARBANTI; ZAVAGLIA; DUEK, 2005). These structures can be designed according to the application and aim to promote the diffusion of healthy tissue cells from the site where they were implanted inside as exemplified Figure 8 (HOKUGO et al., 2006).

Another important point in the manufacture of a structure is the regeneration of tissues using cell growth matrices refers to the controlled degradation of the implanted biomaterial (PATEL; FISHER, 2008). It is usually expected that the cell growth matrix will remain long enough to miscellaneous cells maintained in this biomaterial and tissue microenvironment cells or between biomaterial cells and the extracellular matrix of tissue cells until total regeneration of the injured area (PATEL; FISHER, 2008)

The process of chemical modification, the modulation of parameters such as copolymerization conditions and the molar mass of the polymers used, or even changes in the comonomer ratio are determining factors of the final structural quality of the biomaterial (ATES; HEISE, 2014; JEONG et al., 2004). In addition to issues related to degradation and stiffness, another important point to be considered refers to the porosity of the biomaterial. Thus, the process of developing a support with the control of the size, number, and connectivity of pores are determining characteristics for the quality of the biomaterial. Studies have shown that pore size is directly related to vascularization and the diffusion of nutrients, residues, and oxygen in the regenerating tissue within the biomaterial. And experimental glazing demonstrated that pore diameters greater than 5 μm do not allow good vascularization (BOTCHWEY et al., 2003; TANG et al., 2014).

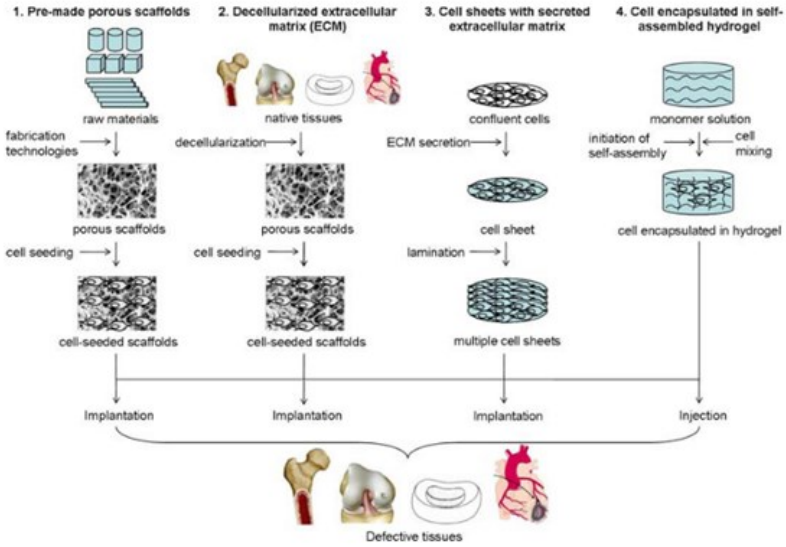

Figure 8. Schematic diagram showing different approaches for Scaffold obtaining for tissue engineering (LEONG, 2008).

Given the complexity of the cellular microenvironment, sometimes chemical modification of the copolymer is not sufficient for tissue development in vitro. In this way, the control over the physical microenvironment includes several electrical, mechanical and magnetic factors, which influence the cellular behaviors of migration, proliferation, differentiation and cellular maturation. Physical factors, unlike biochemical ones, offer unlimited opportunity to stimulate cells. These may be due to the adjustable polymer stiffness depending on the induced cellular behavior or conductive polymers used to stimulate tissues and cells. In addition, electrical stimulation, mechanical stimulation and magnetic stimulation, on the behavior of different tissues and cells grown in functional polymeric structures, aim to enable extrinsic physical cues. cellular and tissue, including cell proliferation, cell migration, among others (TAI,2021).

In addition to the physical microenvironment, cells and tissues in vivo constantly experience evolving mechanical microenvironments, depending on the anatomical location and their stage of development. Thus, physical signals, including morphology, topography, availability of

adhesion sites and mechanical properties of substrates, play a crucial role in cellular behavior. Mechanical properties, including elastic modulus, tensile strength, and fracture toughness at macroscopic and microscopic scales, impact cells in a magnitude-dependent manner. Thus, the need to obtain structures that enable mechanical microenvironments with conditions that favor an accommodating physiological environment for cell survival and differentiation. Furthermore, the biomechanical signals and interactions between cells and the direct cell specification of the ECM as stem cell differentiation are highly sensitive to mechanical inputs, especially the rigidity of adherent surfaces. Based on the mechanosensitive of cells, the application of mechanical forces or stimulation is emerging as an effective modality to guide cellular behaviors, such as proliferation and differentiation, and still form desired tissues under well-controlled tissue morphogenesis (TAI, 2021).

The use of scaffolds in tissue engineering, obtained by electrospinning, allows the creation of synthetic structures that can resemble the extracellular matrix. These structures aim to control intrinsically (i.e. substrate stiffness) or extrinsically (i.e. applied forces) mechanical environments to achieve desired cellular responses that require a 3D microenvironment similar to in vivo conditions to develop a tissue with a structure and function. appropriate.

Electrospinning consists of a simple and easy-to-apply technique that uses electrostatic forces to produce polymer fibers that can present micrometric dimensions reaching nanometric dimensions (BHARDWAJ; KUNDU, 2010; TAYLOR, 1969). The use of this technique is constantly growing, due to its practicality in obtaining three-dimensional surfaces from the deposition of fibers, which can be generated with several polymers, such assynthetic polymers, natural, biodegradable, non-degradable and even the use of mixtures between these materials, which allows its use in various areas of engineering and health (DENG et al., 2007; LEONG, 2008).

From the same type of cell, a growth matrix can be obtained in different formats of supports according to the needs of the patient (BARBANTI et al., 2005). In addition, the dimensions of the solid polymeric support can be designed according to the application mode (Figure 9) (BOTCHWEY et al., 2003). In some cases, these are three-dimensional (3D) structures that can later be applied superficially to the injured site, implanted, or inserted through a surgical procedure in the patient under treatment (KAIGLER et al., 2001).

Studies carried out in tissue and organ regeneration engineering applying biomaterials obtained from electrospinning for the development

of matrices for growth can serve as substrates and provide a better cell-cell or cell-material interaction. The first is to collect a certain tissue or part of an organ through biopsy in the patient who needs to recover an injured tissue or organ. The collected cells must then be dissociated and isolated to allow the cultivation of cells of interest from the tissue or organ in question. This cultivation should occur in a cell growth matrix in the form of support (KAIGLER et al., 2001; MAIA et al., 2013). In the cell-material interaction, it can be implanted directly in the patient, without having had a previous cell culture. Therefore, in this case, a matrix for cell growth may be composed of saline suspension containing polymers, proteins, and growth and cell proliferation factors (KAIGLER et al., 2001).

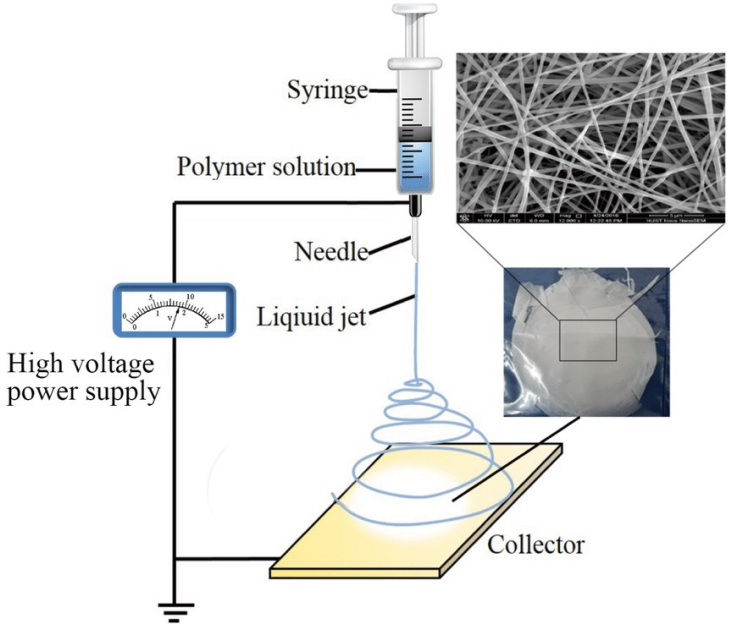

Figure 9. Illustrative scheme for Scaffold obtained from the technique of electrospinning (FENG et al., 2016).

2.4.2 Stabilization of magnetic nanoparticles

Advances in the area of nanotechnology enable the manufacture, characterization, and adequacy of functional properties in magnetic

nanoparticles for biomedical and diagnostic applications as shown Figure 10 (GUPTA; GUPTA, 2005). One class that receives great attention is superparamagnetic nanoparticles, these are constituted by a core of metal or highly magnetic metal oxide, responsible for the superparamagnetic potential. The use of an organic or inorganic polymer coating makes the nanoparticle biocompatible, stable, and can act as a support for biomolecules (ARRUEBO et al., 2007). These particles have dimensions in the order of 10^{-9} m and present different physical, chemical, and biological properties which are due to the increase in the surface area and quantum effects of the particle. The ratio between surface area and volume is an attraction for the functionalization of the surface of nanoparticles. In this way, the properties can be adjusted according to the magnetic monodomains and the coating used for the stabilization of the nanoparticles (GUPTA; WELLS, 2004)

The properties of superparamagnetic nanoparticles are strongly dependent on the size of the particles that make up the material, and when these particles are below a critical size, the properties become differentiated (ZARBIN, 2007). Given this, superparamagnetic nanoparticles become a class of materials with the potential to revolutionize current clinical diagnoses and therapeutic techniques (SUN et al., 2008). Thus, with the decrease in particle size, the domains decrease, which modifies the structure and also the width of the walls that delimit them. Thus, below a certain limit, there is a decrease in system energy due to the formation of multiple domains. That is, below the critical diameter, monodomains have a more favorable configuration to nanoparticles (GUPTA; GUPTA, 2005)

The reduction in particle size leads to a larger number of atoms that constitute the nanoparticle located on the surface which is closely related to the vicinity of the atom inside the particle so that the physical and magnetic properties will be different. However, the potential of these properties is linked to colloidal particle stability, since this stability is dependent on the characteristics of the nanoparticles (PALANISAMY; WANG, 2019). Particle performance is also related to the method used for the synthesis of magnetic nanoparticles and the coating used for colloidal stabilization of particles. Thus, the coating and synthesis method influence properties such as diameter, crystallinity, and magnetic properties.

The stabilization of the nanoparticles consists of decreasing the hydrophobic interactions between the particles, to avoid the agglomeration of particles and inhibit the formation of large agglomerates, avoiding the formation of particles with increased size. The

presence of large clusters exhibit strong magnetic dipole-dipole attractions between them and show ferromagnetic behavior (HAMLEY, 2003), this form of a cluster arouses attractive forces in the other and thus, the adhesion of remaining magnetic particles causes a mutual magnetization, resulting in increased aggregation properties (TEPPER et al., 2003).

To circumvent this situation, since particles are magnetically attracted, flocculation resulting from van der Waals' force, and surface modification is indispensable. For the effective stabilization of iron oxide nanoparticles, it is usually desirable a very high-density of the coating. The addition of a stabilizing agent, such as a surfactant or polymer, added at the time of preparation prevents aggregation of the particulate in the nanoscale (MENDENHALL et al., 1996).

Various materials can be used for the coating of magnetic nanoparticles, which include inorganic and polymeric materials (PALANISAMY; WANG, 2019). Polymeric coating materials can be classified as synthetic and natural. Polymers based on poly (ethylene glycol) (PEG), poly (vinylpyrrolidone) (PVP), poly (vinyl alcohol) (PVA), are examples of synthetic polymeric (GUO et al., 2010; SEO et al., 2018; YU et al., 2012). Natural polymer systems include the use of dextran, chitosan, among others (BADMAN et al., 2020; KHMARA et al., 2019). Some surfactants such as sodium carboxymethylcellulose, sodium oleate, among others can also be used to increase dispersibility in an aqueous medium (ROTH et al., 2016).

Among the polymers, copolymers very promising for the stabilization of magnetic nanoparticles (BASUKI et al., 2014; MOSAFER; TEYMOURI, 2018). The importance of using copolymers in the stabilization of nanoparticles is due to the possibility of modifying the amphipathic characteristic (GUINDANI et al., 2020b). Therefore, the use of copolymers allows different homopolymers to be used for the functionalizing with biomolecules. In addition, the use of polyesters is an alternative for the stabilization of magnetic nanoparticles and subsequent surface functionalization for future biomedical applications (GUINDANI et al., 2019a)

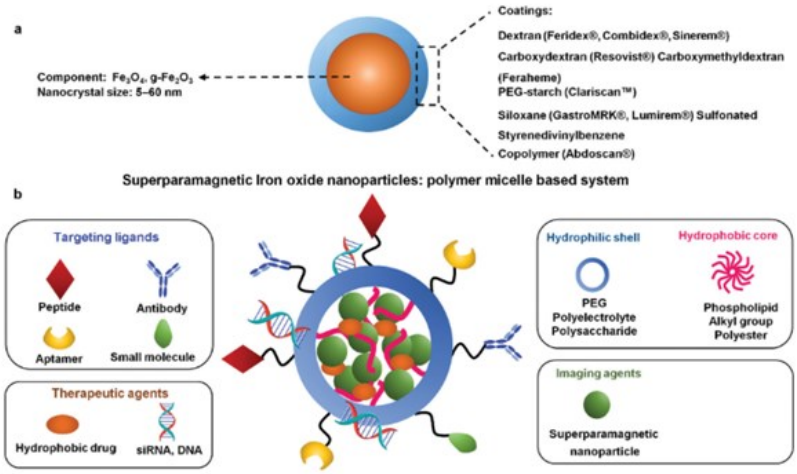

Figure 10. Schematic representation of surface engineering SPIONs for therapeutic applications: (a) SPIONs containing iron oxide as the nucleus with different coating materials and (b) surface engineered SPIONs composed of polymer micelles with a hydrophilic shell and a hydrophobic nucleus. The hydrophilic surface is conjugated with targeting antibodies, peptides, aptamers, and small molecules (PALANISAMY; WANG, 2019).

REFERENCES

ALBERTSSON, Ann Christine e SRIVASTAVA, Rajiv K. Recent developments in enzyme-catalyzed ring-opening polymerization. **Advanced Drug Delivery Reviews**, v. 60, n. 9, p. 1077–1093, 2008.

ALBERTSSON, Ann Christine e VARMA, Indra K. Recent developments in ring opening polymerization of lactones for biomedical applications. **Biomacromolecules**, v. 4, n. 6, p. 1466–1486, 2003.

ARRUEBO, Manuel et al. Magnetic nanoparticles for drug delivery. **Nano Today,** v. 2, n. 3, p. 22–32, 1 Jun 2007.

ATES, Zeliha e HEISE, Andreas. Functional films from unsaturated poly(macrolactones) by thiol-ene cross-linking and functionalisation. **Polymer Chemistry**, v. 5, n. 8, p. 2936–2941, 2014.

ATES, Zeliha e THORNTON, Paul D. e HEISE, Andreas. Side-chain functionalisation of unsaturated polyesters from ring-opening polymerisation of macrolactones by thiol-ene click chemistry. **Polymer Chemistry,** v. 2, n. 2, p. 309–312, 2011.

ATHANASIOU, K. A. et al. Orthopaedic applications for PLA-PGA biodegradable polymers. **Arthroscopy**, v. 14, n. 7, p. 726–737, 1998.

BADMAN, Ryan P. et al. Dextran-coated iron oxide nanoparticle-induced nanotoxicity in neuron cultures. **Scientific Reports**, v. 10, n. 1, p. 1–14, 2020. Disponível em: <https://doi.org/10.1038/s41598-020-67724-w>.

BARBANTI, Samuel H e ZAVAGLIA, Cecília A C e DUEK, Eliana A R. Polímeros Bioreabsorvíveis na Engenharia de Tecidos. **Polímeros**, v. 15, p. 13–21, 2005.

BASUKI, Johan S. et al. A block copolymer-stabilized co-precipitation approach to magnetic iron oxide nanoparticles for potential use as MRI contrast agents. **Polymer Chemistry**, v. 5, n. 7, p. 2611–2620, 2014.

BELTRAME, Jeovandro Maria et al. Covalently bonded n-acetylcysteine-polyester loaded in PCL scaffolds for enhanced interactions with fibroblasts. **ACS Applied Bio Materials**, 2021.

BHARDWAJ, Nandana e KUNDU, Subhas C. Electrospinning: A fascinating fiber fabrication technique. **Biotechnology Advances**, v. 28, n. 3, p. 325–347, 2010.

BOTCHWEY, Edward A. et al. Tissue engineered bone: Measurement of nutrient transport in three-dimensional matrices. **Journal of Biomedical Materials Research**, v. 67A, n. 1, p. 357–367, 2003. Disponível em: <http://doi.wiley.com/10.1002/jbm.a.10111>.

CLAUDINO, Mauro et al. Photoinduced thiol-ene crosslinking of globalide/ε-caprolactone copolymers: Curing performance and resulting thermoset properties. **Journal of Polymer Science, Part A: Polymer Chemistry**, v. 50, n. 1, p. 16–24, 2012.

COULEMBIER, Olivier et al. From controlled ring-opening polymerization to biodegradable aliphatic polyester: Especially poly(β-malic acid) derivatives. **Progress in Polymer Science** (Oxford), v. 31, n. 8, p. 723–747, 2006.

DADFAR, Seyed Mohammadali et al. Iron oxide nanoparticles: Diagnostic,
therapeutic and theranostic applications. **Advanced Drug Delivery Reviews**, v. 138, p.
302–325, 2019.

DENG, Xu-Liang et al. Poly (L-lactic acid)/ hydroxyapatite hybrid nanofibrous scaffolds prepared by electrospinning. **Journal of Biomaterials Science**, Polymer Edition, v. 18, n. 1, p. 117–130, 2007.

FENG C, Hu J, Liu C, Liu S, Liao G, Song L, et al. Association of 17-β Estradiol with Adipose-Derived Stem Cells: New Strategy to Produce Functional Myogenic Differentiated Cells with a Nano-Scaffold for

Tissue Engineering. 2016 PLoS ONE 11(10): e0164918. doi:10.1371/journal. pone.0164918

FUKUDA, Hideki e KONDO, Akihiko e NODA, Hideo. Biodiesel fuel production by transesterification of oils. **Journal of Bioscience and Bioengineering**, v. 92, n. 5, p. 405–416, 2001.

GEUS, Matthijs De. **Enzymatic Catalysis in the Synthesis of New Polymer Architectures and Materials**. [S.l: s.n.], 2007.

GUINDANI, Camila e FEUSER, Paulo Emílio et al. Bovine serum albumin conjugation on poly(methyl methacrylate) nanoparticles for targeted drug delivery applications. **Journal of Drug Delivery Science and Technology**, v. 56, n. January, p. 101490, 2020a. Disponível em: <https://doi.org/10.1016/j.jddst.2019.101490>.

GUINDANI, Camila e CANDIOTTO, Graziâni et al. Controlling the biodegradation rates of poly(globalide-co-ε-caprolactone) copolymers by post polymerization modification. **Polymer Degradation and Stability,** v. 179, 2020b.

GUINDANI, Camila e FREY, Marie Luise et al. Covalently Binding of Bovine Serum Albumin to Unsaturated Poly(Globalide-Co-ε-Caprolactone) Nanoparticles by Thiol-Ene Reactions. **Macromolecular Bioscience,** v. 19, n. 10, 2019a.

GUINDANI, Camila et al. Enzymatic ring opening copolymerization of globalide and ε-caprolactone under supercritical conditions. **Journal of Supercritical Fluids**, v. 128, n. May, p. 404–411, 2017.

GUINDANI, Camila. **ENZYMATIC RING OPENING POLYMERIZATION OF POLY(GLOBALIDE-CO-ε-CAPROLACTONE) BY MEANS OF SUPERCRITICAL TECHNOLOGY AND POST FUNCTIONALIZATION BY THIOL-ENE REACTIONS**. 2018. 163 f. UNIVERSIDADE FEDERAL DE SANTA CATARINA, 2018.

GUINDANI, Camila e DOZORETZ, Pablo et al. N-acetylcysteine side-chain functionalization of poly(globalide-co-ε-caprolactone) through thiol-ene reaction. **Materials Science and Engineering C**, v. 94, p. 477–483, 2019b.

GUO, Zhanhu et al. Effects of iron oxide nanoparticles on polyvinyl alcohol: Interfacial layer and bulk nanocomposites thin film. **Journal of Nanoparticle Research**, v. 12, n. 7, p. 2415–2426, 2010.

GUPTA, Ajay Kumar e GUPTA, Mona. Synthesis and surface engineering of iron oxide nanoparticles for biomedical applications. **Biomaterials**, v. 26, n. 18, p. 3995–4021, 2005.

GUPTA, Ajay Kumar e WELLS, Stephen. Surface-Modified Superparamagnetic Nanoparticles for Drug Delivery: Preparation,

Characterization, and Cytotoxicity Studies. **IEEE Transactions on Nanobioscience**, v. 3, n. 1, p. 66–73, 2004.

HABEYCH, David I. et al. Biocatalytic synthesis of polyesters from sugar-based building blocks using immobilized Candida antarctica lipase B. **Journal of Molecular Catalysis B: Enzymatic**, v. 71, n. 1–2, p. 1–9, 2011. Disponível em: <http://dx.doi.org/10.1016/j.molcatb.2011.02.015>.

HAMLEY, I. W. Nanotechnologie mit weichen Materialien. **Angewandte Chemie**, v. 115, n. 15, p. 1730–1752, 2003.

HENDERSON, Lori A. et al. Enzyme-catalyzed polymerizations of ε-caprolactone: Effects of initiator on product structure, propagation kinetics, and mechanism. **Macromolecules,** v. 29, n. 24, p. 7759–7766, 1996.

HOKUGO, Akishige e TAKAMOTO, Tomoaki e TABATA, Yasuhiko. Preparation of hybrid scaffold from fibrin and biodegradable polymer fiber. **Biomaterials**, v. 27, n. 1, p. 61–67, 2006.

HOYLE, Charles E. e BOWMAN, Christopher N. Thiol-ene click chemistry. **Angewandte Chemie - International Edition**, v. 49, n. 9, p. 1540–1573, 2010.

HOYLE, Charles E e LEE, T A I Yeon e ROPER, Todd. **Thiol – Enes : Chemistry of the Past with Promise for the Future**. v. 42, p. 5301–5338, 2004.

JEONG, Sung In et al. Morphology of elastic poly(L-lactide-co-epsilon-caprolactone) copolymers and in vitro and in vivo degradation behavior of their scaffolds. **Biomacromolecules,** v. 5, n. 4, p. 1303–9, 2004. Disponível em: <http://www.ncbi.nlm.nih.gov/pubmed/15244444>.

JOHNSON, Peter M. e KUNDU, Santanu e BEERS, Kathryn L. Modeling enzymatic kinetic pathways for ring-opening lactone polymerization. **Biomacromolecules**, v. 12, n. 9, p. 3337–3343, 2011.

KAIGLER, Darnell e MOONEY, David e PH, D. Tissue Engineering ' s Impact on Dentistry. **Journal of Dental Education**, v. 65, n. 5, p. 456–462, 2001.

KHMARA, Iryna et al. Chitosan-stabilized iron oxide nanoparticles for magnetic resonance imaging. **Journal of Magnetism and Magnetic Materials**, v. 474, n. November 2018, p. 319–325, 2019. Disponível em: <https://doi.org/10.1016/j.jmmm.2018.11.026>.

KOBAYASHI, Shiro e MAKINO, Akira. Enzymatic polymer synthesis: an opportunity for green polymer chemistry. **Chemical Reviews,** v. 109, n. 11, p. 5288–5353, 2009.

KOLB, Hartmuth C. e FINN, M. G. e SHARPLESS, K. Barry. Click Chemistry: Diverse Chemical Function from a Few Good Reactions. **Angewandte Chemie - International Edition,** v. 40, n. 11, p. 2004–2021, 2001.

LEIRO, Victoria et al. Conjugation Chemistry Principles and Surface Functionalization of Nanomaterials. [S.l.]: **Elsevier Inc.**, 2018. Disponível em: <https://doi.org/10.1016/B978-0-323-50878-0.00002-1>.

LENZ, Robert W. **Biodegradable Polymers**. v. 107, 1993.

LEONG, B P Chan Æ K W. **Scaffolding in tissue engineering : general approaches and tissue-specific considerations**. v. 17, 2008.

LI, Dawei et al. Three-dimensional polycaprolactone scaffold via needleless electrospinning promotes cell proliferation and infiltration. **Colloids and Surfaces B: Biointerfaces**, v. 121, p. 432–443, 2014.

LOWE, Andrew B. **Thiol-ene ‘“ click ”’ reactions and recent applications in polymer and materials synthesis**. p. 17–36, 2010.

MAIA, A L M F et al **Morphological and chemical evaluation of bone with apatite-coated Al 2 O 3 implants as scaffolds for bone repair**. v. 59, p. 533–538, 2013.

MARQUES, A. P. e REIS, R. L. e HUNT, J. A. The biocompatibility of novel starch-based polymers and composites: In vitro studies. **Biomaterials**, v. 23, n. 6, p. 1471–1478, 2002.

MEI, Ying e KUMAR, Ajay e GROSS, Richard A. Probing water-temperature relationships for Lipase-catalyzed lactone ring-opening polymerizations. **Macromolecule**s, v. 35, n. 14, p. 5444–5448, 2002.

MENDENHALL, George David e GENG, Yunpeng e HWANG, James. Optimization of long-term stability of magnetic fluids from magnetite and synthetic polyelectrolytes. **Journal of Colloid and Interface Science**, v. 184, n. 2, p. 519–526, 1996.

MILETIĆ, Nemanja e LOOS, Katja e GROSS, Richard A. **Enzymatic Polymerization of Polyester**. [S.l: s.n.], 2010.

MONTALBETTI, Christian A.G.N. e FALQUE, Virginie. Amide bond formation and peptide coupling. **Tetrahedron**, v. 61, n. 46, p. 10827–10852, 2005.

MOSAFER, Jafar e TEYMOURI, Manouchehr. Comparative study of superparamagnetic iron oxide/doxorubicin co-loaded poly (lactic-co-glycolic acid) nanospheres prepared by different emulsion solvent evaporation methods. **Artificial Cells, Nanomedicine and Biotechnology**, v. 46, n. 6, p. 1146–1155, 2018. Disponível em: <https://doi.org/10.1080/21691401.2017.1362415>.

PACHENCE, James M. e BOHRER, Michael P. e KOHN, Joachim.

Biodegradable polymers. Third Edit ed. [S.l.]: **Elsevier Inc**., 2007. Disponível em: <http://dx.doi.org/10.1016/B978-0-12-370615-7.50027-5>.

PALANISAMY, Sathyadevi e WANG, Yun Ming. Superparamagnetic iron oxide nanoparticulate system: Synthesis, targeting, drug delivery and therapy in cancer. **Dalton Transactions**, v. 48, n. 26, p. 9490–9515, 2019.

PATEL, Minal e FISHER, John P. Biomaterial scaffolds in pediatric tissue engineering. **Pediatric Research**, v. 63, n. 5, p. 497–501, 2008.

QU, Jing et al. Surface design and preparation of multi-functional magnetic nanoparticles for cancer cell targeting, therapy, and imaging. **RSC Advances**, v. 8, n. 62, p. 35437–35447, 2018.

ROTH, Hans Christian et al. Oleate coating of iron oxide nanoparticles in aqueous systems: the role of temperature and surfactant concentration. Journal of **Nanoparticle Research**, v. 18, n. 4, 2016.

SEO, Kyungah et al. Polyvinylpyrrolidone (PVP) effects on iron oxide nanoparticle formation. **Materials Letters**, v. 215, p. 203–206, 2018. Disponível em: <https://doi.org/10.1016/j.matlet.2017.12.107>.

SHEN, Song et al. CMCTS stabilized Fe3O4 particles with extremely low toxicity as
highly efficient near-infrared photothermal agents for in vivo tumor ablation. **Nanoscale**, v. 5, n. 17, p. 8056–8066, 2013.

SUN, Conroy; LEE, Jerry SH; ZHANG, Miqin. Magnetic nanoparticles in MR imaging and drug delivery. **Advanced drug delivery reviews**, v. 60, n. 11, p. 1252-1265, 2008.

TAI, Y.; Banerjee, A.; Goodrich, R.; Jin, L.; Nam, J. Development and Utilization of Multifunctional Polymeric Scaffolds for the Regulation of Physical Cellular Microenvironments. **Polymers** 2021, 13, 3880. https://doi.org/10.3390/polym13223880

TANG, Xiaoyan et al. **Polymeric Biomaterials in Tissue Engineering and Regenerative Medicine**. p. 351–371, 2014.

TAYLOR, G. Electrically Driven Jets. **Proceedings of the Royal Society A: Mathematical, Physical and Engineering Sciences**, v. 313, n. 1515, p. 453–475, 1969. Disponível em: <http://rspa.royalsocietypublishing.org/cgi/doi/10.1098/rspa.1969.0205>.

TEPPER, T. et al. Magneto-optical properties of iron oxide films. **Journal of Applied Physics**, v. 93, n. 10 2, p. 6948–6950, 2003.

TREUEL, Lennart et al. Impact of protein modification on the protein corona on nanoparticles and nanoparticle-cell interactions. **ACS Nano**, v.

8, n. 1, p. 503–513, 2014.
TUNCA, Umit. Orthogonal multiple click reactions in synthetic polymer chemistry. **Journal of Polymer Science, Part A: Polymer Chemistry**, v. 52, n. 22, p. 3147–3165, 2014.
URBANEK, Aneta K. et al. Biochemical properties and biotechnological applications of microbial enzymes involved in the degradation of polyester-type plastics. **Biochimica et Biophysica Acta - Proteins and Proteomics**, v. 1868, n. 2, p. 140315, 2020. Disponível em: <https://doi.org/10.1016/j.bbapap.2019.140315>.
VAN DER MEULEN, Inge et al. Polymers from functional macrolactones as potential biomaterials: Enzymatic ring opening polymerization, biodegradation, and biocompatibility. **Biomacromolecules**, v. 9, n. 12, p. 3404–3410, 2008.
VERT, M. et al. Bioresorbability and biocompatibility of aliphatic polyesters. **Journal of Materials Science: Materials in Medicine**, v. 3, n. 6, p. 432–446, 1992.
VERT, Michel. Degradable and bioresorbable polymers in surgery and in pharmacology: Beliefs and facts. **Journal of Materials Science: Materials in Medicine**, v. 20, n. 2, p. 437–446, 2009.
WILLIAMS, David F. On the mechanisms of biocompatibility. **Biomaterials**, v. 29, n. 20, p. 2941–2953, 2008.
YAO, Xikuang et al. Stimuli-responsive cyclodextrin-based nanoplatforms for cancer treatment and theranostics. **Materials Horizons**, v. 6, n. 5, p. 846–870, 2019.
YU, Miao et al. Dextran and polymer polyethylene glycol (PEG) coating reduce both 5 and 30 nm iron oxide nanoparticle cytotoxicity in 2D and 3D cell culture. **International Journal of Molecular Sciences**, v. 13, n. 5, p. 5554–5570, 2012.
ZARBIN, Aldo J G. QUÍMICA DE (NANO)MATERIAIS Aldo J. G . Zarbin. **Química Nova,** v. 30, n. 6, p. 1469–1479, 2007. Disponível em: <http://quimicanova.sbq.org.br/imagebank/pdf/Vol30No6_1469_15-S07432.pdf>.
ZHANG, Jianxu et al. Recent developments in lipase-catalyzed synthesis of polymeric materials. **Process Biochemistry**, v. 49, n. 5, p. 797–806, 2014.

CHAPTER 3

COVALENTLY BONDED N-ACETYLCYSTEINE-POLYESTER LOADED IN PCL SCAFFOLDS FOR ENHANCED INTERACTIONS WITH FIBROBLASTS

The incorporation of N-acetylcysteine (NAC) in poly(globalide-ε-caprolactone) (PGlCL) to obtain a scaffold from the blend with polycaprolactone (PCL) was studied. The obtaining and characterization of scaffolds through the electrospinning technique were evaluated, followed by the chemical and biological characterization of the material obtained. It was evaluated that the incorporation of NAC allows an improvement in the hydrophilicity and crystallinity of the material. Subsequently, the biocompatibility of the material obtained with short and long-term tests was evaluated. Demonstrating that the incorporation of NAC allows a better adaptation of fibroblasts with the material modified with NAC.

The results presented in this chapter were published in the journal ACS Applied Bio Materials (doi.org/10.1021/acsabm.0c01404).

Graphical Abstract

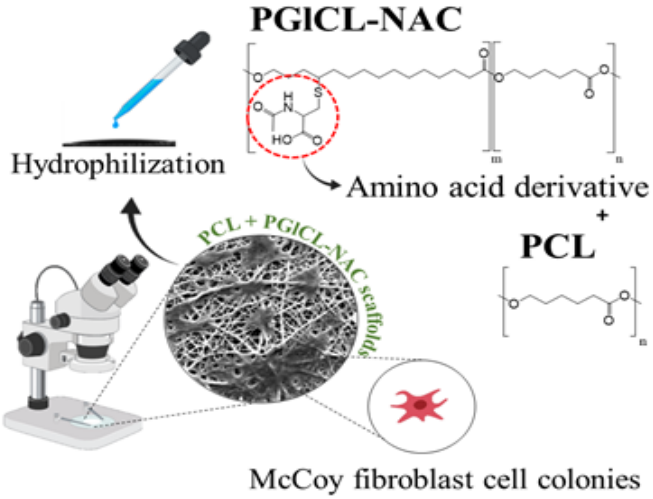

Figure 11: Production of the Scaffold by electrospinning hydrophilic with PGlCLNAC

3.1 ABSTRACT

Poly(ε-caprolactone) (PCL) is commonly used in devices for tissue reconstruction due to its biocompatibility and suitable mechanical properties. However, its high crystallinity and hydrophobicity do not favor cell adhesion and difficult polymer bioresorption. To improve these characteristics, the development of engineered scaffolds for tissue regeneration, based on poly(globalide-co-ε-caprolactone) (PGlCL) covalently bonded with N-acetylcysteine (PGlCL-NAC) was proposed. The scaffolds were obtained from polymer blends of PCL and PGlCL-NAC, using the electrospinning technique. The use of PGlCL-NAC allowed the modification of the physical and chemical properties of PCL electrospun scaffolds, including an expressive reduction in the fiber's diameter, hydrophobicity, and crystallinity. All electrospun scaffolds showed no cytotoxicity against fibroblasts (McCoy cells). *In vitro* biocompatibility assays showed that all tested scaffolds provided high cell viability and proliferation in short-term (NRU, MTT, and nuclear morphology assays) and long-term (clonogenic assay) assays. Nevertheless, PGlCL-NAC based scaffolds have favored the survival and proliferation of the cells in comparison to PCL scaffolds. Cell adhesion on the scaffolds assessed by electronic microscopy images confirmed this behavior. These results suggest that the incorporation of PGlCL-NAC in scaffolds for tissue regeneration could be a promising strategy to improve cell-surface interactions and contribute to the development of more efficient engineered biomedical devices.

3.2 MATERIALS AND METHODS

3.2.1 MATERIALS

Dichloromethane P.A. 99.8% (DCM), chloroform P.A. 99.8%, tetrahydrofuran P.A. 99,9% (THF), ethanol P.A. 99.8% (EtOH), glacial acetic acid P.A. 99.8%, and the radical initiator azobisisobutyronitrile 98% (AIBN) were purchased from Vetec Química (Brazil). Carbon dioxide (99.9% purity) was used as a solvent and it was purchased from White Martins A/S, Brazil. N-acetylcysteine 99.8% (NAC) was purchased from Gemini (Brazil). Novozym 435 (commercial lipase B from *Candida antarctica* immobilized on cross-linked polyacrylate beads) was kindly donated by Novozymes, Brazil, A/S. Globalide (Gl) was a kind gift from Symrise. Polycaprolactone (PCL) (molecular weight 80,000 g/mol) and the monomer ε-caprolactone were purchased from

Sigma-Aldrich. Both globalide and ε-caprolactone (CL) were dried under vacuum for 24 hours and kept in a desiccator over silica and 4 Å molecular sieves. RPMI 1640 medium supplemented with fetal bovine serum (10%), penicillin (100 $U \cdot mL^{-1}$) and streptomycin (100 $\mu g \cdot mL^{-1}$) was purchased from Thermo Fischer Scientific - GIBCO. 3-(4,5-Dimethylthiazol-2-yl)-2,5-diphenyltetrazolium bromide (MTT), red uptake (NRU) and 4',6-diamidino-2-phenylindole, dihydrochloride (DAPI) and phosphate-buffered solution (PBS) (0.1M, pH 7.4) were purchased from Sigma-Aldrich. Water was purified by a Milli-Q water purification system. All biological assays used normal McCoy cell line (murine fibroblast) purchased from Adolfo Lutz Institute (São Paulo, Brazil).

3.2.2 POLY(GLOBALIDE-*co*-E-CAPROLACTONE) SYNTHESIS USING SUPERCRITICAL CARBON DIOXIDE

The synthesis of PGlCL(GUINDANI et al., 2017) was carried out by enzymatic ring-opening polymerization (e-ROP) using the monomers globalide (Gl) and ε-caprolactone (CL) in a mass ratio of 50/50 (Gl/CL). Supercritical carbon dioxide ($scCO_2$) was used as a solvent, and the system was kept at a constant pressure of 120 bar and temperature of 65 °C, for 2 hours. The enzyme content was fixed as 5% relative to the amount of the total monomer, and the CO_2:monomers mass ratio was fixed at 1:2. After polymerization, the material was purified through solubilization in dichloromethane (DCM), followed by the separation of the enzymes and precipitation of the polymer in cold EtOH. DCM and EtOH were used at the volumetric proportion of 1:6. The polymer was then filtered and dried at room temperature, invacum (or under reduced pressure), until constant weight.

3.2.3 MODIFICATION OF PGLCL WITH N-ACETYLCYSTEINE (NAC)

The modification of PGlCL copolymers was performed directly on its double bonds, through thiol-ene reactions, according to the studies performed by Guindani et al.(GUINDANI et al., 2019). NAC was chosen as a functionalizing molecule because it contains a thiol group and because its presence as a pendant group on PGlCL chains confers a desirable hydrophilic characteristic to the final covalently modified

PGlCL-NAC. The copolymer PG1CL and NAC were placed in a vial together with the free radical initiator AIBN, using a mixture of chloroform and acetic acid (3:1 - v:v) as a solvent, under a nitrogen atmosphere. The reaction was performed in an oil bath at 80 °C for 24 h, under continuous magnetic stirring. The amount of NAC used was established as being twice the minimum amount required to functionalize all double bonds. AIBN content was set at 5% (mol/mol) relative to the amount of NAC.

3.2.4 ELECTROSPINNING OF THE MODIFIED POLYESTERS BLENDS

After a series of solubilization tests using different solvents and different concentrations, the electrospun scaffolds were produced using PCL (18% w/v), PCL+PGlCL (18% w/v, PCL:PGlCL= 6:12 w/w) and PCL+PGlCL-NAC (18% w/v, PCL:PGlCL-NAC= 6:12 w/w) dissolved in a solvent mixture of chloroform: DMF (9:1 v/v) (As described in previous works) (BELTRAME, 2018; ZHANG et al., 2020). The solutions were kept under continuous stirring for 24 h at 25 ± 2 °C before electrospinning. Pure PCL and PCL blends with PGlCL and PGlCL-NAC were completely solubilized, yielding solutions and with homogeneous character. For PCL blends, PGlCL covalently bonded to NAC acts as a compatibilizing agent between NAC and PCL. Subsequently, these polymer solutions were transferred to a 5 mL syringe with a 0.723 mm internal diameter needle. In a typical electrospinning experiment, 2 mL of polymeric solution were electrospun at a flow rate of 700 μL h^{-1}, with the help of an infusion pump (New Era Pump Systems NE-300) (Laboratório de Sistemas Porosos - LASIPO/UFSC). The temperature was maintained at 23.0 ± 0.5 °C and the relative humidity was 55 ± 5%. A high voltage source was used, and the potential was set as 18 ± 1 kV. The distance between the needle tip and the grounded collector (aluminum sheet, 6.0 × 6.0 cm^2) was set as 18 cm. The electrospun scaffolds were stored in a humidity-free environment for further testing.

3.2.5 PHYSICO-CHEMICAL CHARACTERIZATION OF THE SCAFFOLDS

The morphology of the electrospun scaffolds was assessed by scanning electron microscopy (SEM) (JEOL JSM-6390LV) at a voltage of 10 kV. A scaffold fragment (0.2 x 0.2 mm^2) was deposited on a stub and covered with a thin layer of gold by sputtering (EM SCD 500

LEICA). For the determination of fiber diameter, 100 measurements were taken based on images obtained. The distribution frequency and mean diameter were determined using the software image J.

To identify the chemical structure of functionalized polymer scaffolds Fourier transform infrared (FTIR-ATR) analysis was performed in a Cary 600 model (Model: Agilent Technologies CARY 600) spectrometer with a ZnSe window Transmission infrared spectra were recorded in a wavenumber range of 650-4000 cm^{-1}.

Melting temperatures and crystallinity of the polymeric materials were determined by differential scanning calorimetry (Jade DSC, Perkin-Elmer) analysis of samples of approximately 5 mg of the dried polymer under nitrogen atmosphere (20 mL min^{-1}), with temperatures ranging from 0 to 150 °C at a heating rate of 10 °C min^{-1}. The thermal history was removed before the analyses (for pure polymer samples) at a heating rate of 20 °C min^{-1} and a cooling rate of 10 °C min^{-1}. For the scaffolds, the first heating runs were used to obtain the thermal properties.

The wettability of the electrospun scaffolds was verified through contact angle measurements. The scaffolds were fixed on glass slides and the contact angle between the polymer films and the water droplets was measured on a goniometer (Ramé-Hart Instrument 250). All measurements were performed in triplicate at room temperature with a constant droplet volume (10 μL).

3.2.6 *IN-VITRO* BIOCOMPATIBILITY ASSAYS

McCoy cells were cultivated in RPMI 1640 medium (GIBCO, Baltimore, USA) supplemented with fetal bovine serum (10%) and penicillin (100 U mL^{-1}) (GIBCO, Baltimore, USA) and streptomycin (100 μg mL^{-1}) (GIBCO, Baltimore, USA). All cells were maintained under controlled conditions (atmosphere containing 5% CO_2; with 95% humidity and at 37 °C) over the period studied. Results are expressed as an average of three independent experiments.

Before the beginning of each biological assay, the polymer scaffolds were sterilized (alcohol 70%; 10 min; repeated at least 3 times) under UV light (365 nm; 10 min). Moreover, only standardized scaffolds with the same dimensions (10 x 10 mm) and thickness (up to 0.2 mm) were used.

The biological tests were carried out in partnership with the clinical analysis department of the Federal University of Parana with professor Karina Bettega Felipe.

3.2.6.1 NRU assay

McCoy cells (1×10^5 cells/well/scaffold) were seeded in the surface of each sterile scaffold placed inside 24-well it was a plate containing a supplemented medium as described before. Then, cells were kept under the same controlled conditions for 24 and 72 h. As a negative control group, wells containing McCoy cells and supplemented medium were analyzed without the presence of a scaffold sample. Control absorbance was considered equivalent to 100% cell viability. At the end of each incubation period, the culture medium was removed. Each scaffold was washed with phosphate-buffered saline pH 7.4 solution, repeating this procedure three times to remove unbound and dead cells. Then, the scaffold received 500 µL of Neutral Red Uptake (NRU) solution (0.1 mg mL^{-1}) for 2 h at 37 °C. Each scaffold was washed three times with phosphate-buffered saline pH 7.4 solution. Were added 500 µL of NaH_2PO_4 0.05M solution with 50% ethanol were added in each scaffold. Finally, the supernatant was transferred from each well (100 µL) to a new well, inside a 96-well plate. The absorbance was measured at 540 nm using a microplate reader (Multiskan FC, Thermo-Scientific, Massachusetts, USA).

3.2.6.2 MTT assay

McCoy cells were seeded and incubated as described in the NRU assay. Then, each well-received 500 µL of 3-(4,5-dimethylthiazol-2-yl)-2,5-diphenyltetrazolium bromide (MTT) solution (0.5 mg mL^{-1}) and kept all plates were incubated for 2 h, at 37 °C. Each scaffold was washed three times with phosphate-buffered saline pH 7.4 solution. Were added 500 µL of DMSO were added to each scaffold. As a negative control group, wells containing McCoy cells and supplemented medium were analyzed without the presence of a scaffold sample. Control absorbance was considered equivalent to 100% cell viability. Finally, the supernatant medium was transferred from each well (100 µL) to a new well, inside a 96-well plate. The absorbance was measured at 570 nm using a microplate reader (Multiskan FC, Thermo-Scientific, Massachusetts, USA).

3.2.6.3 Nuclear morphology assay (NMA)

McCoy cells line at a density of 1 x 10^5 cells mL^{-1} were seeded on the surface of the membrane on a glass slide containing polymer scaffolds soaked with culture medium. After 24 and 72 h of incubation, cells were fixed (5% w/v formaldehyde), colored with DAPI (300 µM Thermo Fisher), and photographed (Leica DM5500 B). Photographic records were used to verify changes in nuclear morphology under physiological conditions and to verify the distribution of cells in the scaffolds, with the help of the software ImageJ. Changes in nuclear morphology can happen for example during cell division processes, and processes associated with cell death. Nuclear condensation and fragmentation can be indicative of apoptosis, while an increase in nucleus size can be seen as indicative of senescence (FILIPPI-CHIELA et al., 2012).

3.2.6.4 Clonogenic assay

Around 234 McCoy cells were seeded over each type of electrospun scaffold, all with the same size (2.5 cm x 4.0 cm), deposited on standard glass slides, and stored in Petri dishes. The scaffolds with cells inside Petri dishes were incubated under controlled conditions for 10 days. The formed cell colonies were fixed overlaying them with sufficient 100% cold methanol for 10 min and then stained with crystal violet (0.04% w/v) for 10 min. After rinsing thoroughly with PBS, all scaffolds were photographed. The number and the area of colonies were determined with the help of the software ImageJ (FRANKEN et al., 2006).

3.2.6.5 Cell adhesion

McCoy cells (2.0×10^4 cells) were seeded inside 24-well plates. After 72 hours of culture, the morphologies of the cells growing over the polymer scaffolds were determined (LI et al., 2014). Briefly, at the end of each time, all cultured cells were fixed by 4% formaldehyde for 20 min at 4 ºC, dehydrated with gradient ethanol, and dried overnight under mechanical airflow kept at room temperature. Then, a piece of each scaffold sample (0.2 x 0.2 mm^2) was deposited on a stub, covered with a thin layer of gold by sputtering, and visualized by SEM (JEOL JSM-6390LV).

3.2.7 STATISTICAL ANALYSIS

The statistical analysis was expressed as a function of the mean and standard deviation. The statistical significance of the differences between the means was determined using ANOVA. Values of *p <0.05, **p <0.01 and ***p <0.001 were considered significant. The GraphPad Prism 6 software was used for statistical analysis.

3.3 RESULTS AND DISCUSSION

3.3.1 POLYMER AND SCAFFOLD PHYSICO-CHEMICAL CHARACTERIZATION

3.3.1.1 **Characterization of the chemical structure of the polymers**

The chemical structures of pure NAC and the electrospun scaffolds (PCL, PCL+PGlCL, and PCL+PGlCL-NAC) were investigated by ATR-FTIR. Figure 12A presents the proposed chemical structures of the polymers, while Figure 12B presents the FTIR spectra obtained for each sample. In the spectrum of NAC, a low-intensity band at 2547 cm^{-1} was observed, being relative to the S-H bond stretch. Two other bands were observed at 1650 and 1541 cm^{-1}, and can be assigned to the stretching of amide I (C=O stretching vibration) and amide II (N-H bending vibration and C-N stretching vibration). A moderate absorption band at 1717 cm^{-1} relative to the C=O stretch was also observed.

Regarding the spectrum of the PCL scaffolds, it was possible to observe a 1720 cm^{-1} band characteristic of the C=O stretch of the ester group, and a second band at 1298 cm^{-1} relative to C-O stretching (also from the ester group) (COLEMAN; ZARIAN, 1979). For the spectrum of PCL+PGlCL scaffolds, the bands obtained are equivalent, none spectrum change was observed. PCL and PGlCL are both polyesters, and what differs them from each other is the number of carbons in their backbones, and the presence of unsaturations on PGlCL, derived from globalide units. However, the concentration of unsaturations in PCL+PGlCL scaffolds is too low and its presence could not be detected by FTIR. Therefore, it is expected that PCL and PGlCL present very similar spectra.

For the PCL+PGlCL-NAC scaffold, the changes were more significant. The absence of the band at 2547 cm^{-1} referring to the S-H group evidences its consumption during the reaction since functionalization happens through thiol-ene reactions. Also, the appearance of two absorption bands at 1643 and 1541 cm^{-1} for the amide I and amide II bands(ATES; HEISE,

2014; PICQUART et al., 1998) indicated a successful functionalization with NAC. In previous studies, Guindani et al (GUINDANI et al., 2019) have analyzed the PGlCL and PGlCL-NAC samples by ^{1}H NMR, and the consumption of the double bonds was observed (53% double bonds consumption).

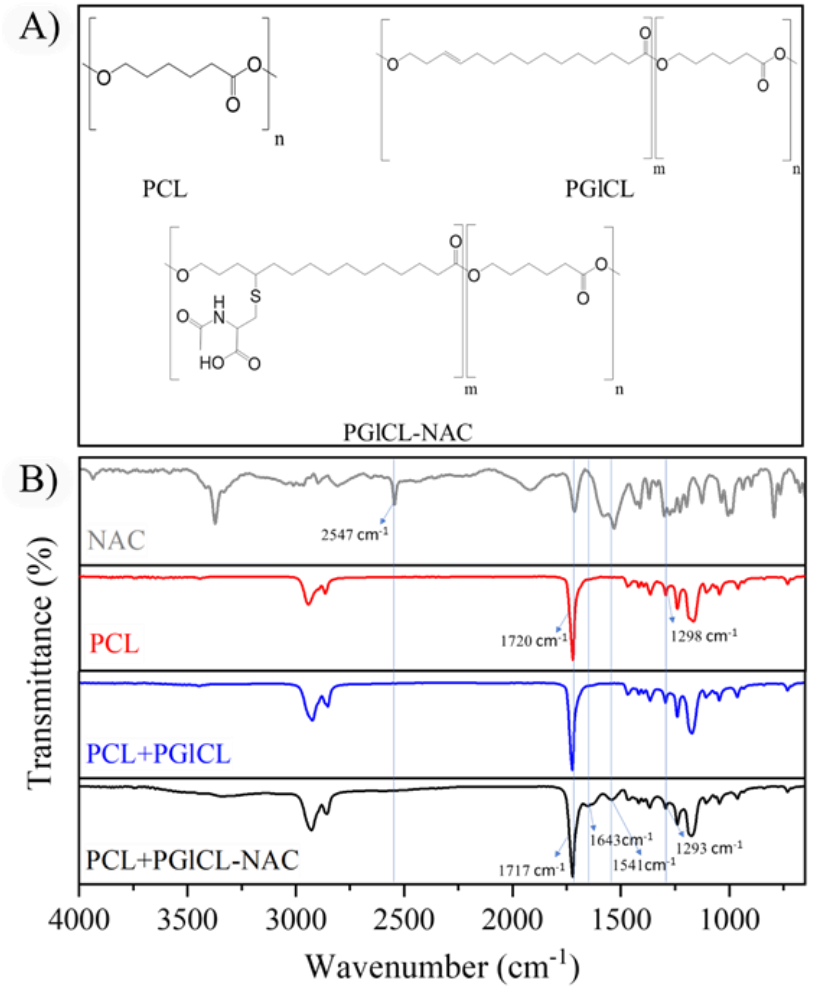

Figure 12. (A) Molecular structures of polymers and (B) FTIR spectra of pure NAC and the scaffolds of PCL, PCL+PGlCL, and PCL+PGlCL-NAC.

3.3.1.2 Thermal properties

Differential scanning calorimetry (DSC) analysis was performed to determine the thermal properties of the polymers and electrospun scaffolds. The thermograms are shown in Figure 13, and the thermal data are presented in Table 1. The thermal properties of the polymers were obtained from the second heating run, after the removal of the thermal history. For the electrospun scaffolds, the data were obtained from the first heating run, to evaluate the phase morphology of the scaffolds after the electrospinning process.

Analyzing the thermograms corresponding to the polymers, for PCL, it was observed a characteristic melting peak at 57 °C. Guindani and collaborators have previously determined the thermal properties for PGlCL (GUINDANI et al., 2017), finding the characteristic melting peak at 39 °C, and PGlCL-NAC (GUINDANI et al., 2019), which did not present any melting peak, which is a typical of amorphous materials.

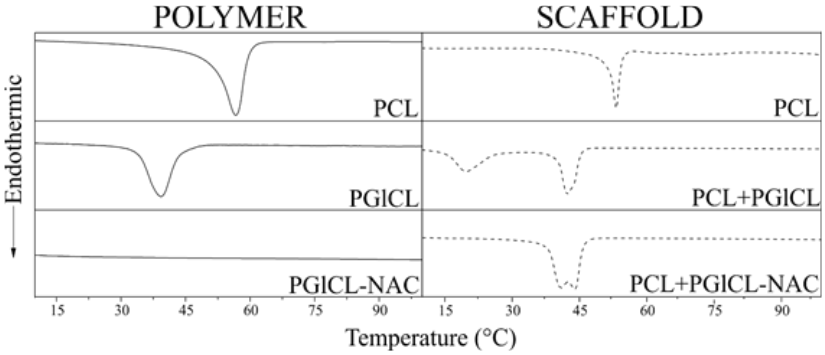

Figure 13. Thermograms of the polymer and electrospun scaffolds.

PCL electrospun scaffolds presented a melting peak at 55 °C. For the electrospun blends, PCL+PGlCL scaffolds presented two melting peaks: the first, at 19 °C, probably rich in PGlCL chains, and another peak at 47 °C, probably rich in PCL chains. PCL+PG1CL-NAC scaffolds presented only one peak, observed at 46 °C, which should be related to the presence of crystalline domains formed by PCL chains, since PG1CL-NAC is an amorphous material, and did not present any melting peak. In comparison to the pure polymers, the electrospun blends presented a decrease in their melting temperatures, which is indicative of less stable crystalline domains (CANEVAROLO JR., 2006).

Table 1. Thermal properties of the polymers and electrospun scaffolds.

	Material	T_m 1 (°C)	T_m 2 (°C)	ΔH_m 1 (J/g)	ΔH_m 2 (J/g)	X_c 1 (%)	X_c 2 (%)	X_{cT} (%)
Polymer	PCL	-	57	-	96	-	70	70
	PGlCL[19]	39	-	92	-	68	-	68
	PGlCL-NAC [17]	-	-	-	-	-	-	-
Electrospun scaffold	PCL	-	55	-	60	-	44	44
	PCL+PGlCL	19	47	7.6	56	5	41	46
	PCL+PGlCL-NAC	-	46	-	40	-	29	29

T_m 1: The first peak melting temperature; T_m 2: Second peak melting temperature; ΔH_m1: First peak heat of fusion; ΔH_m 2: Second peak heat of fusion; X_c: Degree of crystallinity, calculated from the heat of fusion of a PCL 100% crystalline sample (CRESCENZI et al., 1972).

Comparing the thermal data of pure PCL and PCL scaffolds, it was possible to observe a reduction in the crystallinity degree from approximately 70% to 44% after the electrospinning process. Similar behavior was observed for PCL+PGlCL blends. According to Table 1, the polymer samples of PGlCL and PCL have a crystallinity of 68% and 70%, respectively. After the electrospinning process, the overall degree of crystallinity obtained for the PCL+PGlCL scaffold was reduced to 46%, similarly to what occurred to PCL scaffolds. Finally, after the introduction of NAC modified polymers in the blends, to form PCL+PGlCL-NAC scaffolds, the degree of crystallinity decreased from 44 to 46% (PCL and PCL+PGlCL scaffolds) to only 29%. These decreases in the degree of crystallinity were directly related to the reduction in the number of crystalline domains in the material, due to fast evaporation rates of the solvent during electrospinning.

The decrease of the melting temperature is indicative that the energy level necessary to overcome the secondary intermolecular forces between the chains of the crystalline phase is lower, and it becomes easier to destroy the regular structure of packaging (CANEVAROLO JR., 2006). The overall heat of fusion (and consequently the degree of crystallinity) is related to the number of crystalline domains. The formation of these crystalline domains in the polymer scaffolds can be influenced by different factors, such as their chemical composition and also the electrospinning process. Even when using similar polymeric materials in the blend composition (PCL and PGlCL), the intermolecular electrostatic interactions between the species interfere in the formation and stability of the crystalline structure, causing changes in T_m, ΔH_m, and X_c (COLEMAN; ZARIAN, 1979). Regarding process conditions, the fast evaporation of the solvent during the electrospinning can also influence the kinetics of the crystalline arrangement, leading to the formation of less stable domains in the scaffolds (CRESCENZI et al., 1972). The reduction in the amount and stability of the crystalline domains of the scaffolds are crucial for the improvement of water uptake, implying faster bioresorption/biodegradation rates of the material in biological media (GUINDANI et al., 2020).

3.3.1.3 Fiber morphology and wettability

The morphology and the fiber diameter of the electrospun scaffolds (PCL, PCL+PGlCL, and PCL+PGlCL-NAC) were described in Figure 14. SEM images show that all obtained scaffolds presented uniform cylindrical shapes, without the presence of beads. Besides, it was not

observed any phase separation or surface defects for PCL+PGlCL-NAC fibers. This means that covalently binding NAC to PGlCL was a successful strategy of compatibilization of NAC with PCL that could be applied to a wide range of other functionalizing polar molecules. The fiber average diameter depended on the scaffold composition (PIRES et al., 2019). The average fiber diameter was 733 ± 256 nm for PCL scaffolds, 114 ± 29 nm for PGlCL scaffolds, and 132 ± 43 nm for PCL+PGlCL-NAC. The reduction in the concentration of PCL produced significant changes in fiber diameter and morphology. PCL has a much higher molecular weight (Mn = 80,000 Da) than PGlCL (Mn= 16,000 Da (SEYEDNEJAD et al., 2011) and PGlCL-NAC. This means that the partial substitution of PCL by PGlCL or PGlCL-NAC caused a decrease in the viscosity of the solution, which allowed the production of fibers with reduced diameters (CANEVAROLO JR., 2006; ZHANG et al., 2020).

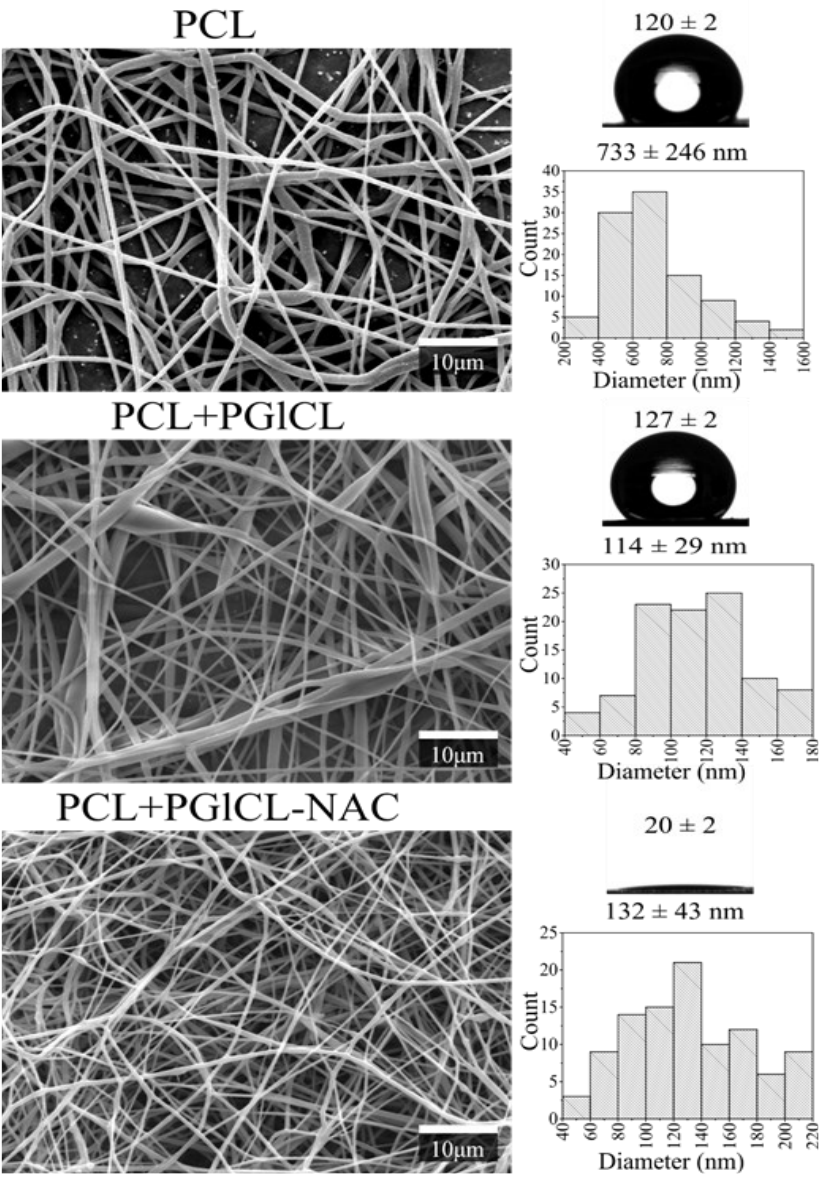

Figure 14. SEM images, fiber diameter distribution, and contact angle with water of the electrospun scaffolds.

PCL+PGlCL-NAC and PCL+PGlCL presented a narrow fiber size distribution when compared to the PCL. The size range of PCL+PGlCL

and PCL+PGlCL-NAC fibers were between 40 - 220 nm, whereas PCL the fiber sizes ranged from 200 to 1600 nm as observed in Figure 14.

The contact angle between the scaffolds surface and water was measured in a goniometer. The values and images are presented in Figure 14. PCL and PCL+PGLCL electrospun scaffolds presented contact angle values of respectively 120° ± 2 and 127° ± 2, being considered very hydrophobic materials (ZHENG et al., 2005). The use of PGlCL-NAC in a blend with PCL provided a meaningful reduction in the contact angle values to 20° ± 2. The presence of NAC hydrophilic groups, such as -(C=O)NH- and -COOH on the scaffold surface provided enhanced interaction between the scaffold and water through hydrogen bonds, causing the reduction of hydrophilicity, in comparison to PCL and PCL+PGlCL may scaffold (GUINDANI et al., 2017). These results are in accordance with those obtained by Guindani et al., 2019) for PGlCL and PGlCL-NAC films. The modification of PGlCL with NAC was reported to cause a decrease in the partition coefficient logarithm for n-octanol/water mixture (log $P_{o/w}$) values, i.e. an increase in hydrophilicity and thus a higher affinity to water (GUINDANI et al., 2020).

Biomaterials that present surfaces with a certain degree of hydrophilicity are desired for applications in tissue engineering. Cell attachment is usually poor on scaffolds with lower surface energy (hydrophobic, high contact angle), in comparison to scaffolds that present high surface energy (more hydrophilic, low contact angle) surfaces, suggesting PGlCL-NAC are potential candidates for application in tissue engineering (GUELCHER; HOLLINGER, 2006; SYROMOTINA et al., 2016).

3.3.2 BIOCOMPATIBILITY ASSAYS

3.3.2.1 Short-term cell viability and proliferation

The short-term viability of the cells on the electrospun scaffolds was evaluated to check if the presence of the electrospun scaffolds can cause any effect that disturbs the functions of the cells. The quantitative results of the metabolic activity of the cells were evaluated by MTT (mitochondrial activity) and NRU (lysosomal activity) assays. The mitochondrial activity is essential for the supply of energy to the cell, while the lysosomal activity is associated with the cell autophagy process (BOYA et al., 2013). Mitochondria and lysosomes are fundamental

organelles for cell metabolism, and any dysfunction in these organelles can cause serious damage to cell proliferation and cause cell death (TODKAR et al., 2017). Table 2 shows these results in terms of the percentage of viable cells.

Table 2. Cell viability was determined by NRU and MTT assays after incubation on electrospun polymer scaffolds in 24 h and 72 h.

Sample	NRU assay (% of viable cells)		MTT assay (% of viable cells)	
	24 h	72 h	24 h	72 h
PCL	97.2 ± 7.6	98.7 ± 1.8	122.1 ± 2.4	125.5 ± 3.7
PCL+PGlCL	101.8 ± 7.6	103.7 ± 5.8	146.9 ± 2.8	153.9 ± 3.0
PCL+PGlCL-NAC	126.7 ±4.6	145.7 ± 4.4**	166.9 ± 1.6*	170.4 ± 1.7***

Statistical analysis was performed using one-way ANOVA. *($p < 0.05$), **($p<0.01$), ***($p<0.001$) indicate statistical difference relative to PCL.

For the first 24 h, the percentage of viable cells for all tested samples were very similar to each other, being also similar to the control. For NRU assay, no statistical difference was observed when comparing the viability of the cells exposed to PCL+PGlCL-NAC and PCL electrospun scaffolds. For MTT assay, cells in contact with PCL+PGlCL-NAC electrospun scaffolds presented slightly higher viability in comparison to cells exposed to PCL scaffolds, with a statistical level of significance ($p < 0.05$). In the 72 h test, for NRU assay, a higher number of viable cells was found on PCL+PGlCL-NAC scaffolds, in comparison to the number of viable cells found on PCL scaffolds, and this difference showed a statistical level of significance ($p<0.01$). For MTT assay, this trend was maintained the same, but the difference presented a higher level of statistical significance ($p<0.001$).

These results indicate that the use of the NAC modified polymer in the composition of the electrospun scaffolds did not present any kind of cytotoxic effect to the cells, up to 72 h of incubation. The presence of PGlCL-NAC in the composition of the electrospun scaffolds increased the biocompatibility and provided favorable conditions for the proliferation of viable fibroblast cells, in comparison to PCL scaffolds.

The nuclear morphology assay (NMA) makes it possible to identify possible changes in the cell nucleus that result from the interaction between adhesion proteins and the scaffold surface (CHEN et al., 2009; HUANG et al., 2016). Changes in nuclear cell morphology may be indicative of cytotoxicity, cellular senescence, and apoptosis. Also, it makes it possible to monitor the migratory state of the cells to its distribution on surface (ISER et al., 2016).

In this assay, McCoy cells were cultured on the surface of the scaffold and incubated for periods of 24 h and 72 h. Cell nuclei were stained with a fluorescent dye (DAPI) and fluorescence microscopy images enabled the visualization of the cell nuclei on the scaffolds after 72 h in Figure 15A. Fluorescence images showed that the cells adapted well to all tested scaffolds, spreading themselves over the surfaces during the entire incubation periods observed, which can be observed under bright-field microscopy. This behavior provides us evidence that the cell migration process has not been hindered.

The percentage of normal, senescent, and apoptotic cell nuclei after 72 h of incubation on the electrospun scaffolds is presented in Figure 15B. The percentage of normal nuclei remained much superior in comparison to the percentage of senescent and apoptotic nuclei for all tested scaffolds. No significant differences were observed in the percentage of normal nuclei for the different electrospun scaffolds evaluated. These results

confirm the data obtained by metabolic assays and show that PCL+PGlCL-NAC scaffolds can be compared to PCL scaffolds, not inducing cytotoxicity and showing potential to be employed in biomedical applications.

Figure 15C shows that after an incubation time of 72 h, there was an increase of 32% in the number of normal nuclei on PCL+PGlCL-NAC scaffolds, in comparison to PCL scaffolds (significant difference, $p<0.01$). These results confirm that the introduction of NAC-modified polymer in the blends has favored cell proliferation on the scaffolds, as suggested by the results of NRU and MTT assays.

It is well known in the scientific literature that the fiber diameter and the wettability of the surfaces are two factors that play a very important role in cell proliferation (CHEN et al., 2007; DOWLING et al., 2011). The decrease in fiber diameter is frequently associated with higher degrees of cell proliferation, while hydrophilic surfaces are more suitable for cell adhesion and proliferation (CHRISTOPHERSON et al., 2009; SYROMOTINA et al., 2016). All results obtained in short-term assays are in accordance with these findings, which leads us to conclude that the incorporation of PGlCL-NAC in the blends implied in higher McCoy's fibroblasts proliferation on PCL+PGlCL-NAC scaffolds, in comparison to PCL scaffolds.

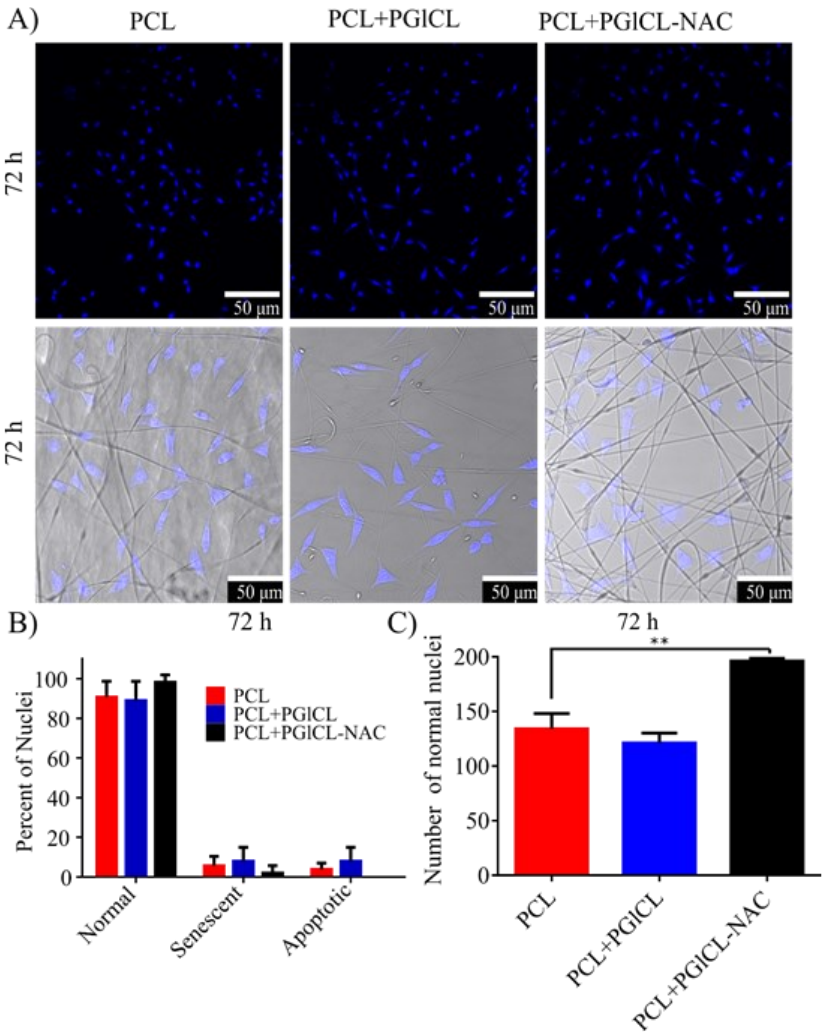

Figure 15. Nuclear morphometric analysis (NMA) performed using Fluorescence Microscopy (A) Fluorescence images of the cells adhered on the electrospun scaffolds for 72 h (dark field and bright field) of incubation, using a magnification objective x 20. (B) Percentage of normal, senescent, and apoptotic cell nuclei after 72 h of incubation on the electrospun scaffolds. (C) The number of normal cell nuclei on the electrospun scaffolds after an incubation time of 72 h and statistical analysis was performed using one-way ANOVA **($p<0.01$) relative to PCL.

3.3.2.2 Long-term cell proliferation

Clonogenic assay was performed to evaluate McCoy cell's ability to form colonies on the electrospun scaffolds from a single cell unit, in a long-term assay. Cell proliferation was evaluated after a long-term incubation period of 10 days. The data were presented in Figure 16, as the number and area of colonies formed after 10 days of incubation of the cells on the scaffolds.

Figure 16 shows that similarly as in short-term assays, long-term incubation of McCoy fibroblast cells on PCL+PGlCL-NAC electrospun scaffolds had a superior performance in terms of triggering cell proliferation when compared to PCL electrospun scaffolds. Besides, it is possible to observe in the photographic images that larger colonies were formed on PCL+PGlCL-NAC electrospun scaffolds, in comparison to PCL scaffolds (colonies area presented significant difference, $p<0.01$), which indicates good adaptability of the cells on the surface enabling its proliferation. Similarly, the addition of alginate in PCL scaffolds allows greater biocompatibility, favoring the formation of cell colonies due to the increased hydrophilicity (HU et al., 2019).

The number of colonies formed on PCL+PGlCL-NAC scaffolds was also superior to the number of colonies formed on PCL scaffolds (significant difference, $p<0.05$), which suggests that PCL+PGlCL-NAC scaffolds present characteristics that favor the adhesion of McCoy fibroblast cells on its surface.

The long-term proliferation results can also be expressed for each sample in terms of efficiency of colony formation, which is the ratio between the number of colonies and the number of seeded cells, expressed in percentage. The calculated efficiency of colony formation is 23% for PCL scaffolds, 15% for PCL+PGlCL scaffolds, and 42% for PCL+PGlCL-NAC scaffolds. These results are in agreement with the trend obtained in the short-term assays and enable a clearer comprehension of the good performance of PCL+PGlCL-NAC scaffolds as a biomaterial, also when exposed to longer-term contact to fibroblast cells.

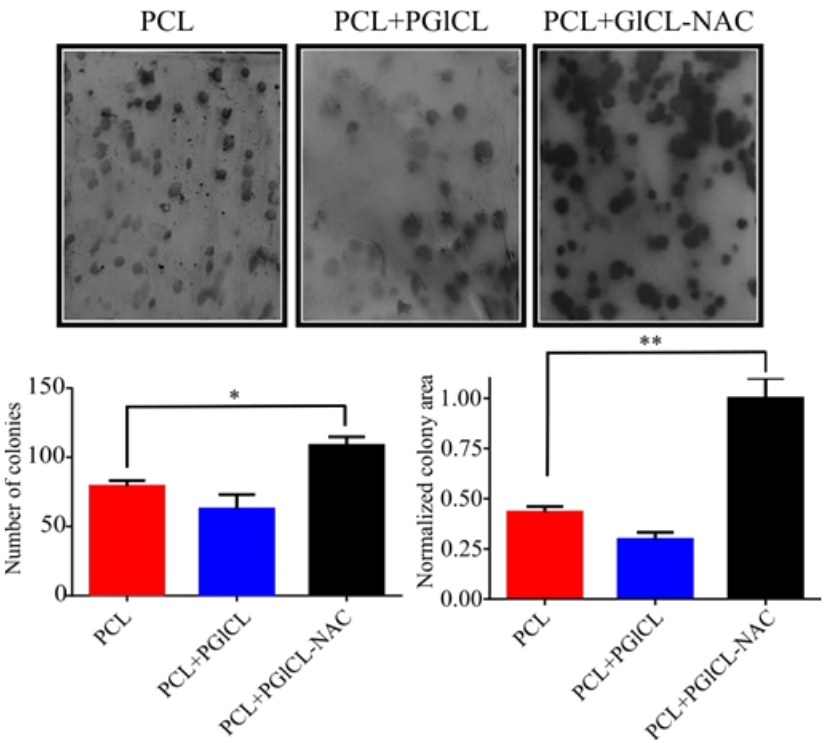

Figure 16. Long-term viability and proliferation of McCoy cells proliferation determined by Clonogenic assay. Colony formation was evaluated for the electrospun scaffolds during an incubation time of 10 days. The number and area of the colonies on the scaffold were quantified and statistical analysis was performed using one-way ANOVA * ($p<0.05$) and **($p<0.01$) indicate statistical difference relative to PCL.

3.3.2.3 Cell adhesion on polymer scaffolds

Cell adhesion is considered an intrinsic property of McCoy cells that regulates subsequent processes, such as cell growth and proliferation over extracellular matrix (ECM) (or a biomaterial that simulates ECM) (DENG et al., 2007). The adhesion process depends on the good interaction between cells and the biomaterial (SCHAFFNER; DARD, 2003).

In this assay, McCoy fibroblast cells were seeded on the electrospun scaffolds and the interaction between cells and scaffolds was observed with the help of scanning electron microscopy (SEM) images.

Figure 17 presents the SEM images of cell interaction with PCL, PCL+PGlCL, and PCL+PGlCL-NAC electrospun scaffolds for 72 h. Cell adhesion could be observed for all samples, and the images are in complete accordance with the behavior observed in the short-term cell viability and proliferation assays. SEM images also allowed the visualization of the effect of the use of NAC modified polymers in the cell-surface interactions. The successful cell adhesion on PCL+PGlCL-NAC electrospun scaffolds allowed the formation of larger and thicker cell colonies in comparison to PCL and PCL+PGlCL scaffolds.

Cell adhesion is a requisite for cell proliferation, so some of the factors that increase cell proliferation are the same that improve cell adhesion, including fiber diameter and the hydrophilicity of the scaffolds. A larger specific surface area is reported as one of the possible reasons for the better attachment of cells on small-sized fibers scaffolds when allied to other factors that improve cell adaptability to the scaffold. Since more adhesion proteins could be absorbed on them, scaffolds with higher specific areas offer a larger number of available adhesion points for cell attachment (CHEN et al., 2007; SANTILLÁN et al., 2019). Cell attachment, on the other hand, is favored on more hydrophilic scaffolds, since it presents higher surface energy(PIRES et al., 2019). Another fact that has to be considered is that NAC is a cysteine derivative, an amino acid that is one of the main components of fibroblast receptors (BURRUS et al., 1992). Therefore, there is probably a broad range of specific interactions that NAC might be establishing with fibroblast receptors (e.g. integrins) by acting as a signaling molecule, thus enabling improved fibroblast adhesion to the scaffold containing PGlCL-NAC (MAO et al., 2010). Therefore, it is possible to understand that for these reasons the use of NAC covalently bonded to PGlCL on PCL+PGlCL-NAC scaffolds provided better adaptability conditions for cell adhesion and consequently cell proliferation, as shown in section 3.2.

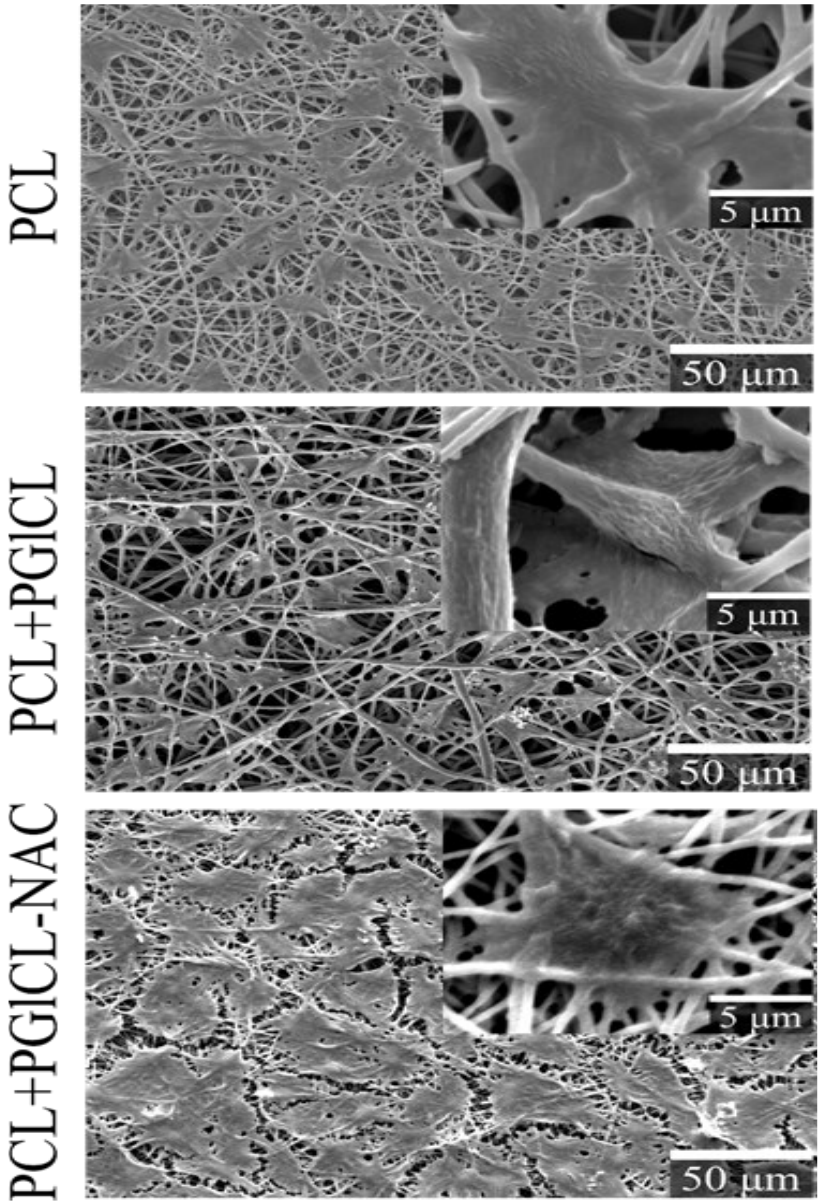

Figure 17. SEM images were obtained after McCoy cells incubation on the electrospun scaffolds after 72 h.

3.4 CONCLUSION

In this study, we successfully produced electrospun polymeric scaffolds composed of a polymeric blend between PCL and PGlCL-NAC, a copolyester covalently bonded with N-acetylcysteine, with enhanced potential for biomedical applications, in comparison to the well-known PCL scaffolds. PCL+PGlCL-NAC scaffolds presented uniform morphology, reduced fiber diameter, hydrophobicity, and crystallinity in comparison to PCL scaffolds. These characteristics led to improved cell adhesion and cell proliferation on PCL+PGlCL-NAC scaffolds while maintaining cell viability, showing its potential as a biomaterial. Furthermore, its lower degree of crystallinity is also indicative of faster degradation rates which are desirable for many applications in tissue engineering. The results obtained in this work could be are an important contribution to the development of new engineered devices for medical applications, especially in tissue engineering, where cell adhesion and proliferation are crucial features.

REFERENCES

ATES, Zeliha e HEISE, Andreas. Functional films from unsaturated poly(macrolactones) by thiol–ene cross-linking and functionalisation. **Polymer Chemistry**, v. 5, n. 8, p. 2936, 2014.

BELTRAME, Jeovandro. **Desenvolvimento de matriz extracelular eletrofiada para aplicação na engenharia de tecidos.** (Mestrado em Engenharia Química). Departamento de Pós Graduação em Engenharia Química, Universidade Federal de Santa Catarina, Florianópolis, 2018.

BOYA, Patricia e REGGIORI, Fulvio e CODOGNO, Patrice. Emerging regulation and functions of autophagy. **Nature Cell Biology**, v. 15, n. 7, p. 713–720, 2013.

BURRUS, L W et al. Identification of a cysteine-rich receptor for fibroblast growth factors**. Molecular and Cellular Biology**, v. 12, n. 12, p. 5600–5609, 1992.

CANEVAROLO JR., Sebastião Vicente. Ciência dos Polímeros - Um texto básico para tecnólogos e engenheiros. 2ª Edição ed. São Paulo: **Artliber**, 2006.

CHEN, Fei et al. Antioxidant and antibacterial activities of eugenol and carvacrol-grafted chitosan nanoparticles. **Biotechnology and Bioengineering,** v. 104, n. 1, p. 30–39, 2009.

CHEN, Ming et al. Role of fiber diameter in adhesion and proliferation of NIH 3T3 fibroblast on electrospun polycaprolactone scaffolds. **Tissue Engineering**, v. 13, n. 3, p. 579–587, 2007.

CHRISTOPHERSON, Gregory T. e SONG, Hongjun e MAO, Hai Quan. The influence of fiber diameter of electrospun substrates on neural stem cell differentiation and proliferation. **Biomaterials**, v. 30, n. 4, p. 556–564, 2009. Disponível em: <http://dx.doi.org/10.1016/j.biomaterials.2008.10.004>.

COLEMAN, M M e ZARIAN, J. Fourier-Transform Infrared Studies of Polymer Blends II. Poly(\(\varepsilon\)-Caprolaxtone)-Poly(vinyl Chloride) System. **Journal of Polymer Science: Polymer Physics Edition**, v. 17, p. 837–850, 1979.

CRESCENZI, V. et al. Thermodynamics of fusion of poly-β-propiolactone and poly-ε-caprolactone. comparative analysis of the melting of aliphatic polylactone and polyester chains. **European Polymer Journal**, v. 8, n. 3, p. 449–463, 1972.

DENG, Xu-Liang et al. Poly (L-lactic acid)/ hydroxyapatite hybrid nanofibrous scaffolds prepared by electrospinning. **Journal of Biomaterials Science, Polymer Edition**, v. 18, n. 1, p. 117–130, 2007.

DOWLING, Denis P. et al. Effect of surface wettability and topography on the adhesion of osteosarcoma cells on plasma-modified polystyrene. **Journal of Biomaterials Applications**, v. 26, n. 3, p. 327–347, 2011.

FILIPPI-CHIELA, Eduardo C. et al. Nuclear morphometric analysis (NMA): Screening of senescence, apoptosis and nuclear irregularities. **PLoS ONE**, v. 7, n. 8, 2012.

FRANKEN, Nicolaas A P et al. Clonogenic assay of cells in vitro. **Nature Protocols,** v. 1, n. 5, p. 2315–2319, 2006. Disponível em: <http://www.nature.com/doifinder/10.1038/nprot.2006.339>.

GUELCHER, Scott A. e HOLLINGER, Jeffrey O. An Introduction to Biomaterials. MICHAEL R. NEUMAN (Org.). . **The Biomedical Engineering Series.** Boca Raton: CRC Press, 2006. .

GUINDANI, Camila et al. Controlling the biodegradation rates of poly(globalide-co-ε-caprolactone) copolymers by post polymerization modification. **Polymer Degradation and Stability**, v. 179, 2020.

GUINDANI, Camila et al. Enzymatic ring opening copolymerization of globalide and ε-caprolactone under supercritical conditions. **Journal of Supercritical Fluids**, v. 128, n. May, p. 404–411, 2017.

GUINDANI, Camila et al. N-acetylcysteine side-chain functionalization of poly(globalide-co-ε-caprolactone) through thiol-ene reaction. **Materials Science and Engineering C**, v. 94, p. 477–483, 2019.

HU, Wei Wen e LIN, Cheng Hsien e HONG, Zhen Jie. The enrichment of cancer stem cells using composite alginate/polycaprolactone nanofibers. **Carbohydrate Polymers**, v. 206, n. 300, p. 70–79, 2019. Disponível em: <https://doi.org/10.1016/j.carbpol.2018.10.087>.

HUANG, Chen-yu e HU, Keng-hsiang e WEI, Zung-hang. Comparison of cell behavior on pva / pva-gelatin electrospun nanofibers with random and aligned configuration. **Nature Publishing Group**, n. April, p. 1–8, 2016. Disponível em: <http://dx.doi.org/10.1038/srep37960>.

ISER, Isabele C. et al. Conditioned Medium from Adipose-Derived Stem Cells (ADSCs) Promotes Epithelial-to-Mesenchymal-Like Transition (EMT-Like) in Glioma Cells In vitro. **Molecular Neurobiology**, v. 53, n. 10, p. 7184–7199, 2016. Disponível em: <http://dx.doi.org/10.1007/s12035-015-9585-4>.

LI, Dawei et al. Three-dimensional polycaprolactone scaffold via needleless electrospinning promotes cell proliferation and infiltration. **Colloids and Surfaces B: Biointerfaces**, v. 121, p. 432–443, 2014.

MAO, Gaowei et al. N-acetyl-L-cysteine increases MnSOD activity and enhances the recruitment of quiescent human fibroblasts to the proliferation cycle during wound healing. **Molecular biology reports,** v. 43, n. 1, p. 31-39, 2016.

PICQUART, Michel et al. Spectroscopic study of N-acetylcysteine and N-acetylcystine r hydrogen peroxide complexation. **Chemical Physics**, v. 228, p. 279–291, 1998.

PIRES, Filipa et al. Polycaprolactone/Gelatin Nanofiber Membranes Containing EGCG-Loaded Liposomes and Their Potential Use for Skin Regeneration. **ACS Applied Bio Materials**, v. 2, n. 11, p. 4790–4800, 2019.

SANTILLÁN, Jaime et al. Fabrication and Evaluation of Polycaprolactone Beads-on-String Membranes for Applications in Bone Tissue Regeneration. **ACS Applied Bio Materials**, v. 2, n. 3, p. 1031–1040, 2019.

SCHAFFNER, P e DARD, M M. Cellular and Molecular Life Sciences Structure and function of RGD peptides involved in bone biology. **CMLS, Cell. Mol. Life Sci**., v. 60, p. 119–132, 2003.

SEYEDNEJAD, Hajar e GHASSEMI, Amir H. et al. Functional aliphatic polyesters for biomedical and pharmaceutical applications. **Journal of Controlled Release,** v. 152, n. 1, p. 168–176, 2011. Disponível em: <http://dx.doi.org/10.1016/j.jconrel.2010.12.016>.

SYROMOTINA, D. S. et al. Surface wettability and energy effects on the

biological performance of poly-3-hydroxybutyrate films treated with RF plasma. **Materials Science and Engineering C**, v. 62, p. 450–457, 2016.
TODKAR, Kiran e ILAMATHI, Hema S. e GERMAIN, Marc. Mitochondria and lysosomes: Discovering bonds. **Frontiers in Cell and Developmental Biology,** v. 5, n. DEC, p. 1–7, 2017.
ZHANG, Yu et al. Preparation of electrospun nanofibrous polycaprolactone scaffolds using nontoxic ethylene carbonate and glacial acetic acid solvent system. **Journal of Applied Polymer Science**, v. 137, n. 8, p. 2–9, 2020.
ZHENG, Chang Ji et al. Fatty acid synthesis is a target for antibacterial activity of unsaturated fatty acids. **FEBS Letters**, v. 579, n. 23, p. 5157–5162, Set 2005.

CHAPTER 4

SPIONS STABILIZATION WITH A CYSTEINE-MODIFIED COPOLYESTER: A POSSIBLE NOVEL NANOPLATFORM FOR TRIGGERED RELEASE

The modification of PGlCL with cysteine (Cys) via thiol-ene reaction followed by stabilization of superparamagnetic iron oxide nanoparticles (SPIONs) was studied. Subsequently, folic acid was conjugated on the surface of SPIONs and evaluated when the release was triggered in the presence of enzymes. The obtaining and characterization of modified PGlCLCys was evaluated. The improvement in the material's hydrophilicity and crystallinity enabled its use for SPION stabilization. With that in the sequence, it was characterized as to its use for the stabilization of SPIONs. It was evaluated for the cytotoxicity of SPIONs. Finally, bioconjugation with folic acid (SPION@PGlCLCys_FA) and subsequent triggered release. In this way, the present work can be treated as a model where FA can be replaced by other molecules of high biological interest (for example, peptides, antibodies, drugs) allowing better performance in diagnostic or theranostic applications.

The results presented in this chapter were submitted to publication in the journal ACS Bioconjugate Chemistry.

Graphical abstract

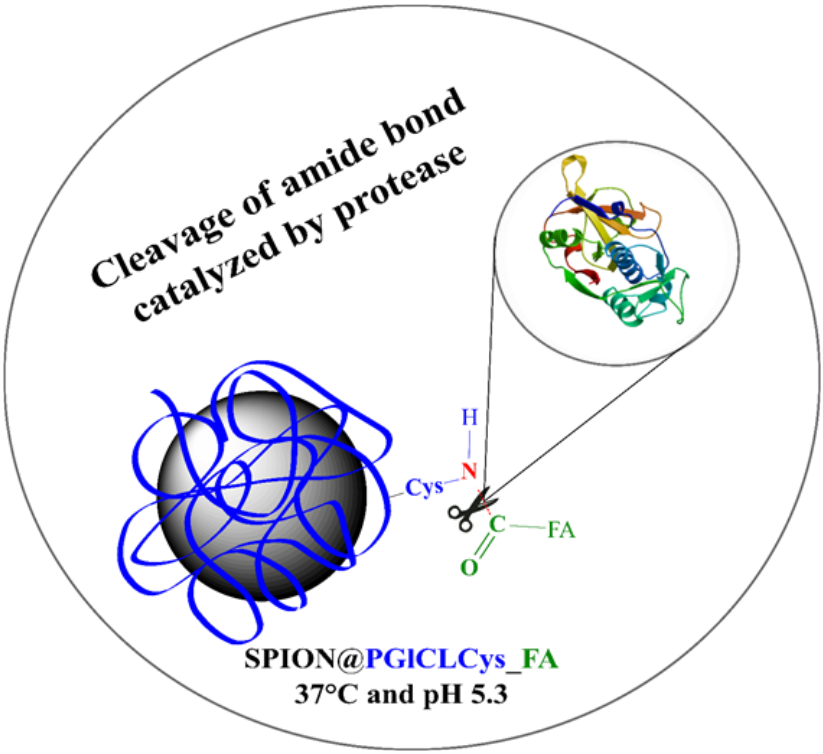

Figure 18. Triggered cleavage of amide bond catalyzed by protease Bromelain with ph 5.3.

4.1 ABSTRACT

Superparamagnetic iron oxide nanoparticles (SPIONs) have their use approved for the diagnosis/treatment of malignant tumors, and can be metabolized by the organism. To prevent embolism caused by these nanoparticles they need to be coated with biocompatible and non-cytotoxic materials. Here, we synthesized an unsaturated and biocompatible copolyester called poly(globalide-co-ε-caprolactone) (PGlCL). In sequence PGlCL was modified with the amino acid cysteine (Cys) via a thiol-ene reaction, and used for the coating and stabilization of the SPIONS (SPION@PGlCLCys). PGlCL is a non-toxic polymer, and

the incorporation of cysteine reduced the crystallinity and increased hydrophilicity. Additionally, cysteine pendant groups at the particles surface allowed the direct bioconjugation of biomolecules that establish specific interactions with MDA-MB 231 tumor cells. The bioconjugation of folic acid (FA) was carried out directly on the amine groups of cysteine molecules present in the SPION@PGlCLCys surface (SPION@PGlCLCys_FA) by carbodiimide-mediated coupling, leading to the formation of amide bonds, with a conjugation efficiency of 67%. Next, FA release from the nanoparticle surface was evaluated using a protease at 37 ºC and pH ~ 5.3 phosphate buffer. It was found that 35% of all folic acid conjugated to the SPIONS were released after 24 h, demonstrating that the release was triggered by the enzyme that cleaved the amide bonds. MTT assay revealed that SPION@PGlCLCys_FA are not toxic to L929 and MDA-MB 231 cell lines. Thus, after a successful bioconjugation and subsequent triggered release of FA, we understand that SPION@PGlCLCys_FA can be treated as a model where FA can be replaced by other molecules of high biological interest (e.g. peptides, antibodies, drugs) enabling improved performance in diagnosis or theranostic applications.

4.2 MATERIALS AND METHODS

4.2.1 MATERIALS

Acetone P.A 99.8%, chloroform P.A. 99.8%, dichloromethane P.A. 99.8% (DCM), dimethylformamide P.A 99.5%, dimethyl sulfoxide P.A 99,7%, ethanol P.A. 99.8% (EtOH), tetrahydrofuran P.A. 99.8% (THF), toluene P.A. 99.0% were purchased from Merk (Brazil). The photoinitiator 2,2-dimethoxy-2-phenylacetophenone (DMPA) CAS:24650-42-8 was kindly donated by IGM resins. Iron (III) chloride hexahydrate ($FeCl_3 \cdot 6H_2O$), iron (II) chloride tetrahydrate ($FeCl \cdot 4H_2O$), ammonium hydroxide (NH_4OH). Folic acid (FA) 98% (Vetec), 1-ethyl-3-(3-dimethyl aminopropyl) carbodiimide hydrochloride (EDC), N-Hydroxysuccinimide (NHS) were purchased from Sigma-Aldrich. Bromelain enzyme (Sigma-Aldrich). Cysteine 99.8% (Cys) was purchased from Gemini (Brazil). Novozym 435 (commercial lipase B from Candida Antarctica immobilized on cross-linked polyacrylate beads) was kindly donated by Novozymes, Brazil, A/S. Globalide (Gl)

was a kind gift from Symrise. Globalide and ε-caprolactone (CL) were dried under vacuum for 24 hours and kept in a desiccator over silica and 4 Å molecular sieves. Water was purified by a Milli-Q water purification system.

4.2.2 CHARACTERIZATIONS

4.2.2.1 Physical-chemical characterization of poly(globalide-co-ε-caprolactone)

Proton nuclear magnetic resonance (^{1}H NMR) analysis were performed on Bruker AC-200F NMR equipment, operating at 200 MHz. Chemical shifts are reported in ppm relative to tetramethylsilane (TMS) 0.01% (vol%) (δ=0.00). All samples were solubilized in $CDCl_3$ (δ = 7.27 for ^{1}H NMR).

Poly(globalide-co-ε-caprolactone) ^{1}H NMR ($CDCl_3$ 200 MHz): δ(ppm) 5.49 – 5.32 (m, CH=CH); 4.10 – 4.04 (m, $CH_2O(C=O)$).

Poly(globalide-co-ε-caprolactone) - Cys RMN ^{1}H ($CDCl_3$ 200 MHz): δ(ppm) 5.49 – 5.32 (m, CH=CH); 4.10 – 4.04 (m, $CH_2O(C=O)$); 2.90 – 2.70 (m, S-CH_2).

Molecular weight distributions were determined by Gel Permeation Chromatography (GPC). 0.02 g of the copolymer was dissolved in 4 mL of tetrahydrofuran (THF) and the solution obtained was filtered (pore: 0.45 µm, diameter: 33 mm) before the analysis. The analysis was performed using a high-performance liquid chromatography equipment (HPLC, model LC 20-A, Shimadzu) and Shim Pack columns of the GPC800 series (GPC 801, GPC 804, and GPC 807), also from Shimadzu. As eluent, THF was used at a volumetric flow rate of 1 mL min^{-1} at 40°C. Calibration was achieved using polystyrene standards. Polystyrene standards with molecular weights ranging from 580 to 9.225 × 10^6 g·mol^{-1} were used to construct the standard curve.

Fourier transform infrared spectroscopy (FTIR) was used to identify the chemical structure of the cysteine-modified copolymer. The analysis was performed on a Prestige 21 spectrophotometer (Shimadzu IR) using the KBr tableting technique for obtaining a transparent tablet. The spectra were recorded in a wavenumber range of 400-4000 cm^{-1}.

Differential scanning calorimetry (DSC) was used to measure melting temperatures and melting enthalpy (degree of crystallinity) of the polymeric materials using a Jade DSC (Perkin-Elmer). For the analysis, approximately 5 mg of the dried polymer was analyzed under nitrogen

atmosphere (20 mL·min^{-1}), with temperatures ranging from 0 to 150 °C and a heating rate of 10 °C · min^{-1}. The thermal history was removed before the analyses (for pure polymer samples) at a heating rate of 20 °C min^{-1} and a cooling rate of 10 °C min^{-1}. The second heating runs were used for the polyester to obtain the thermal properties.

$$C\% = \frac{\Delta \text{Hreal}}{\Delta \text{H100\%}} * 100$$

where, ΔHreal is the enthalpy of melting of the sample and ΔH 100% is the enthalpy of melting of the 100% crystalline polymer.

For the contact angle assay, PGlCL and PGlCL-Cys films were produced, by depositing copolymer solutions (100 mg:mL - Chloroform: DMF 9:1) on microscope slides. The contact angle between the polymeric films and the water drops was measured in a goniometer (Ramé-Hart Instrument Co. - Ramé-Hart 250). For this assay, samples were analyzed in triplicate at room temperature, using 10 μL drop volume.

4.2.2.2 Physical-chemical characterization of Superparamagnetic Iron Oxide Nanoparticles (SPIONs)

Fourier transform infrared spectroscopy (FTIR) analysis of the SPIONS and SPION@PGlCLCys were performed on a Prestige 21 spectrometer (Shimadzu IR) using a KBr tableting technique for obtaining a transparent tablet. Spectra were recorded in a wavenumber range of 400-4000 cm^{-1}.

Transmission electron microscopy and selected area electron diffraction (TEM/SAED) images were obtained on a JEM-1011 TEM microscope at an acceleration voltage of 100 kV.

Powder X-ray diffraction (XRD) analysis were performed on a Rigaku_MiniFlex 600 diffractometer with graphite monochromatized CuKα (λ = 1.5418 A°), with maximum voltage and current at 40 kV and 40 mA, respectively, with a 2θ °/min scan rate in the range of 20 to 80° with 0.05° steps.

Magnetic properties of SPION@ PGlCLCys were measured in a vibrating sample magnetometer (VSM) (Microsense EV9 Model). For the VSM analysis, the samples were dried, pressed and held in a quartz cylinder holder.

Thermogravimetric analysis (TGA) was performed under a nitrogen atmosphere at a heating rate of 10°C · min^{-1} from room temperature to 900 °C, in a STA 449-F3 Jupiter (2012) equipment.

The particle size distribution and zeta potential were measured by dynamic light scattering (DLS) using a Zetasizer 3000 HSA (Malvern Instruments) equipment.

4.2.2.3 Synthesis of poly(globalide-co-ε-caprolactone) by e-ROP

The synthesis of PGlCL was carried out by enzymatic ring-opening polymerization (e-ROP) using the monomers globalide (Gl) and ε-caprolactone (CL) in a 50/50 mass ratio (Gl/CL) (GUINDANI et al., 2017) (Figure 19A). Toluene was used as a solvent, and the system was maintained at a temperature of 65 °C for 2 hours. The enzyme content was fixed in 5 wt.% relative to the total mass of monomer, and the solvent:monomers mass ratio was fixed at 1:2. After polymerization, the material was solubilized in dichloromethane (DCM), and the immobilized enzyme (NZ-435) was filtered. The copolymer was precipitated in a mixture of cold EtOH: acetone (70:30 v:v). The obtained copolymer was then filtered and dried at room temperature, under vacuum, up to constant weight.

4.2.2.4 Modification of PGlCL with Cysteine via thiol-ene reaction

The post-polymerization modification of PGlCL was carried out by photopolymerization using thiol-ene reactions using a DMPA photoinitiator, directly on PGlCL unsaturations (ATES; HEISE, 2014) (Figure 19B). Cysteine was chosen as a functionalizing molecule because it contains a thiol group and because its presence as a pendent group on PGlCL chains confers desirable hydrophilic characteristic and enables the covalent conjugation of high biological interest molecules to the nanoparticle surface.

For the modification procedure, the copolymer PGlCL (0.300 g) and Cys (0.224 g) were placed in a flask with the photoinitiator DMPA (0.016 g), using a mixture of chloroform and DMF (2:1 - v: v) as a solvent, under nitrogen atmosphere. The reaction was carried out in a UV chamber for a period of 4 h, under continuous magnetic stirring. The amount of Cys used was stablished to be twice the minimum required to react with all double bonds.

4.2.2.5 Synthesis of Superparamagnetic Iron Oxide Nanoparticles (SPIONs)

SPIONs were synthesized by Fe_3O_4 co-precipitation method (ZOTTIS et al., 2015) (Figure 19C). PGlCLCys will be used as the stabilizing agent. First, solutions of $FeCl_2 \cdot 4H_2O$ (2.0 mmol) and $FeCl_3 \cdot 6.H_2O$ (4.0 mmol) salts will be prepared in the proportion of 1:2 (mol/mol) dissolved in 1 mL of 1M HCl solution under an inert atmosphere, to avoid oxidation of Fe (II). 100 mL of deionized water is heated up to 80 °C, then the solution containing Fe^{3+} and Fe^{2+} was added under nitrogen flow. When the solution reached 90ºC, 40 mL of NH_4OH (25% v:v) was added, reaching pH ~ 10. Next, the modified copolymer (PGlCLCys) was added to the system (Fe^{+3} : PGlCLCys = 8:1 mol/mol) , and the system was kept under contant stirring at 90 °C during one hour. The appearance of a dark brown/black color in the solution is indicative of the formation of stabilized iron oxide, forming SPION@PGlCLCys. After that time, SPIONs were separated with a magnet and washed with distilled water. Afterwards, the sample was frozen and lyophilized for the subsequent analyses.

4.2.2.6 Conjugation of SPIONs with Folic Acid

Folic acid was modified by the carbodiime approach (GUO et al., 2013) (Figure 19D). Folic acid (2 mmol), NHS (2 mmol) and EDC·HCl (2.2 mmol) were dissolved in 100 mL DMSO. The mixture purged with nitrogen, and the reaction was carried out overnight, under constant stirring, at room temperature and protected from light. DMSO and unreacted folic acid were removed by dialysis (Spectra-Por 100-500 Da, Biontech CE Tubing) in a buffer solution (PBS, pH 8.0) for four days, replacing the buffer solution daily. After dialysis, the FA+NHS solution was lyophilized.

For the conjugation of folic acid to the SPIONs surface, the amount of cysteine in the copolymer was calculated based on the consumption of the double bonds of the copolymer, determined by ^1H NMR analysis. Two ratios between amine groups (PGlCLCys) and carboxylic acid groups (FA+NHS) were evaluated: a stoichiometric ratio of 1:1; and with an excess of FA+NHS, where a ratio of 2:1 was used. 5 mg of SPION@PGlCLCys were dispersed in phosphate buffer (pH ~ 8.0) with the help of a sonicator. After complete dispersion of the

SPION@PGlCLCys, the amounts of FA+NHS 0.160 mg and 0.260 mg were added to falcon tubes containing SPION@PGlCLCys. The system was purged with nitrogen, and left in a Klein-type shaker for 24 hours. Afterwards, magnetic separation was performed and samples were submitted to 3 washing cycles, collecting the supernatant for FA quantification. The amount of FA conjugated to the SPION@PGlCLCys was calculated based on a FA calibration curve built at 283 nm using an UV-vis equipment.

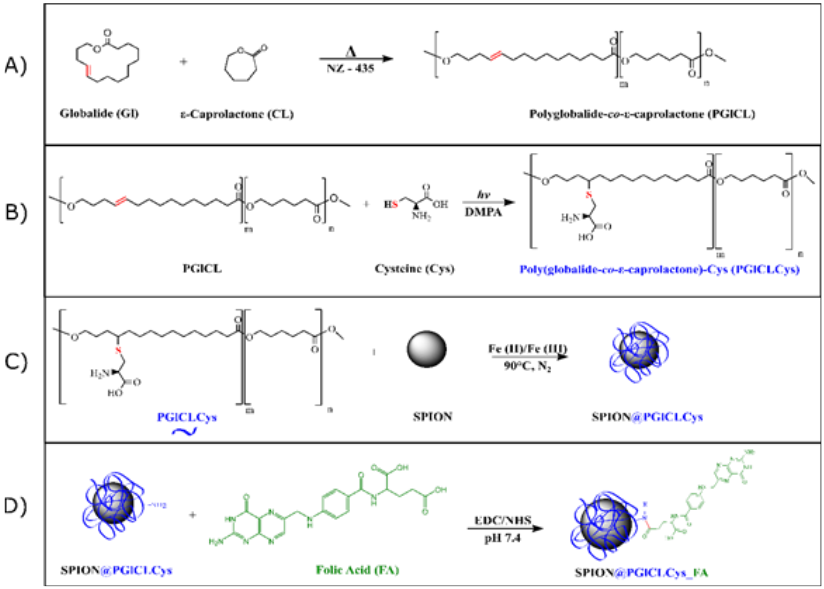

Figure 19. Representative scheme of the reaction steps to obtain PGlCL and its modification with cysteine followed by stabilization of SPIONs. A) Enzymatic Ring-Opening Polymerization reaction (e-ROP). B) Modification reaction with the amino acid cysteine (Cys) via thiol-ene reaction to obtain PGlCLCys. C) Synthesis and stabilization of SPIONs with PGlCLCys and D) Conjugation of SPIONs with FA.

4.2.2.7 Cell culture

All biological assays used normal L929 and breast carcinoma-derived MDA-MB 231 cells lines. L929 and MDA-MB 231 were cultivated in RPMI 1640 medium (GIBCO, Baltimore, USA) supplemented with fetal bovine serum (10%), penicillin (100 U/mL) (GIBCO, Baltimore, USA), streptomycin (100 µg/mL) (GIBCO,

Baltimore, USA) and Glutamine 2mM. All cells were maintained under controlled conditions (37 °C in a 5% CO_2 atmosphere with 95% air humidity) over the period studied (24 and 72h). Results are expressed as an average of three independent experiments.

4.2.2.7.1 In vitro cell viability of SPION@PGlCLCys and SPION@PGlCLCys_FA

The cell viabilities of L929 and MDA-MB 231 exposed to SPION@PGlCLCys and SPION@PGlCLCys_FA were measured using the MTT assay (MOSSMAN, 1983). $7.5x10^3$ cells/well (24 h assay) and 5.0×10^3 cells/well (72 h assay) were seeded in 96-well plates. At confluence, cells were exposed to different nanoparticle concentrations (0.0001, 0.001, 0.01, 0.1, 1, 10 and 100 $\mu g \cdot mL^{-1}$) and incubated at 37 °C and pH 7.4 for 24 h and 72 h for each cell. After incubation, cells were washed twice with PBS and incubated for 2 h with MTT (0.5 $mg \cdot mL^{-1}$) (ZOTTIS et al., 2015). Subsequently, the formed formazan crystals were solubilized by the addition of DMSO (100 µl/well), and colored solutions were read at 570 nm. For all tested conditions, the respective blanks were analyzed. The experiments were performed independently for each cell line and in triplicate, and the results are presented as cell viability.

4.2.2.8 Release FA with Enzymatic

The release of the folic acid conjugated to the SPION@PGlCLCys was studied under the lysosomal condition (pH = 5.3), taking 400 µg of SPION@PGlCLCys_FA and 400 µg of Bromelain protease in 2 mL of PBS (0.1 M solution, pH = 5.3) at 37 °C. The FA release was evaluated for 12 h, 24 h, 48 h and 72 h (GUPTA; BHARGAVA; BAHADUR, 2014). Magnetic separation was performed and the samples were submitted to 3 washing cycles, collecting the supernatant for FA quantification. The amount of released FA was calculated based on a FA standard curve built using an UV-vis (283 nm) equipment.

4.2.2.9 Computational Section

The theoretical values of the logarithm of partition coefficient (log P) obtained in the present work were based on the Density Functional Theory (DFT) (CHU; LEUNG, 2001; JUNG et al., 2006). The simulated molecules were generated and analyzed by the software Avogadro(HANWELL et al., 2012) version (1.2.0).

First, the molecular geometry of PGlCL, PGlCLCys, AF and PGlCLCys_FA were optimized to the ground state geometry of these molecules in different media such as gas phase, n-octanol and water. The optimized structures were confirmed as real minima by vibration analysis (no imaginary frequency was detected) (NEDYALKOVA et al., 2019). Through the thermodynamic properties obtained by the DFT calculations it is possible to obtain the Gibbs free energy in different media and the partition coefficient.

The partition coefficient (P) can be defined as the ratio between the concentration of a solute in two phases of a mixture that contains two immiscible solvents at equilibrium (GARRIDO et al., 2011). The logarithm of partition coefficients for n-octanol/water mixtures ($\log P^{O/W}$) can be obtained according to (NEDYALKOVA et al., 2019):

$$\log P^{O/W} = \frac{\Delta G^{W}_{solv} - \Delta G^{O}_{solv}}{2.303RT}$$

where $\Delta G_{solv} = G^{X} - G$ is the Gibbs free energy of solvation, G and G^{X} are respectively the Gibbs free energy in gas phase and in the solvent. The superscripts (X = W and X = O) represent respectively the water and n-octanol solvents, while R is the ideal gas constant (8.314 J/K-mol^{-1}).

The results were obtained at the reaction conditions (25 °C and 1.0 atm), using the Becke-three-parameter Lee-Yang-Parr (B3LYP) model as hybrid functional, along with a split-valence double-zeta polarized basis set, based on Gaussian type orbitals (6-31G**)(CANDIOTTO et al., 2020). The Gibbs free energy of solvation in water and n-octanol were computed using the solvation model based on electronic density (SMD) (BAUER et al., 2018). All DFT calculations were performed using the ORCA 5.0.2 package (BAUER et al., 2018).

4.3 RESULTS AND DISCUSSION

Figure 19 shows the steps involved in the development of the nanoplatform. In a first stage, the copolymer PGlCL was synthesized via enzymatic ring-opening polymerization (e-ROP). Subsequently, the modification of the copolymer with the amino acid cysteine was carried out through photoinitiated thiol-ene reactions. The modified copolymer PGlCLCys was then used for the stabilization of the SPIONS, and the amine groups from the cysteine in the SPION@PGlCLCys allow the incorporation of folic acid (FA) via carbodiimide chemistry.

4.3.1 SYNTHESIS, MODIFICATION AND CHARACTERIZATION OF PGLCLCYS

The synthesis of PGlCL (50:50) was carried out via e-ROP using toluene as solvent at a fixed mass ratio of 2:1 (monomer:solvent). The number (Mn) and weight (Mw) average molecular weights of PGlCL determined by gel permeation chromatography (GPC) were 24,500 $g \cdot mol^{-1}$ and 57,000 $g \cdot mol^{-1}$, respectively. In sequence, the copolyester was modified with cysteine via thiol-ene reaction by photoinitiation with DMPA (PGlCLCys).

The modification of the polymer with cysteine was verified by FT-IR (Figure 20A). For PGlCL a band was observed in 1635 cm^{-1} referring to the elongation of the alkene group (-C=C-) present in the PGlCL. The same band could not be observed in the PGlCLCys spectrum. Additionally, the appearance of bands at 674 cm^{-1} (-C-S-C-) and at 1580 cm^{-1} ($-C-NH_2$) confirms the incorporation of cysteine to the copolymer. The nonappearance of bands at 2550 cm^{-1} (-C-SH) indicates the absence of free cysteine in the modified polymer.

The degree of modification of PGlCL with cysteine was determined by ^1H NMR analysis (Figure 20B) based on the integral of the double bond (-C=C-, at 5.40 ppm) peak areas of the globalide monomer units in the copolymer (results in Table 3). For integration, the peak of ester methylene at 4.06 ppm was used as a reference, since the amount of ester methylene remains constant. A 18% consumption of double bonds was observed after the reaction with cysteine, indicating the coupling of cysteine to 18% of the globalide monomer units of PGlCL. The modification was also evidenced by the emergence of the $-S-CH_2-$ group at 2.90-2.70 ppm. The crystallinity of the polyesters was measured by

DSC and the degree of crystallinity was determined by the relationship between the ΔH_m of each sample and the theoretical value of a 100% crystalline PCL sample (More details in Table 4). The melting temperature (T_m) for PCLGl was 38°C and after modification T_m was reduced to 32°C. At the same time, the crystallinity decreased from 44% to 30% after the reaction with the amino acid (Figure 20C). The modification of the polyester with cysteine has also affected its hydrophobic character, reducing the value of the contact angle with water from 77° to 56° (Figure. 20C). The increase in the hydrophilicity of the polymer is endorsed by the prediction of the partition coefficient (log P) through DFT calculations (for details, see Section 4.2.2.9 and Table 5). The polymer PGlCL presented log P = 5.53, while after the modification with cysteine, this value decreased to log P = 3.54, indicating an increase in hydrophilicity.

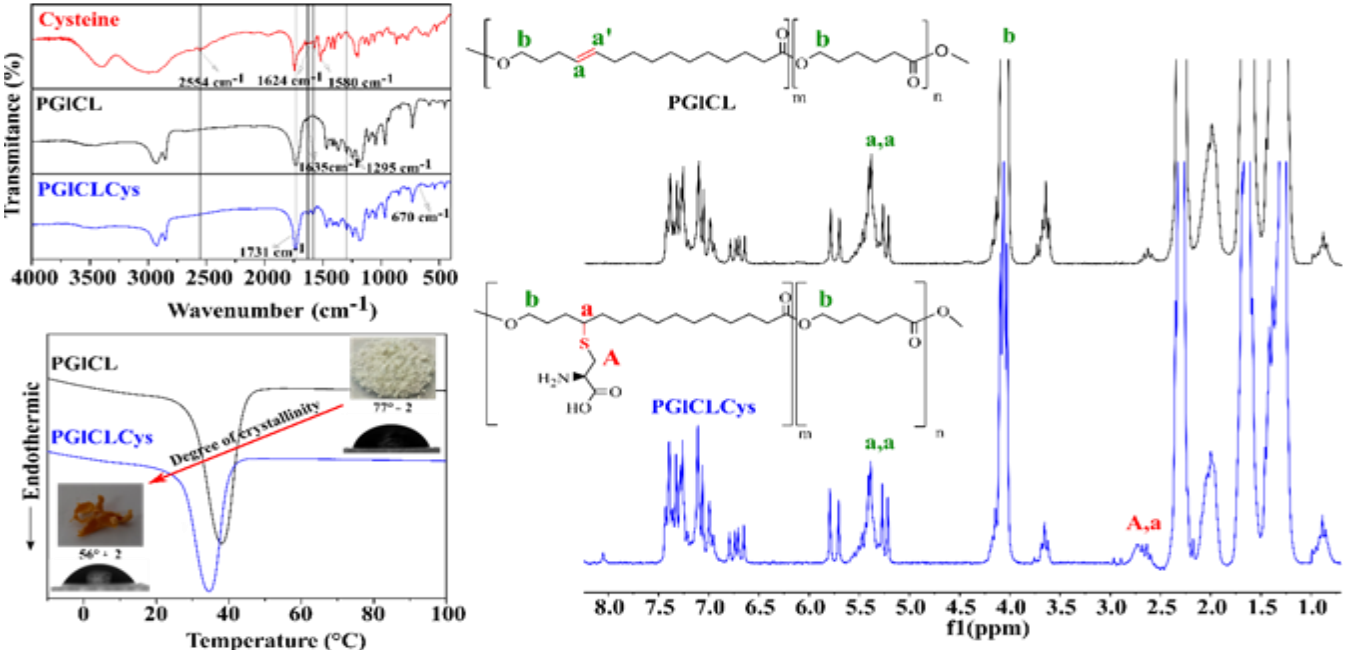

Figura 20. (A) FTIR spectra of pure Cys and respective copolymers PGlCL and PGlCLCys. (B) ^{1}H NMR spectra of PGlCL and PGlCLCys (50/50 Gl/CL ratio) and their respective peak attributions to the chemical structure of the polymers. (C) Second run DSC heating curves of PGlCL and PGlCLCys with different Gl/CL ratios, with the contact angle values as well as the reduction in the degree of crystallinity obtained.

Table 3. Thiol-ene reaction conversion calculated based on the consumption of the double bonds present in PGlCL chains, determined by ^{1}H NMR.

	Integration by corresponding peak (ppm)			
Sample	**Double Bond (5.40 ppm)**	**Reference (4.06 ppm)**	**Cysteine (2.90 – 2.70 ppm)**	**Double bond Conversion (%)**
PGlCL	1.00	1.00	-	-
PGlCLCys	0.82	1.00	3.00	18%

Table 4. Thermal properties of the polymers, determined by DSC.

Sample	**Tm_1 (°C)**	**Tm_2 (°C)**	**ΔH (J/g)**	**Xc (%)**
PGlCL	38	ND	59.22	44
PGlCLCys	32	ND	40.6	30

*Xc: degree of crystallinity, calculated from the heat of fusion of a PCL 100% crystalline sample (CRESCENZI et al., 1972).

Table 5. Gibbs free energy calculated at 1 atm and 25 °C using DFT/B3LYP/6-31G** with water and n-octanol solvents in SMD model.

Compound	**Gas-phase**	**Water**		**n-octanol**	
	G (Kcal/mol)	G^{W}_{solv} (Kcal/mol)	ΔG^{W}_{solv} (Kcal/mol)	G^{O}_{solv} (Kcal/mol)	ΔG^{O}_{solv} (Kcal/mol)
PGlCL	344.3180	348.5650	4.2473	341.0100	3.3081
PGlCLCys	407.4900	416.9260	9.4357	412.0820	4.5921
PGlCLCys AF	609.0233	615.9962	6.9728	614.8832	5.8599

Table 5 presents the calculated Gibbs free energy (G) and the Gibbs free energy of solvation (G_{solv}) in gas-phase, water and n-octanol. ΔG_{solv} was calculated as the difference between the Gibbs free energy of solvation and gas-phase Gibbs free energy.

4.3.2 STABILIZATITON SPIONS WITH PGLCLCYS

The synthesis of SPIONS and further stabilization with PGlCLCys (SPION@PGlCLCys) was performed according to the co-precipitation approach with modifications (BEE; MASSART; NEVEU, 1995; ZOTTIS; et al., 2015).

The SPION@PGlCLCys exhibited a number average size of 7.2 ± 2.2 nm (Figure 21A and Figure 21D), determined by transmission electron microscopy (TEM-100 kV), and a monomodal distribution, as well as high crystallinity (Figure 21B) determined by selected area electron diffraction (SAED) technique. The average crystalline domains and core size were around 7.6 nm as estimated from the results of X-ray powder diffraction (XRPD) analysis (Figure 21C). The lattice parameter obtained after Rietveld refinement (a = 8.36154 Å) applied to the XRPD data (0.252 nm to (311)) is consistent with the value of 8.46 Å based on the (220) interplanar spacing of 0.299 nm obtained using SAED (Table A1 and Figure A1, Figure A2 and Figure A3, see APPENDIX A). Thus, the results obtained are equivalent to other studies (HABIBI, 2014) related to the spinel structure of Fe_3O_4 and standard measurements (a = 8.3940 Å) (for more details, see Table A6, APPENDIX A).

The superparamagnetic behaviour of magnetite SPIONs@PGlCLCys observed by VSM analysis corroborates the core size below 15 nm(LEE; HYEON, 2012) and the successful stabilization of the SPIONS, presenting a saturation magnetization of 60 $emu \cdot g^{-1}$ (for details, see Figure A6, see APPENDIX A). The coating of the SPIONs by PGlCLCys was also evidenced by the FTIR spectra (Figure A4, see ANNEX A), indicated by vibration frequencies at 1736 cm^{-1} (elongation -C=O), associated with a carboxyl group and elongation of the amine group at 1643 cm^{-1} ($-NH_2$). TGA results (Figure A5, APPENDIX A) show that the mass loss assigned to PGlCLCys was 13.3 %, while 1.7 % is referent to water evaporation. Dynamic Light Scattering (DLS) measurements (Figure A7, APPENDIX A) also indicated that SPIONs@PGlCLCys are stable in aqueous media after being dispersed in buffer solution (zeta potential of -35.4 mV) at pH = 8.0, (Figure A8, see APPENDIX A), close to physiological conditions.

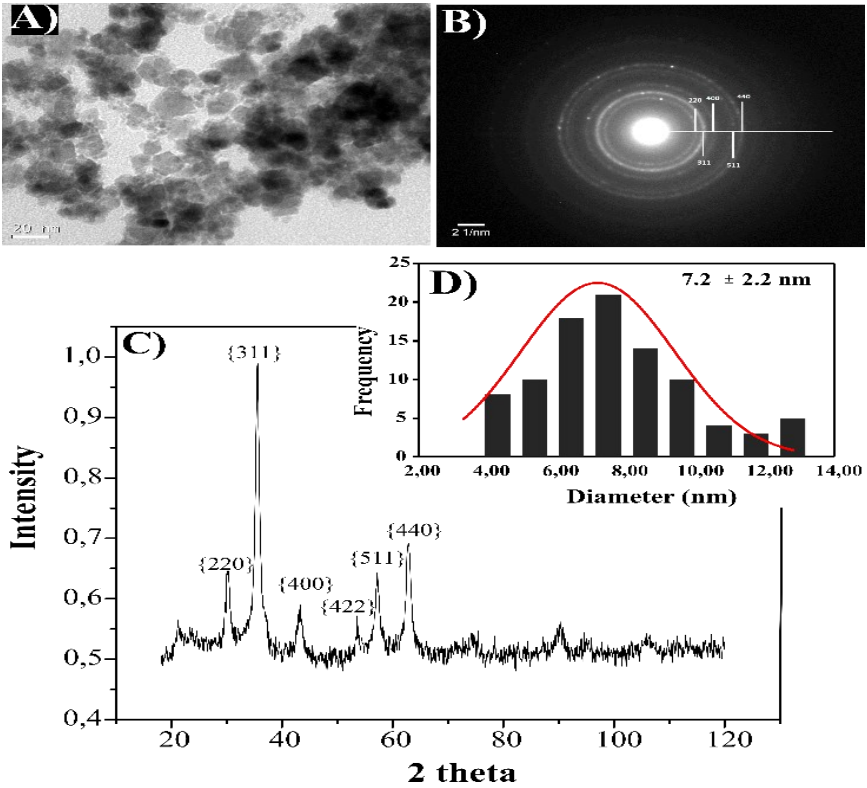

Figure 21. SPION@PGlCLCYS (A) Low magnification TEM image; (B) SAED; (C) XRPD diffractogram with diffraction peaks indexed to the spinel iron oxide phase. (D) Particle size distribution of the magnetic nanoparticles obtained from the TEM images.

4.3.3 CONJUGATION OF FOLIC ACID TO THE SURFACE OF THE SPION@PGLCLCys AND SUBSEQUENT RELEASE

Since SPION@PGlCLCys are stable in aqueous medium, their surface was covalently conjugated with FA by carbodiimide approach, aiming the targeting of folate receptors in breast cancer. The amount of FA covalently bonded to the SPION@PGlCLCys was determined by UV-vis spectrometry, by using a FA calibration curve in pH = 8.0 buffer at 286 nm (further details see Figure A9, APPENDIX A). Considering an NH_2:COOH stoichiometric balance of 1:1 and 1:2, the percentages of

conjugation of FA on the SPIONs surface were 57.7%, 74.2% respectively, relative to the available sites for conjugation. After FA conjugation, PGlCLCys_FA presented an estimated log P value of 0.81. Such hydrophilic characteristic must be highlighted, since the hydrophilization of nanoparticles is commonly reported as a strategy to increase its circulation time in the blood stream(YOO; CHAMBERS; MITRAGOTRI, 2010).

The cytotoxicity of SPION@PGlCLCys and SPION@PGlCLCys_FA were evaluated by MTT assay, using L929 and MDA-MB 231 cell lines (for details see Figure A10 and Figure A11, APPENDIX A). Cell viability reached 100% for all tested samples, in the concentration range of 1.10^{-4} ppm to 100 ppm, for 24 h and 72 h, and both test cell lines. Finally, the release profile of the folic acid conjugated on the surface of the SPIONS@PGlCLCys was evaluated. Bromelain was used as a protease to simulate a possible triggered release via lysosomal protease at 37 ^{o}C and pH ~ 5.4, similar to cellular pH, to verify the cleavage of the amide bond formed in the conjugation of FA to the surface of SPION@PGlCLCys nm. The results showed that the protease cleaves approximately 35% of the bonds within 24 h (Figure 22). This is the main route for drug release, since for the assay at the same pH but without enzyme, no release occurs. Thus, after a successful conjugation and subsequent triggered release of FA, we understand that SPION@PGlCLCys_FA can be treated as a model where FA can be replaced by other molecules of high biological interest (e.g. peptides, antibodies, drugs) enabling improved performance in diagnosis or theranostic applications. This work proposes the development of a superparamagnetic nanodevice that can be decorated in many ways through conjugation techniques, offering a platform for the preparation of high-performance tumor theranostic probes and other biomedical applications.

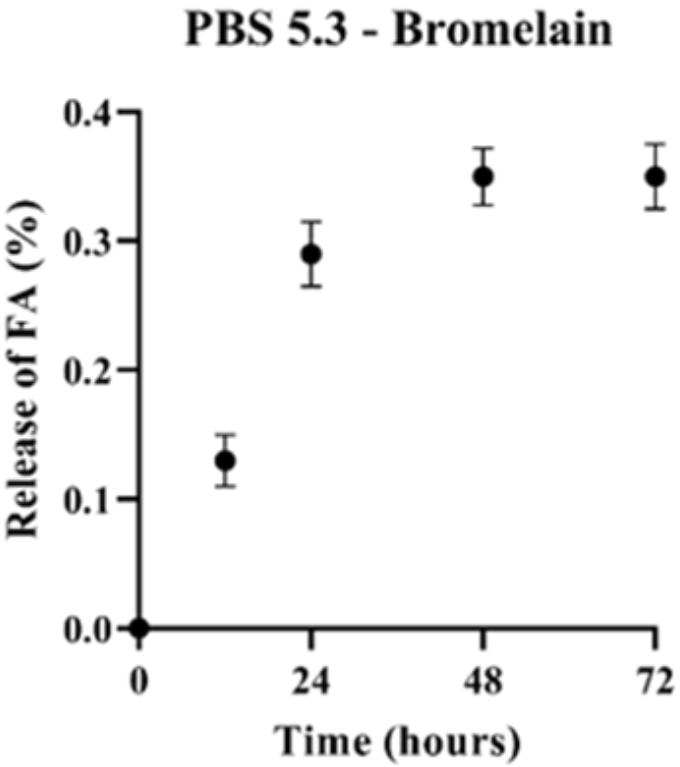

Figure 22. FA release from SPIONS@PGlCLCys_FA at pH 5.3.

4.4 CONCLUSION

The folic acid conjugation on the surface of SPIONS stabilized with cysteine-modified polyester enables demonstrating that these nanoparticles interact non-toxically with cells and that it is possible to release the conjugated (bio)molecules by protease cleavage. This strategy can provide a platform for chemically combining different components to achieve different functionalities and applications for SPIONS stabilized with a modified copolyester.

REFERENCES

ATES, Zeliha e HEISE, Andreas. Functional films from unsaturated poly(macrolactones) by thiol–ene cross-linking and functionalisation. **Polymer Chemistry**, v. 5, n. 8, p. 2936, 2014.

BAUER, Kristin N.; LIU, Lei; WAGNER, Manfred; ANDRIENKO, Denis; WURM, Frederik R. Mechanistic study on the hydrolytic degradation of polyphosphates. **European Polymer Journal**, vol. 108, no. August, p. 286–294, 2018. https://doi.org/10.1016/j.eurpolymj.2018.08.058.

BEE, A. e MASSART, R. e NEVEU, S. Synthesis of very fine maghemite particles. **Journal of Magnetism and Magnetic Materials**, v. 149, n. 1–2, p. 6–9, Ago 1995. Disponível em: <https://linkinghub.elsevier.com/retrieve/pii/0304885395003177>. Acesso em: 10 fev 2021.

CANDIOTTO, Graziâni; GIRO, Ronaldo; HORTA, Bruno A.C.; ROSSELLI, Flávia P.; DE CICCO, Marcelo; ACHETE, Carlos A.; CREMONA, Marco; CAPAZ, Rodrigo B. Emission redshift in DCM2-doped Alq3 caused by nonlinear Stark shifts and Förster-mediated exciton diffusion. **Physical Review B**, vol. 102, no. 23, p. 1–7, 2020. https://doi.org/10.1103/PhysRevB.102.235401.

CHU, Cho Ho; LEUNG, Chi Wai. The convolution equation of Choquet and Deny on [IN]-groups. **Integral Equations and Operator Theory**, vol. 40, no. 4, p. 391–402, 2001. https://doi.org/10.1007/BF01198136.

CRESCENZI, V.; MANZINI, G.; CALZOLARI, G.; BORRI, C. Thermodynamics of fusion of poly-β-propiolactone and poly-ε-caprolactone. comparative analysis of the melting of aliphatic polylactone and polyester chains. **European Polymer Journal**, vol. 8, no. 3, p. 449–463, 1972.

GARRIDO, Nuno M.; JORGE, Miguel; QUEIMADA, António J.; MACEDO, Eugénia A.; ECONOMOU, Ioannis G. Using molecular simulation to predict solute solvation and partition coefficients in solvents of different polarity. **Physical Chemistry Chemical Physics,** vol. 13, no. 20, p. 9155–9164, 2011. https://doi.org/10.1039/c1cp20110g.

GUINDANI, Camila; DOZORETZ, Pablo; VENERAL, Josamaique G.; DA SILVA, Deivid M.; ARAÚJO, Pedro H.H.; FERREIRA, Sandra R.S.; DE OLIVEIRA, Débora. Enzymatic ring opening copolymerization of

globalide and ε-caprolactone under supercritical conditions. **Journal of Supercritical Fluids**, vol. 128, no. May, p. 404–411, 2017. https://doi.org/10.1016/j.supflu.2017.06.008.

GUO, Xing; SHI, Chunli; WANG, Jie; DI, Shubin; ZHOU, Shaobing. PH-triggered intracellular release from actively targeting polymer micelles. **Biomaterials**, vol. 34, no. 18, p. 4544–4554, 2013. DOI 10.1016/j.biomaterials.2013.02.071. Available at: http://dx.doi.org/10.1016/j.biomaterials.2013.02.071.

GUPTA, Jagriti; BHARGAVA, Parag; BAHADUR, D. Methotrexate conjugated magnetic nanoparticle for targeted drug delivery and thermal therapy. **Journal of Applied Physics**, vol. 115, no. 17, p. 2012–2015, 2014. https://doi.org/10.1063/1.4866080.

HABIBI, Neda. Preparation of biocompatible magnetite-carboxymethyl cellulose nanocomposite: Characterization of nanocomposite by FTIR, XRD, FESEM and TEM. **Spectrochimica Acta - Part A: Molecular and Biomolecular Spectroscopy**, v. 131, p. 55–58, 2014. Disponível em: <http://dx.doi.org/10.1016/j.saa.2014.04.039>.

HANWELL, Marcus D; CURTIS, Donald E; LONIE, David C; VANDERMEERSCH, Tim; ZUREK, Eva; HUTCHISON, Geoffrey R. Avogadro: an advanced semantic chemical editor, visualization, and analysis platform. **Journal of Cheminformatics**, vol. 4, no. 1, p. 17, 13 Dec. 2012. DOI 10.1186/1758-2946-4-17. Available at: https://linkinghub.elsevier.com/retrieve/pii/S0001870814001959.

JUNG, Ji-Youn et al. Involvement of Bcl-2 family and caspases cascade in sodium fluoride-induced apoptosis of human gingival fibroblasts. **Korean Journal of Physiology & Pharmacology**, v. 10, n. 5, p. 289-294, 2006.

KIM, Sun Hun; KIM, Won Jae. Involvement of Bcl-2 family and caspases cascade in sodium fluoride-induced apoptosis of human gingival fibroblasts. **Korean Journal of Physiology and Pharmacology**, vol. 10, no. 5, p. 289–295, 2006.

LEE, Nohyun e HYEON, Taeghwan. Designed synthesis of uniformly sized iron oxide nanoparticles for efficient magnetic resonance imaging contrast agents. **Chemical Society Reviews**, v. 41, n. 7, p. 2575–2589, 2012.

MOSMANN T. Rapid colorimetric assay for cellular growth and survival: application to proliferation and cytotoxicity assays. **J Immunol Methods**, vol. 65, no. 1–2, p. 55–63, 1983.

NEDYALKOVA, Miroslava A.; MADURGA, Sergio; TOBISZEWSKI, Marek; SIMEONOV, Vasil. Calculating the Partition Coefficients of

Organic Solvents in Octanol/Water and Octanol/Air. **Journal of Chemical Information and Modeling**, vol. 59, no. 5, p. 2257–2263, 2019. https://doi.org/10.1021/acs.jcim.9b00212.

YOO, Jin-Wook e CHAMBERS, Elizabeth e MITRAGOTRI, Samir. Factors that Control the Circulation Time of Nanoparticles in Blood: Challenges, Solutions and Future Prospects. **Current Pharmaceutical Design**, v. 16, n. 21, p. 2298–2307, 2010.

ZOTTIS, Alexandre DA et al. Pheomelanin-coated iron oxide magnetic nanoparticles: a promising candidate for negative T 2 contrast enhancement in magnetic resonance imaging. **Chemical Communications**, v. 51, n. 56, p. 11194-11197, 2015.

CHAPTER 5

5 CONCLUDING REMARKS

In this work, the synthesis and modification of the copolymer poly(globalide-co-ε-caprolactone)(PGlCL) was carried out using synthetic methods to minimize the use of harmful reagents aiming future biomedical applications.

Modification reactions via thiol-ene reaction were used to modify the structure of PGlCL with the conjugation of N-acetylcysteine (NAC) and cysteine (Cys). With this, it was possible to obtain copolymers PGLCLNAC and PGlCLCYs, the presence of the side groups allowed the increase of hydrophilicity and reduction of crystallinity for both polymers.

PGlCLNAC was used for the production of electrospun scaffolds mixed with polycaprolactone (PCL). The presence of the modified copolyester with the amino acid derivative made it possible to obtain fibers with uniform distribution and nanometric diameters. The reduction of crystallinity and hydrophobicity of the scaffold, when compared to pure PCL, was also observed. These characteristics provided the scaffold with better adhesion and cell proliferation, showing its potential as a biomaterial.

PGlCLCys was used for the production of superparamagnetic iron oxide nanoparticles (SPIONs). The modification of the copolyester with the amino acid provided a good interaction with the metallic core of the particle, stabilizing the nanoparticle and allowing the production of nanoparticles with a hydrophilic surface. The conjugation of biomolecules on the surface of SPIONs with folic acid was possible through covalent bonding. Furthermore, the study of enzyme triggered release at controlled pH demonstrated the potential application of these nanoparticles as future drug carriers for the diagnosis and treatment of cancer.

This work consisted of an unprecedented study involving the modification of a copolyester for the production of scaffolds and of SPIONs aiming the development of materials for medical applications. It was possible to understand the effect of the copolyester modification and the implications on the final properties of the copolymer as a function of the molecule used. It was possible to show that these modifications enable the modulation of the properties aiming applications of these copolymers

for the production of smart devices. There are still many challenges to be overcome regarding syntheses and modifications, new strategies can be explored. Finally, this work should contribute to the progress of chemistry, chemical engineering, biomedical engineering and may serve as a support for future work aimed at studying biomaterials.

APPENDIX A

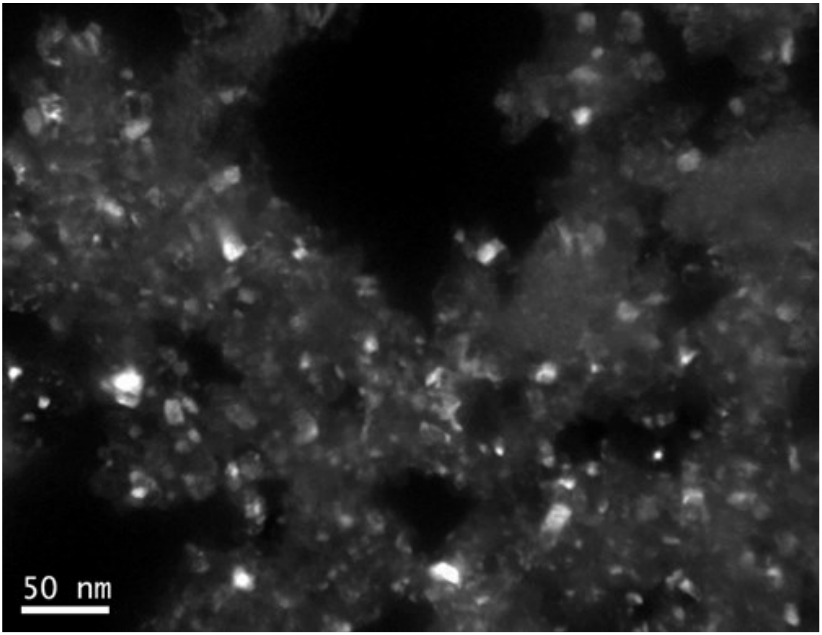

Figure A1. TEM dark field image showing individual crystalline particles (DF-TEM) of SPION@PGlCLCys.

The dark field TEM image (Figure A2) was crucial for the identification of individual nanoparticles, enabling the measurement of the size of nanoparticles. Since the samples tends to agglomerate, the conventional bright field TEM image shows superposed nanoparticles. The dark field technique otherwise makes visible only certain particles with particular geometrical orientation glow facilitating the identification of single-particle boundaries.

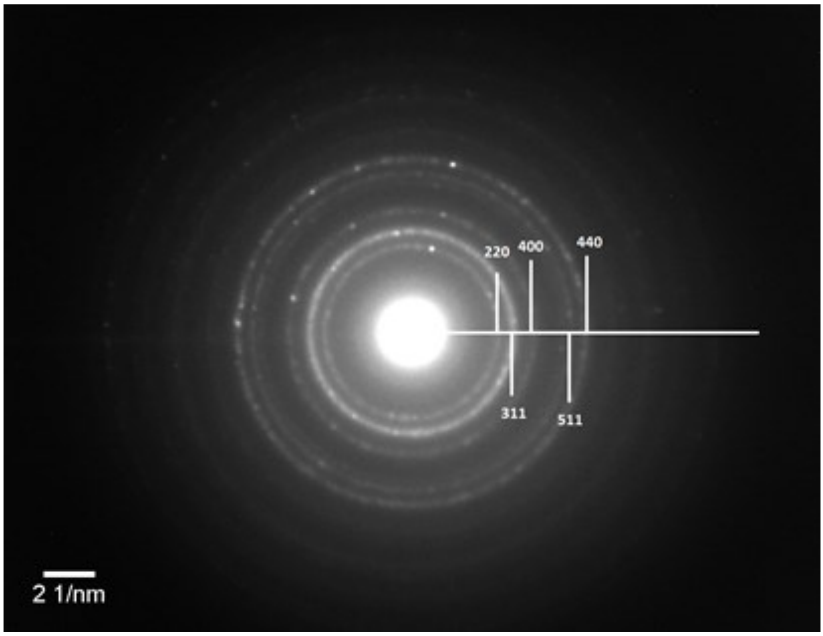

Figure A2. Selected area electron diffraction (SAED) image showing indexed diffraction rings corresponding to magnetite crystallographic planes of SPION@PGlCLCys.

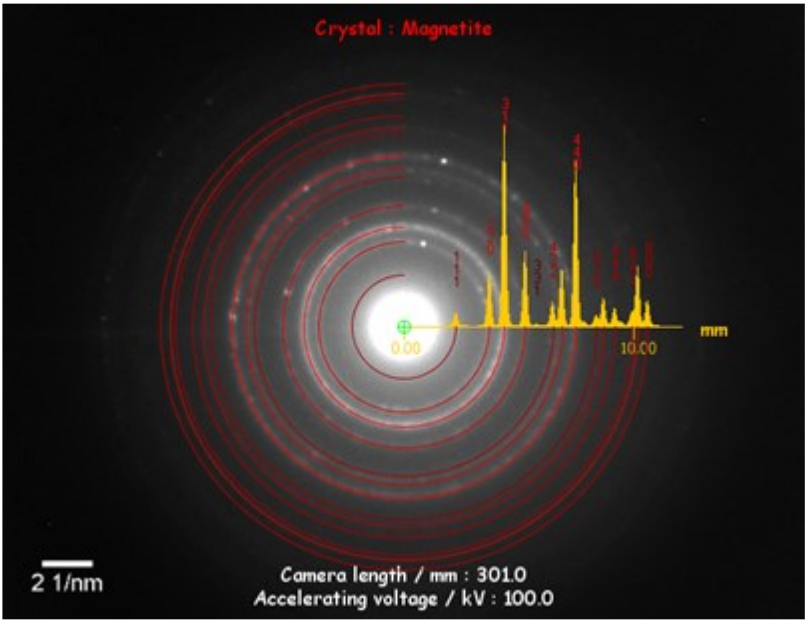

Figure A3. SAED image with Indexed diffraction pattern of magnetite and simulated diffraction ring pattern matching the results for the SPION@PGlCLCys sample.

X-ray diffraction (XRD) analysis was used to characterize the crystallite size, phase, and crystallization of SPIONS**.** According to the half-maximum full width (FWHM) of (311) reflections, the mean size of the Fe_3O_4 (JCPDS: 88-0315) nanocrystalline particles was calculated as 7.662 nm. In addition, the crystal cell dimension of (311) reflections were calculated to be a = 0.83615 nm using for quantitative analysis the Rietveld approach and the GSAS software.

Table A1. Interplanar distance.

Plane (hkl)	Measured Distance d (nm)	Theoretical Distance[17] d (nm)
220	0.299	0.297
311	0.255	0.253
400	0.212	0.210
511	0.162	0.162
440	0.149	0.148

Table A1 shows the measured interplanar distances obtained by transmission electron microscopy - selected area electron diffraction (TEM–SAED). The values are compared with theoretical values of magnetite (FLEET, 1981) and a good agreement is observed.

To calculate the unit cell, the plane distance was used and the distance calculated with the equation for cubic cells:

$$d_{(hkl)} = \frac{a_0}{\sqrt{h^2 + k^2 + l^2}}$$

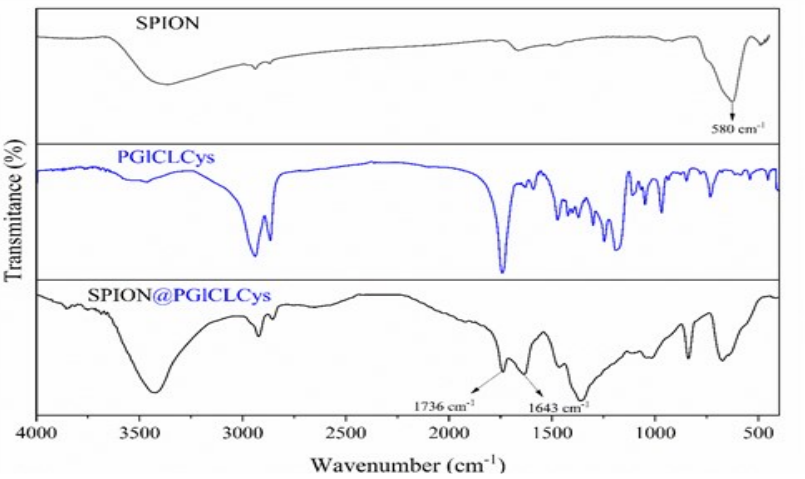

Figure A4. FT-IR spectra for SPIONs, and modified copolymer (PGlCLCys) and after stabilization of magnetic nanoparticles (SPION@PGlCLCys).

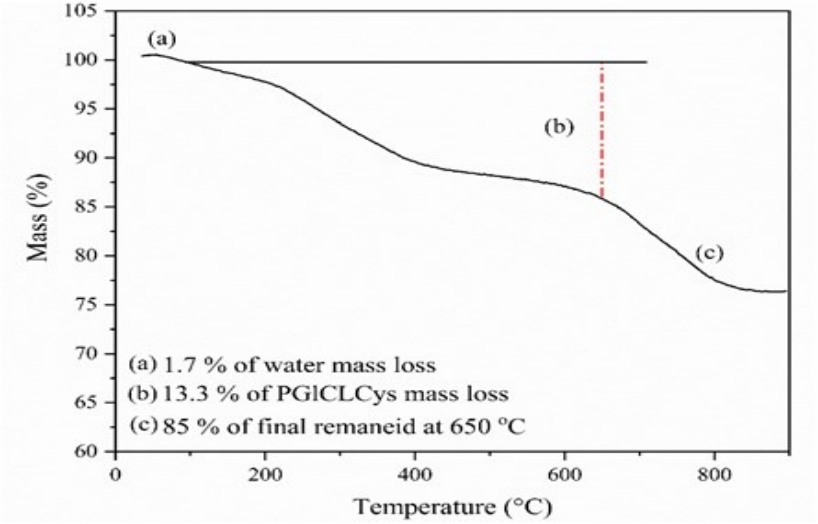

Figure A5. Thermogravimetric analysis of SPION@PGlCLCys.

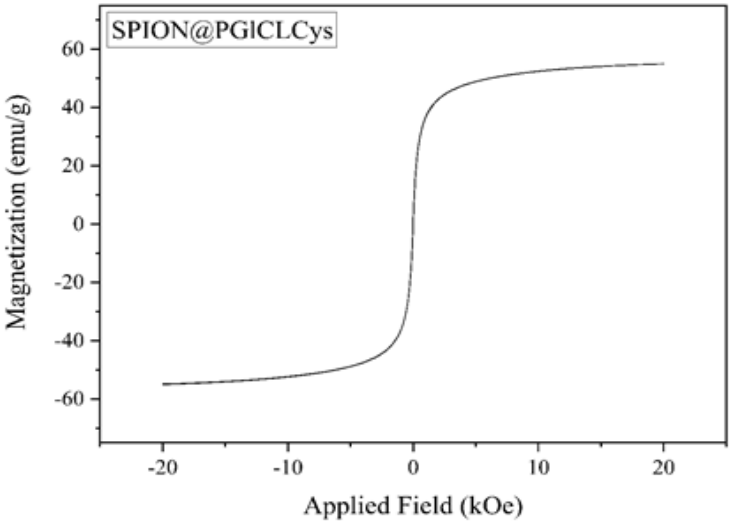

Figure A6. VSM analysis of SPION@PGlCLCys.

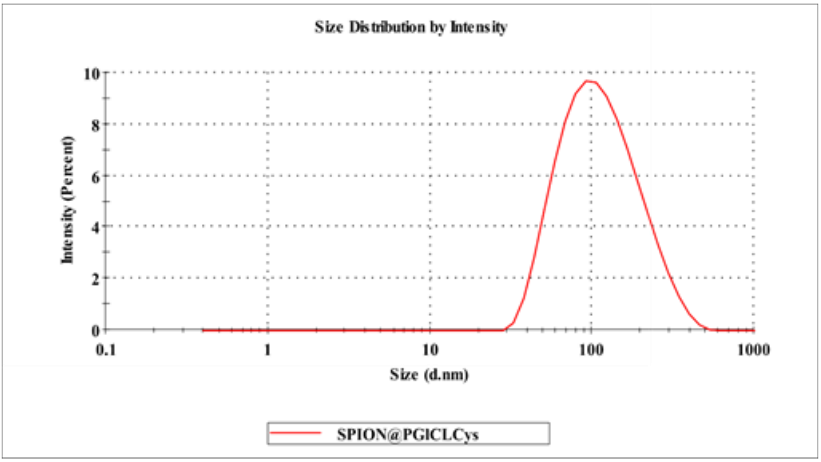

Figure A7. DLS analysis of SPION@PGlCLCys.

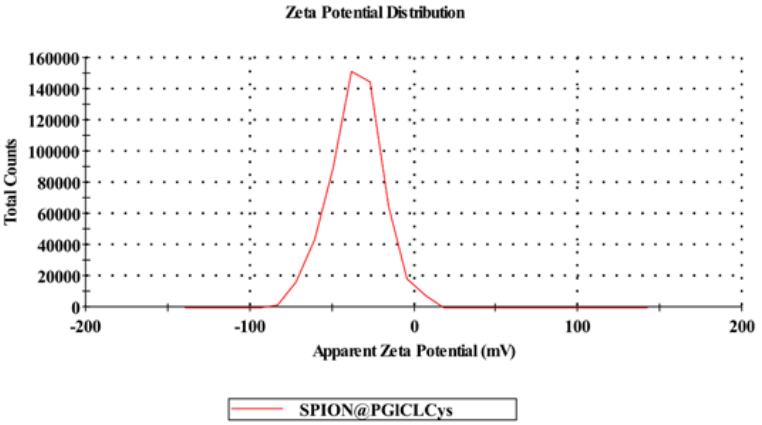

Figure A8. Zeta potential surface analysis of SPION@PGlCLCys (ζ= -35.4mV) stabilized in buffer solution (pH=8.0).

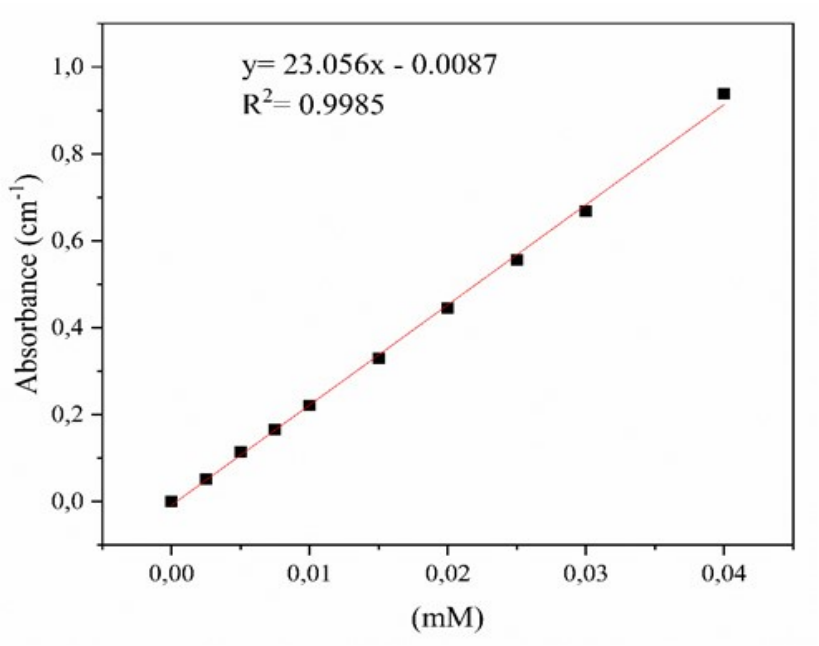

Figure A9. UV-vis calibration curve for Folic Acid in buffer solution (pH=8.0) at 283 nm.

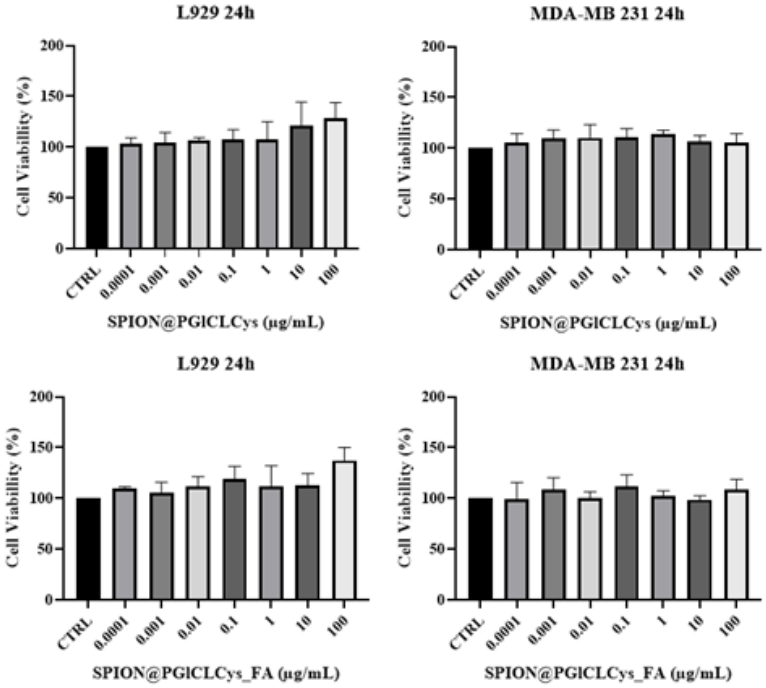

Figure A10. MTT assay of SPION@PGlCLCys and SPION@PGlCLCys_FA showing cells viability of the SPION as a function of nanoparticles concentration (0.0001 to 100 $\mu g \cdot mL^{-1}$) for 24 h. All SPIONs tested at different concentrations did not exert difference (ANOVA) in relations to the control group n=3.

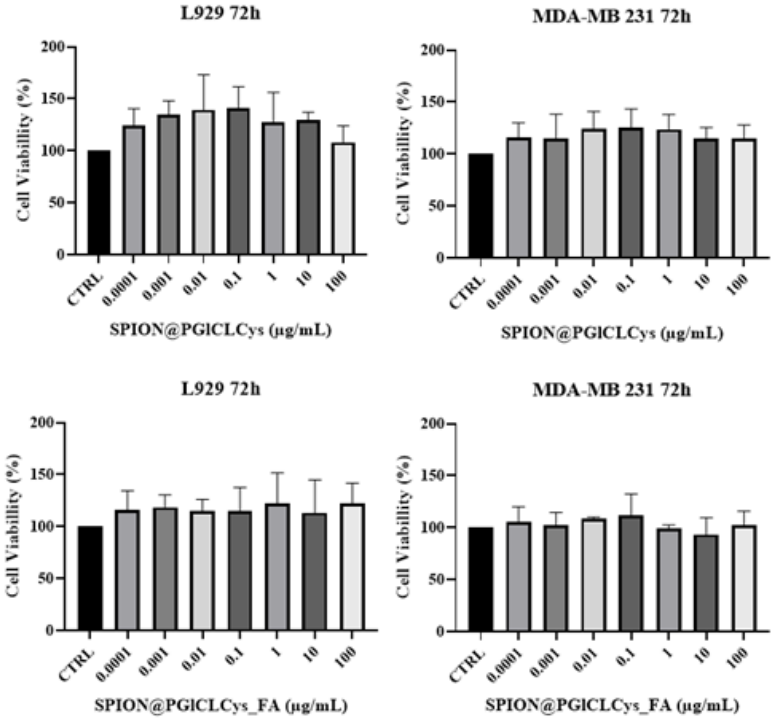

Figure A11. MTT assay of SPION@PGlCLCys and SPION@PGlCLCys_FA showing cells viability of the SPION as a function of nanoparticles concentration (0.0001 to 100 µg·mL^{-1}) for 72 h. All SPIONs tested at different concentrations did not exert difference (ANOVA) in relations to the control group n=3.